VALIDATION REPORT - SWIR

Technical Note

ESA project METHANE+ led by SRON

Task 2, WP 2000, Deliverable 3 (D3) SWIR

Lead authors:
Alba Lorente (SRON), Michael Buchwitz (IUP-UB)

Co-authors:
Tobias Borsdorff (SRON), Oliver Schneising (IUP-UB)

Change log

Version	Date	Status	Authors	Reason for change
0.01	xx-Jan-2021	In preparation	…	New document
0.1	2-Feb-2021			IUP-UB input added by Michael Buchwitz and Oliver Schneising
	23-Mar-2021			SRON input added
0.9	8 April 2021			Edited
1.0	28 April 2021	Approved	See cover page	Reviews by ESA included
1.9 Draft	25-Jan-2022	In preparation	M. Buchwitz	New section 4.5 added to present additional comparisons
1.9 Draft	24-Feb-2022	In preparation	A. Lorente	Several changes but mainly Sects. 1 (overview table added), 2, 4.1.4, 4.5.
1.9 Draft	28-Feb-2022	In preparation	M. Buchwitz	Improved table 1. Additional information on WFMD v1.5 added in Sect. 4.5
1.9	17-Mar-2022	In preparation	A. Lorente	Integrate comments from partners Editing
2.0	29-Apr-2022	Final		approved by ESA, identical to v1.9

Authors

SRON:

- Alba Lorente
- Tobias Borsdorff

IUP-UB:

- Michael Buchwitz
- Oliver Schneising

Table of Contents

1. Overview

The purpose of the Validation Report for the short-wave infrared (VR SWIR) technical note is on the one hand to assess the data quality of the different products by validation with external independent reference measurements and on the other hand to work out differences of the data products by detailed inter-comparison between them. This information is crucial for next steps of the project in which these data products are assimilated in the inverse modelling systems to infer fluxes global fluxes.

SRON the Netherlands Institute for Space Research develops the retrieval algorithm for the operational processing of TROPOMI XCH_4 data by ESA. Furthermore, in the software deployment cycle SRON provides a scientific beta product that already includes updates and improvements of the XCH_4 retrieval. SRON focused in this project in providing the SRON S5P-RemoTeC scientific TROPOMI XCH_4 product with the latest updates that will be implemented in the operational processing in the processor update in June 2021 and November 2021. The focus in the project is to validate this scientific (beta) product to assess the quality of data after the improvements have been implemented (Sect. 2). Furthermore, SRON focusses on the analysis over regions that are challenging for the retrieval to asses that the developments implemented in the SRON S5P-RemoTeC scientific product work in the right direction (Sect. 4.1). In Sect. 4.5 additional ongoing improvements of the SRON S5P-RemoTeC XCH_4 scientific product are presented.

The Institute of Environmental Physics of the University of Bremen (IUP-UB) focussed in this project on the following aspects: (i) Provision of a S5P/TROPOMI XCH_4 data set retrieved with the scientific algorithm “Weighting Function Modified Differential Optical Absorption Spectroscopy” (WFM-DOAS or WFMD). This data set is referred to as WFMD data set in this document. (ii) Validation of this WFMD data set by comparisons with TCCON ground-based XCH_4 retrievals (Sect. 3). (iii) Comparisons of the WFMD data set with the operational Copernicus S5P TROPOMI XCH_4 product (referred to as OPER product in Sect. 4.2) focussing on selected regions showing locally elevated methane (Sect. 4.2). In addition, comparisons have been conducted with the SRON S5P-RemoTeC scientific TROPOMI XCH_4 product generated at SRON with an improved version of the operational algorithm (Sect. 4.3, referred to as OPERbeta in that section). The comparisons listed above have been carried out with product XCH_4 WFMD version 1.2. Additional comparisons are presented in Sect. 4.5 using XCH_4 WFMD version 1.5.

Table 1 shows the different SWIR XCH4 data products validated and compared in this report.

Table 1: SWIR XCH_4 products and the corresponding versions used in the validation report

WFM-DOAS from IUP-UB	Version 1.2 (Schneising et al., 2019). Additional comparisons with version 1.5 (Schneising et al., 2021b, 2021c) in Sect. 4.5.
SRON S5P-RemoTec scientific	Version 14_14, 18_17 (extra updates in Sect. 4.5) Note: version 14_14 is referred to as OPERbeta in Sect. 4.3)
Operational S5P TROPOMI XCH4 product	Version v1.2.x and v1.3.x (referred to as OPER in Sect 4.2)

2. SRON SWIR XCH4 TROPOMI product

In this section the scientific SRON S5P-RemoTeC TROPOMI CH_4 dataset is presented. SRON develops the retrieval algorithm for the operational processing of TROPOMI XCH_4 data done by ESA. In the software deployment cycle, SRON provides a scientific beta product that already includes updates and improvements of the XCH_4 retrieval. In the duration of the Methane+ project, two different versions of the scientific product were provided, as developments led to improvements of the data product that were of significance to the project.

The scientific SRON S5P-RemoTeC XCH_4 product version 14_14 covers the time period November 2017 to December 2020, and it is described in detail in Lorente et al. (2021). The scientific SRON S5P-RemoTeC algorithm version 14_14 was implemented in the operational algorithm in the processor update version v2.2.0 in June 2021. The updates of the scientific SRON S5P-RemoTeC retrieval algorithm v14_14 to retrieve TROPOMI XCH_4 relate to the regularization scheme, the selection of the spectroscopic database and a more sophisticated a posteriori correction for the albedo dependence. The regularization scheme is updated with a constant regularization parameter for both CH_4 and the retrieved scattering parameters, which stabilizes the retrieval and yields less scatter in the TROPOPOMI XCH_4 data (Lorente et al., 2021). The spectroscopic database has been updated to the Scientific Exploitation of Operational Missions – Improved Atmospheric Spectroscopy Databases database (the SEOM-IAS database) (Birk et al. (2017), Hase et al. (2018)), that was derived in a dedicated project for the improvement of spectroscopic databases for the interpretation of TROPOMI observations. The use of the SEOM-IAS database provides better fitting results in the retrieved XCH_4 compared to the HITRAN 2008 and HITRAN 2016 database (Lorente et al. 2021). The most relevant update is the implementation of an a posteriori correction that is fully independent of any reference data that has been derived using only TROPOMI XCH_4 data. The correction is more accurate than the one implemented at the beginning of the mission, as it corrects more accurately the strong XCH_4 underestimation at low surface albedo scenes and also corrects for the positive bias in scenes with high surface albedo. All these updates have resulted in a TROPOMI XCH_4 product with high quality as demonstrated by the validation with independent ground-based measurements and the comparison with GOSAT satellite XCH_4 data (Lorente et al., 2021).

The scientific SRON S5P-RemoTeC XCH_4 product version 18_17 covers the time period March 2018 to 28 September 2021. The scientific SRON S5P-RemoTeC algorithm version 18_17 was implemented in the operational algorithm in the processor update v2.3.1 in November 2021. The main change in version 18_17 with respect to version 14_14 is that version 18_17 contains measurements over the ocean under sun-glint geometry, and the regularization of two scattering parameters instead of three. The changes on the retrieved XCH_4 over land due to the change in the regularization are not significant.

Table 2 summarizes the main characteristics of the different versions for the SRON S5P-RemoTeC scientific algorithm delivered in the duration of the Methane+ project, and its correspondence with the different versions of the operational processor. Please be aware that the changes in the operational processing take effect from the day of the activation onwards.

Table 2: Main differences between SRON RemoTeC S5P XCH4 scientific product and operational product for the different versions.

	SRON RemoTeC-S5P Scientific v18_17 Operational v2.3.1	**SRON RemoTeC-S5P Scientific v14_14 Operational v2.2.0**	**SRON RemoTeC-S5P Operational v1.2.x, v1.3.x**
Coverage	Land and ocean	Land	Land
Regularization	Scattering layer altitude fixed to prior (3000 m)	Constant regularization different for XCH4 and scattering parameters	L-Curve
Cross-section	SEOM-IAS	SEOM-IAS	HITRAN 2008
Bias correction	Land: same as v14_14/v2.2.0 Ocean: correction factor	Independent B-Spline fit to surface albedo	Based on GOSAT linear fit to surface albedo
Altitude DEM	SRTM15'' (in v18_17) GMTED2010 S5P (in oper v2.3.1)	SRTM15'' (in v14_17) GMTED2010 S5P (in oper v2.2.0)	GMTED2010 S5P
Reference	Updated ATBD (Hasekamp et al., 2019)	Lorente et al. (2021)	Hu et al. (2016)

The algorithm has been designed to provide accurate and precise retrievals for clear-sky scenes with minor scattering by aerosols and optically thin cirrus. Thus a strict cloud filter is applied based on observations of the Visible Infrared Imaging Radiometer Suite (VIIRS) aboard the Suomi-NPP and other retrieved parameters. A posteriori correction to the retrieved XCH_4 over land is applied to account for the dependence on the retrieved surface albedo in the short-wave infrared (SWIR) spectral band, explained in detail in Lorente et al. (2021). The results shown in this section refer to the corrected XCH_4 product unless stated otherwise. The data over oceans were derived from measurements under sun-glint geometries. These retrievals do not show a specific dependency with signal or albedo as data over land, so we apply a correction based on the XCH4 distribution over land. A demonstration of the dataset is shown in

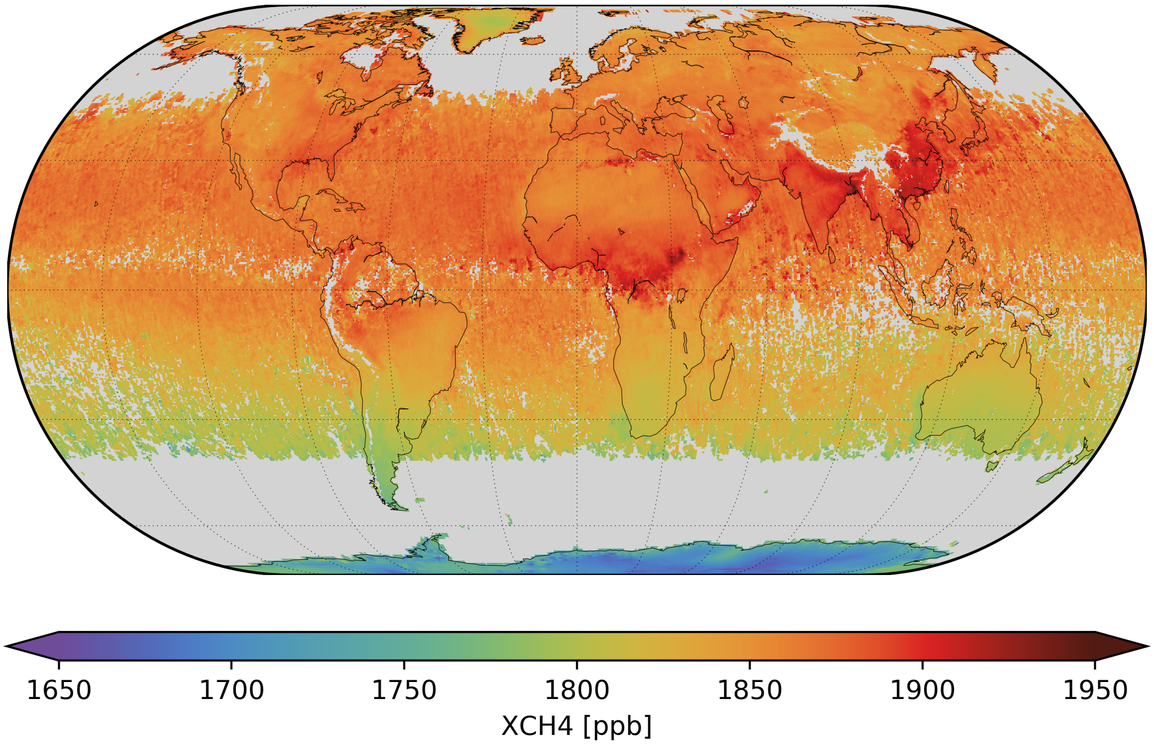

Figure 1 which represents a yearly average of XCH_4 retrieved with the SRON S5P-RemoTeC scientific algorithm version 18_17 from TROPOMI measurements.

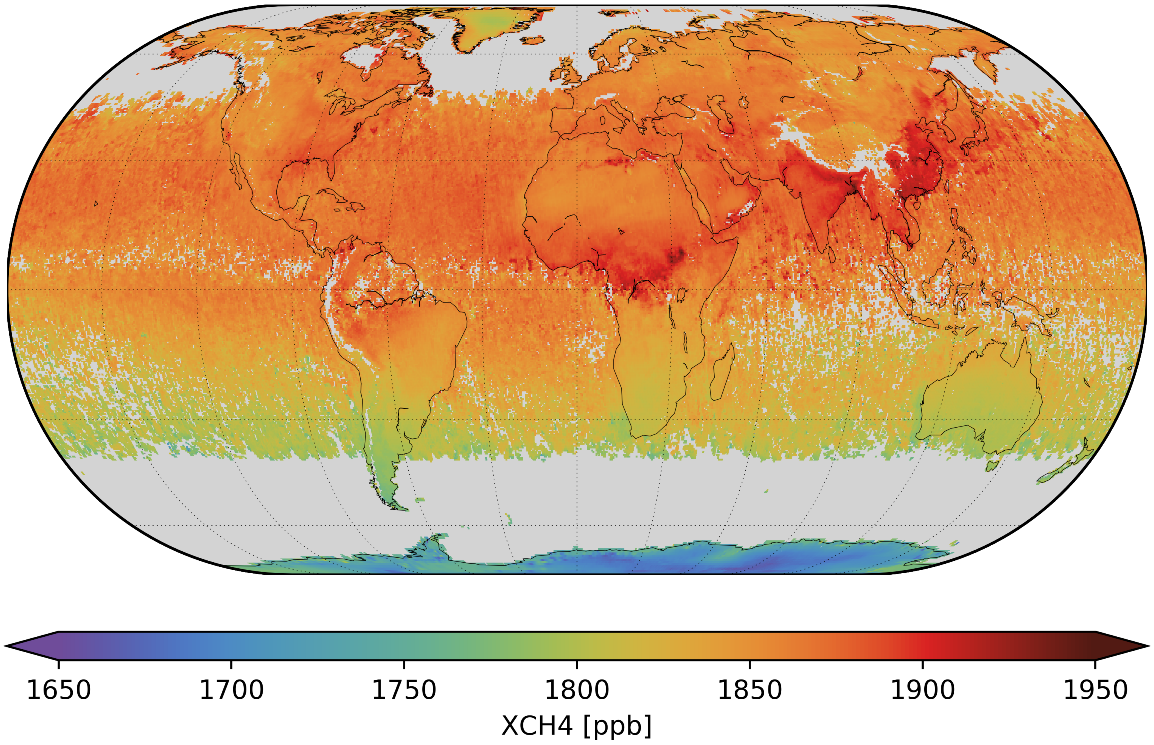

Figure 1: Global averaged TROPOMI XCH_4 distribution for the period 1 Jan 2020 31 Dec 2020 represented on a cylindrical equal-area grid with 0.3° x 0.5° resolution at the Equator based on retrievals of the SRON S5P-RemoTeC scientific algorithm version 18_17.

2.1. TCCON Validation of TROPOMI XCH_4

For the validation of TROPOMI XCH_4 data, ground-based measurements from the TCCON network are used. The TCCON network of ground-based Fourier transform spectrometers (FTS) is the state-of-art validation system for satellite measurements. Additionally, EM27/SUN spectrometers have been developed and the COllaborative Carbon Column Observing Network (COCCON) has been created (Frey et al., 2019), with the added value that it is more feasible to place this type of instruments at location where TCCON is less represented (e.g., high surface albedo, high latitudes). In this project and in the operational validation of TROPOMI XCH_4 only TCCON data has been considered, but there have been already some studies where TROPOMI XCH_4 data has been validated against measurements from the COCCON network (e.g., Tu et al., 2020).

2.1.1. TCCON Validation of TROPOMI XCH4 over land

The SRON S5P-RemoTec scientific XCH_4 dataset is validated with independent XCH_4 retrievals from ground-based Fourier Transform measurements (FTIR) performed by the Total Carbon Column Observing Network (TCCON). (Wunch et al., 2011). All the ground-based measurements are processed using the GGG2014 standard retrieval code (Wunch et al., 2015) and are freely available at https://tccondata.org/. We used 13 ground-based stations located in both the Northern and Southern Hemisphere, and we validate the data for a period of 2 years (January 2018– December 2019).

A TCCON station can be overpassed by TROPOMI one or two times a day. For the validation, we average the TROPOMI XCH_4 retrievals from one orbit overpass within a radius around each station of 300 km. The selection of the radius is based on a trade-off between having enough data for a robust validation and statistics. For a stricter collocation criterion of 100 km radius, the number of points is reduced significantly, but the results of the validation do not change. The average retrieved TROPOMI XCH_4 is then compared with the average of the retrievals from a TCCON stations that fall withing ± 2 hours of the TROPOMI overpass time.

For each TCCON station we calculate a mean bias and its standard deviation from the time series of collocated XCH_4 retrievals which quantifies the data quality on a regional scale. To analyse the global agreement between TCCON and TROPOMI we furthermore compute the average of the station biases and its standard deviation as a measure of the station-to-station variability.

Different instruments have different vertical sensitivities and the retrievals also use different apriori profiles. In order to account for this in the validation, column averaging kernels can be taken into consideration. However, if the vertical sensitivities are similar as is the case for TROPOMI and TCCON, the smoothing effect is negligible (Sha et al., 2021).

Figure 2 shows the time series of the average XCH_4 retrievals of TROPOMI in comparison with the collocated measurements of each TCCON station averaged within ± 2 hours of the TROPOMI overpass time. The TROPOMI data can clearly capture the temporal variability of XCH_4 in good agreement with the one measured by the ground-based stations such as the seasonal cycle and the year-to-year increase in XCH_4 concentrations. Figure 3 shows the same as Figure 2 but for version 18_17, with the time series extended further in time.

A summary of the validation results is given in Figure 4 for version 14_14; Figure 4a shows the mean bias and the standard deviation for each of the stations and Figure 4b shows a correlation plot of all the paired collocations between TCCON and TROPOMI retrievals. The average bias for all the stations is -0.2% (-3.4 ppb) and the station-to-station variability is 0.3%. Before the correction, the agreement is -0.9% (-17 ppb) and the station-to-station variability is 0.6%. Figure 5 shows the same results but for version 18_17. The average bias for all the stations is -0.3% (-5.4 ppb) and the. station-to-station variability is 0.3%. With this we can conclude that the scientific SRON

S5P RemoTeC TROPOMI XCH_4 data set is well within the mission requirements of 1%, even before the posterior correction is applied.

The validation at high latitude stations such as East Trout Lake and Sodankylä show that there is a seasonality in the bias between TROPOMI and TCCON XCH_4 which is positive during the February-April period and changes to negative bias around May, increasing then to reach high negative bias in autumn. This seasonality correlates with the presence of snow on the region where the stations are located, as indicated by low surface albedo retrieved in the SWIR together with high surface albedo in the NIR (not shown).

To filter for such scenes covered with snow or ice, Wunch et al. (2011) introduced the so-called blended albedo, which combines the surface albedo retrieved in the NIR and SWIR. Scenes covered by snow are characterized by low spectrum intensity in the SWIR, so the signal to noise ratio is a limiting factor for the TROPOMI retrieval performance under these conditions.

By applying a threshold value between 0.85-0.95 for the blended albedo these problematic scenes could be removed. Hence, the influence of snow should be considered when using TROPOMI XCH_4 data over snow-covered scenes, especially for high latitudes.

2.1.2. TCCON validation of TROPOMI XCH4 over the oceans (sun-glint geometries)

XCH_4 retrievals over the oceans under sun-glint geometry is an extension of the scientific TROPOMI data product provided in version 18_17. The stations selected for validation of ocean measurements are those located on islands and close to the coastline, as is typically done for greenhouse gas measurements of other instruments like GOSATT and OCO-2.

Figure 6 shows the time series of TROPOMI and TCCON XCH4 measurements and Figure 7 the summary of the collocations. Here, the validation results for some of the stations are based on very little data available for the analysed period, thus the statistics shown should be considered with this in mind.

Similarly as over land, we can conclude that the variability in XCH_4 as captured by the ground-based measurements stations is in good agreement with the one measured by TROPOMI. The overall bias is -8.4 ppb and the station-to-station variability is 6.3 ppb. Before the correction, the bias is -15.5 ppb. The station-to-station variability does not change as the correction is constant and equal for all retrievals. The magnitude of the bias and its variability is similar to the ones found for the validation of the XCH_4 data product over land.

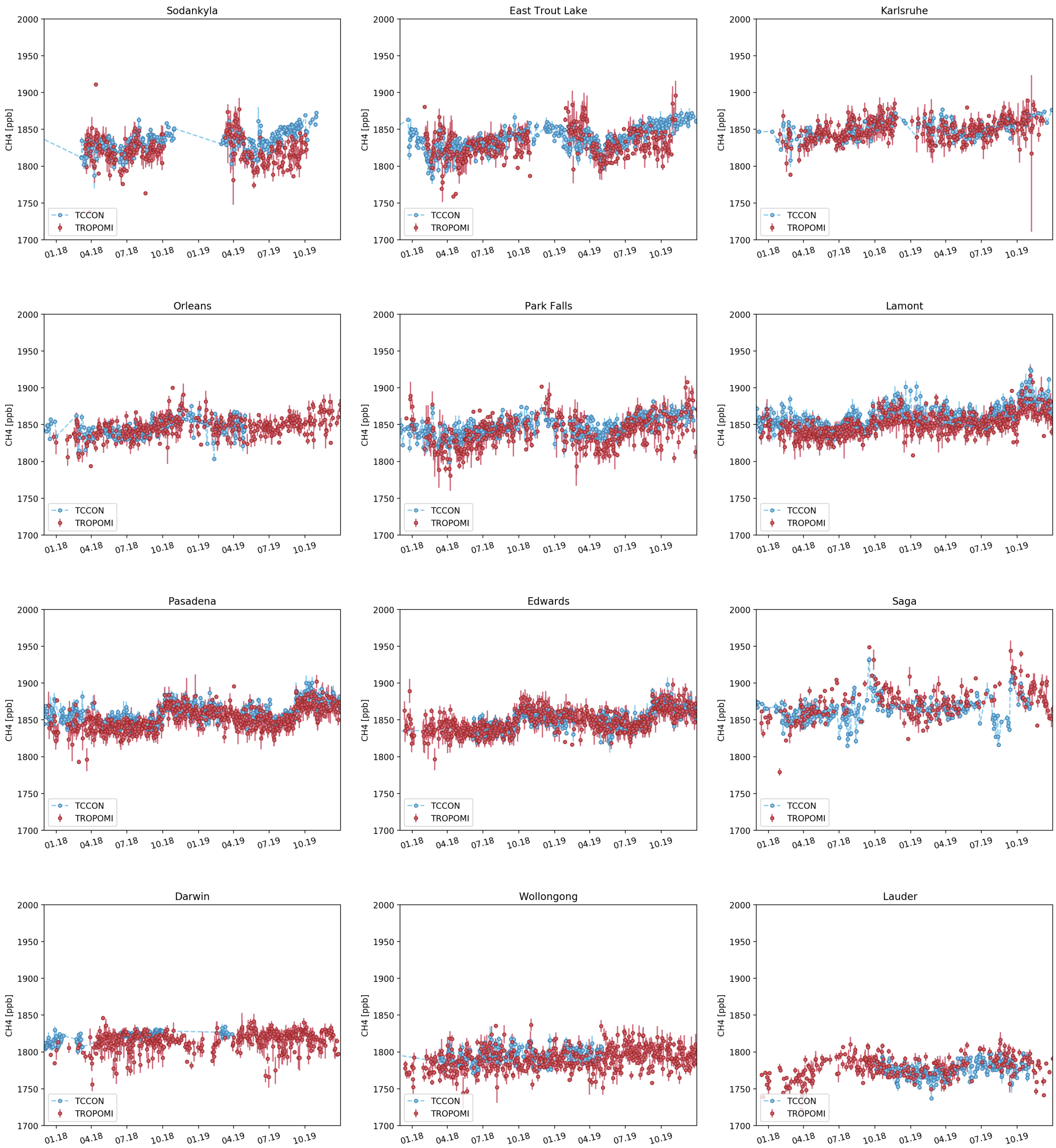

Figure 2: Time series of daily averaged XCH_4 measurements from TROPOMI (red) and TCCON (blue) for the period 1 of Jan 2018–31 of Dec 2019.

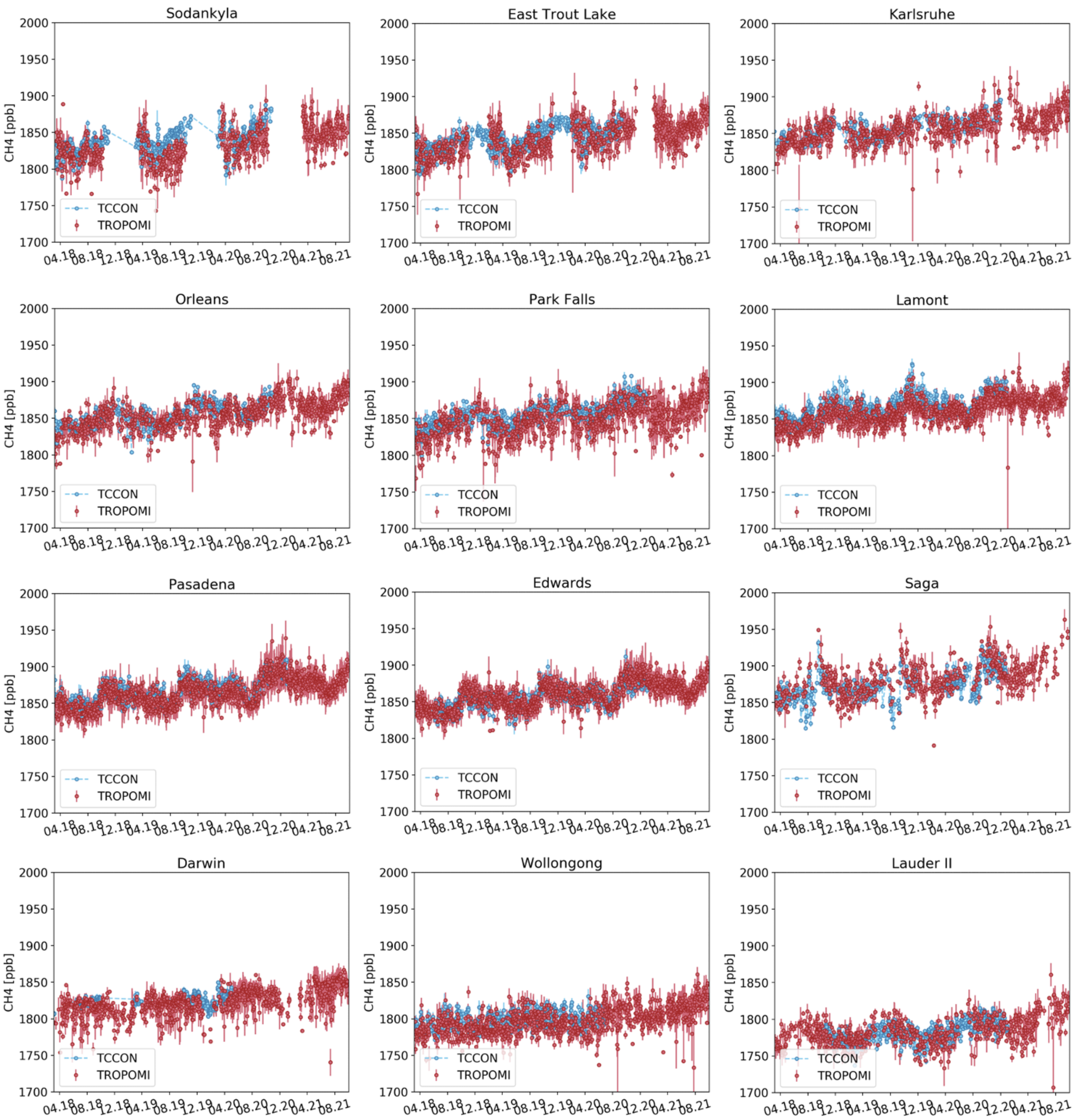

Figure 3: same as Figure 2 but for version 18_17 and extended time period (1 of Mar 2018–28 of Sep 2020).

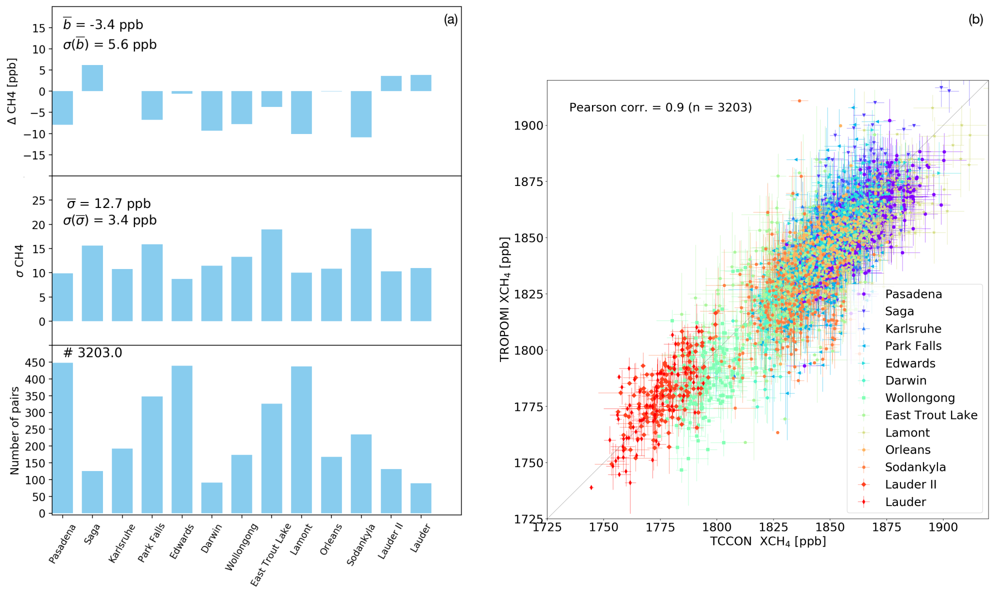

Figure 4: Mean differences between TROPOMI and TCCON XCH4 (ΔXCH4), the standard deviation of the differences (σXCH_4) and the number of collocations for each of the stations. (b) Correlation of daily average XCH_4 measured by TROPOMI and TCCON for all the stations.

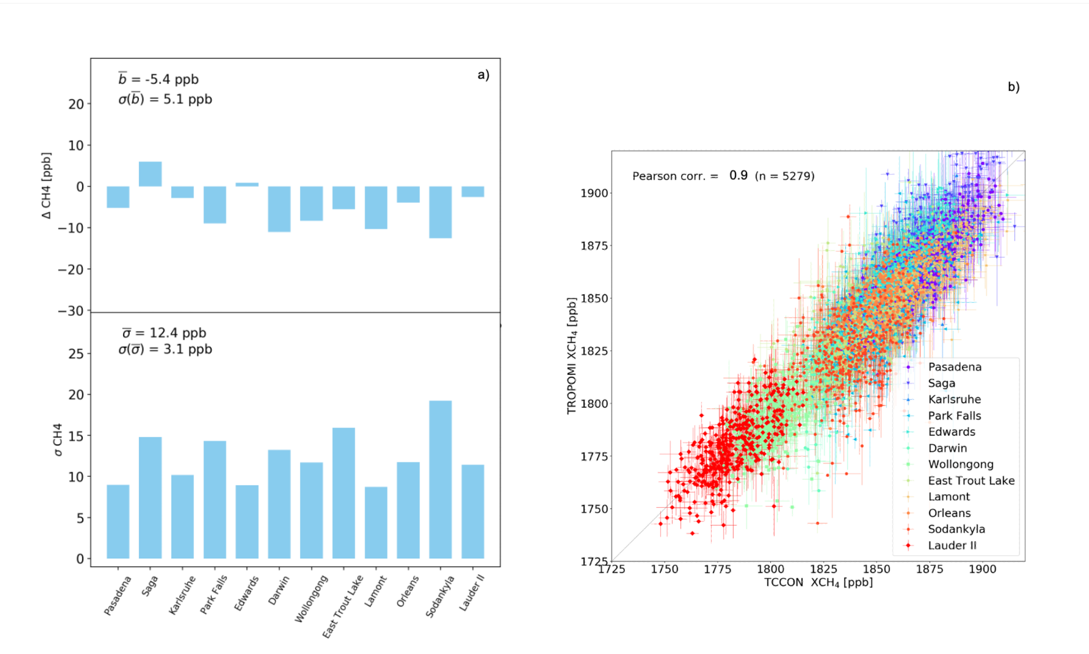

Figure 5: Same as Figure 4 but for version 18_17.

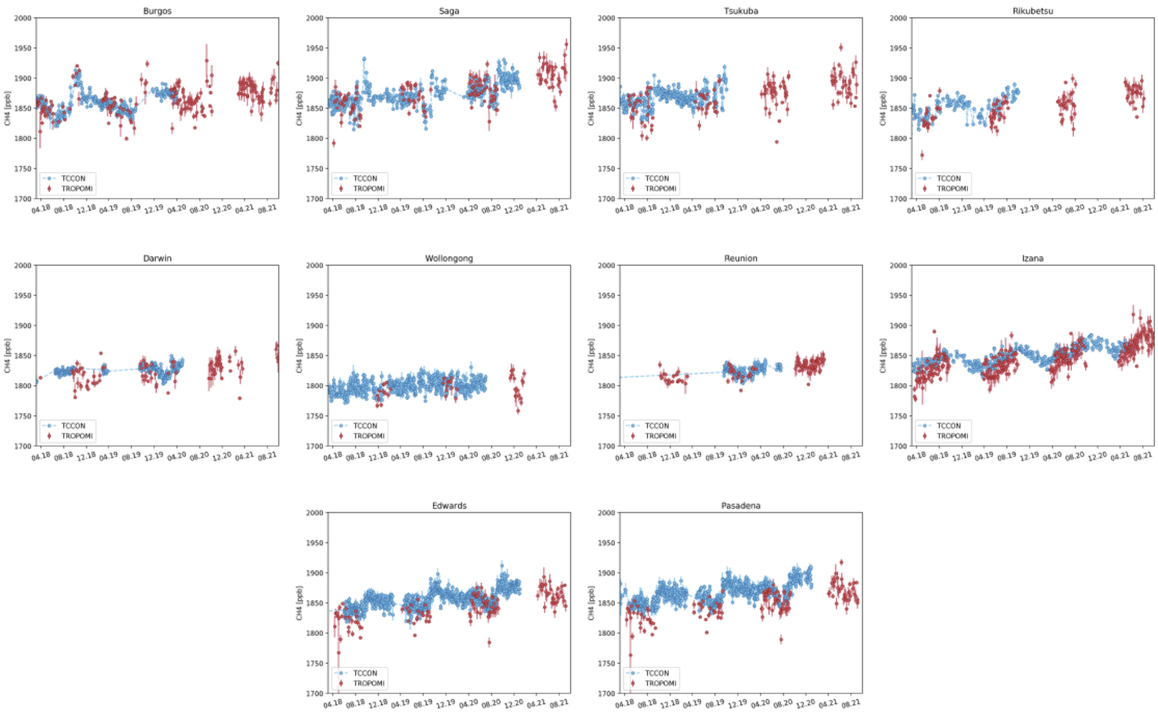

Figure 6: Time series of daily averaged XCH_4 measurements from TROPOMI over ocean for sunglint geometries (red) and TCCON (blue) for the period 1 of Mar 2018–28 of Sep 2020.

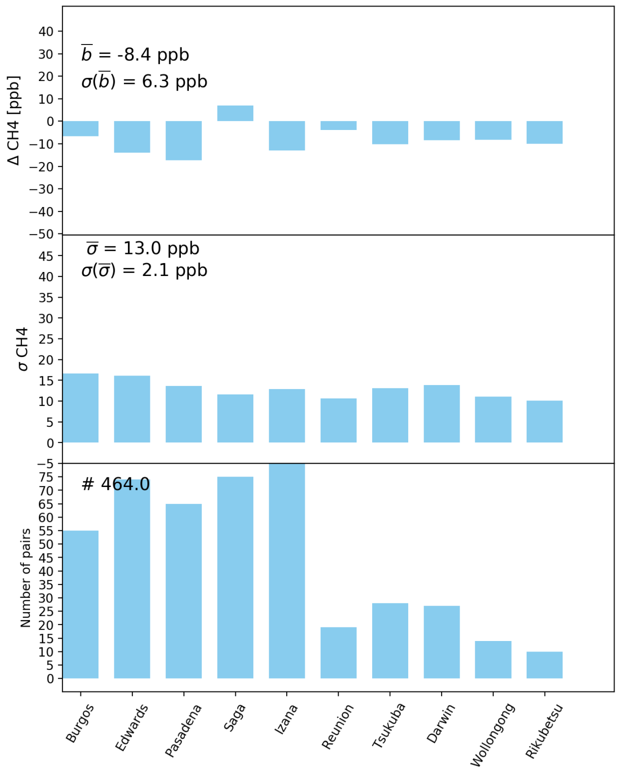

Figure 7: Mean differences between TROPOMI ocean measurements and TCCON XCH4 (ΔXCH4), the standard deviation of the differences (σXCH_4) and the number of collocations for each of the stations.

2.2. Intercomparision of TROPOMI and GOSAT XCH_4

A global impression of the data quality of the scientific TROPOMI XCH_4 data product can be obtained by satellite intercomparison with XCH_4 retrievals from measurements by the Thermal and Near Infrared Sensor for Carbon Observation Fourier transform spectrometer (TANSO-FTS) on board the Greenhouse gases Observing SATellite (GOSAT) satellite.

For this we use the GOSAT proxy XCH_4 data product that is retrieved using the RemoTeC/proxy retrieval algorithm. The proxy approach assumes that the light path modifications in the atmosphere are the same for the target absorber and the proxy absorber CO_2, whose prior is assumed to be known with high accuracy (Frankenberg et al, 2005). There is also a full-physics data product from GOSAT measurements, however the data yield of the full-physics GOSAT product is smaller due to the strict filtering needed to minimize the scattering-related error.

For the analysis over land, we compare XCH_4 retrieved from TROPOMI (version v14_14) and GOSAT measurements for a period of 2 years (January 2018– December 2019). We compare daily collocations averaged to a 2 x 2 degree grid.

The comparison yields a mean bias of -10.3 ± 16.8 ppb; overall compared to GOSAT, TROPOMI XCH_4 is lower, especially in the regions around the tropics. The overall underestimation is stronger in the non-corrected XCH4, reflecting that the albedo correction improves the TROPOMI XCH4 that is too low in areas where the surface albedo is low. This bias between TROPOMI and GOSAT is still under investigation and most probably reflects a different approach in the correction for the signal dependent bias in the XCH_4 retrieval.

The good agreement between TROPOMI and GOSAT, which is of the same order of magnitude as the agreement with TCCON, highlights the high quality of the scientific S5P-RemoTeC XCH_4 dataset.

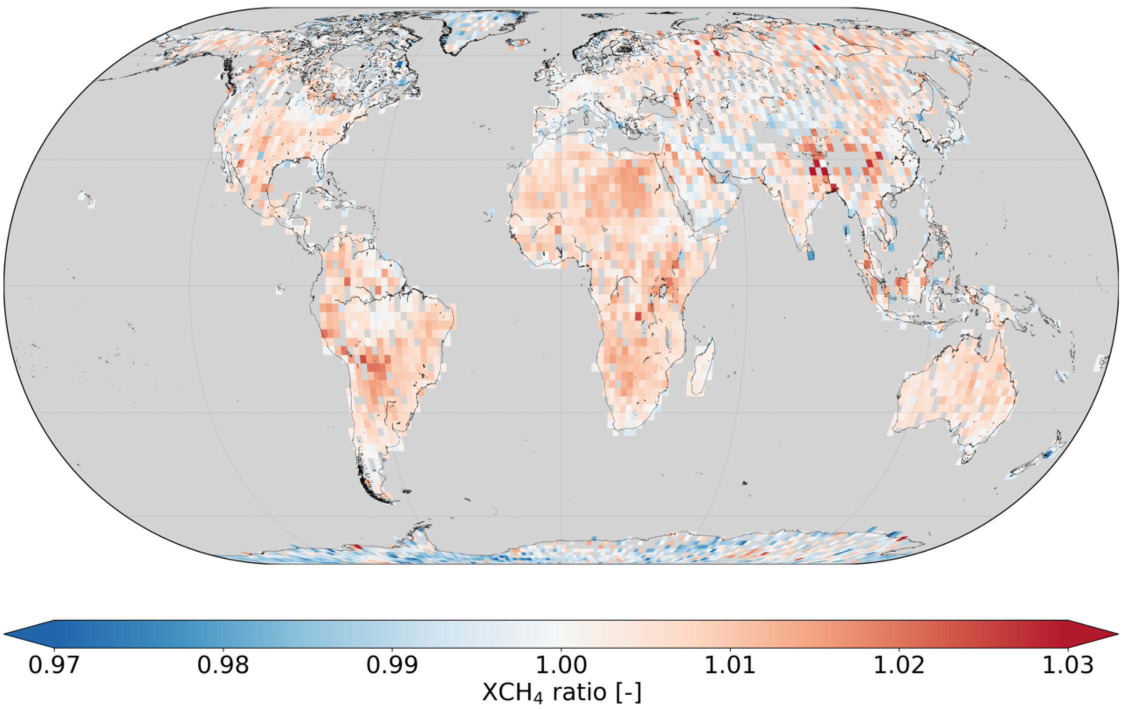

Figure 8: Global distribution of the ratio of GOSAT to TROPOMI XCH_4 v14_14. Daily collocations are averaged to a 2° x 2° grid.

We perform a similar intercomparison as the one above for version 18_17, also including ocean measurements over sun-glint geometries for the period 1 March 2018–31 December 2020. Over land, the comparison results in a bias after correction of -13.8 ± 16.1 ppb (-0.7 ± 0.8 %) and a Pearson's correlation coefficient of 0.87. Over ocean, the comparison results in a bias of -4.4 ± 15.7 ppb (-0.2 ± 0.9 %).

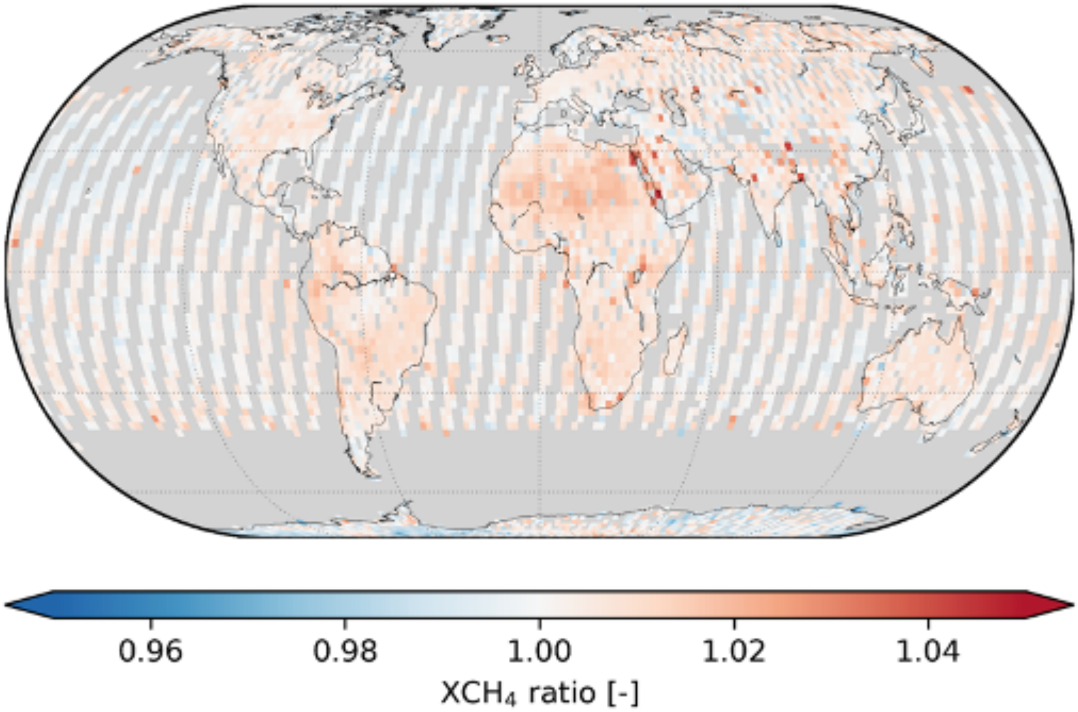

Figure 9: Global distribution of the ratio of GOSAT to TROPOMI XCH_4 for version v18_17. Daily collocations are averaged to a 2° x 2° grid for the period 1 March 2018–31 December 2020.

3. Validation of IUP-UB SWIR XCH_4 TROPOMI product

In this section the validation of the scientific TROPOMI/WFMD version 1.2 XCH_4 data product is described (see Schneising et al., 2019, 2020, for details). This product covers the time period November 2017 to July 2020.

How this product "looks like" is shown in Figure 10-Figure 12. The global distribution of retrieved XCH_4 is shown in Figure 10. Clearly visible is the interhemispheric gradient with larger values on the Northern Hemisphere, where the majority of sources is located, superimposed by enhancements over prominent source regions like China, India, or Southeast Asia. The data set includes measurements over the ocean and inland water. The product has also significant coverage at high latitudes as can be seen in the zoom on the artic region shown in Figure 11.

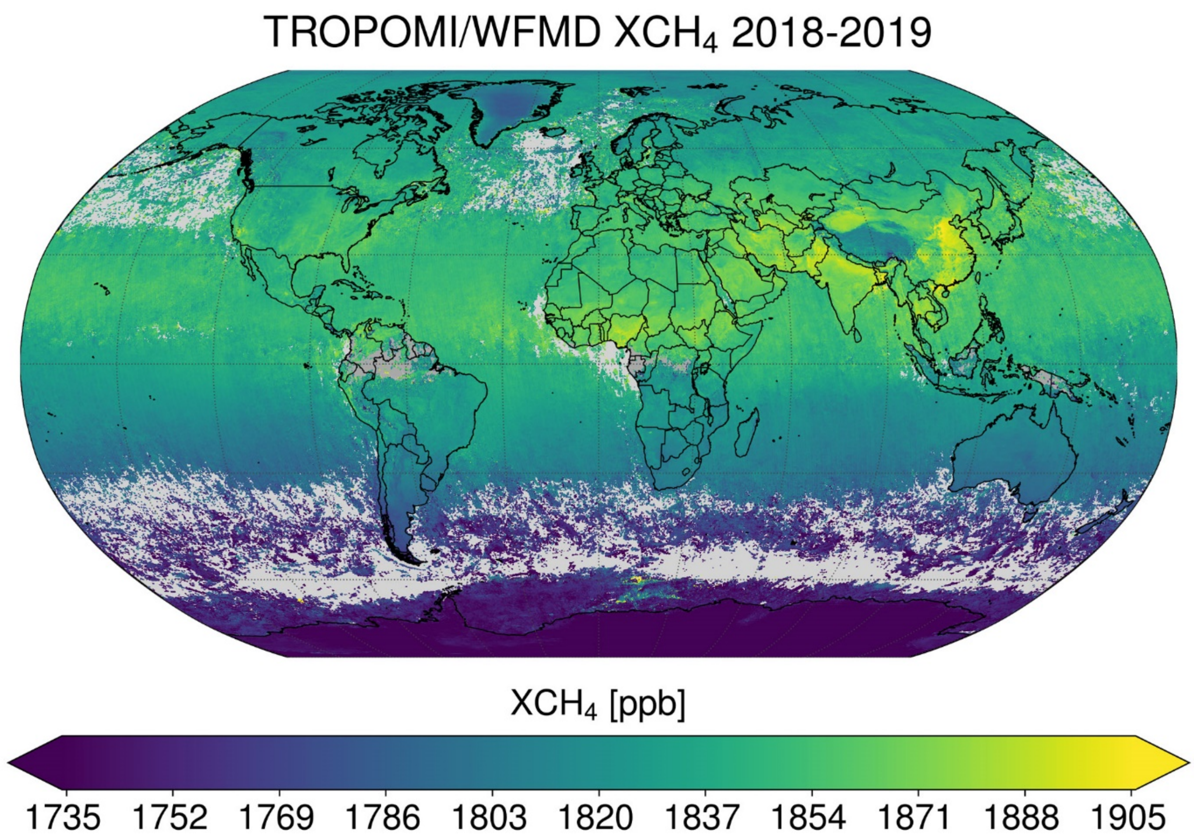

Figure 10: Biennial mean (2018-2019) of retrieved TROPOMI/WFMD v1.2 methane.

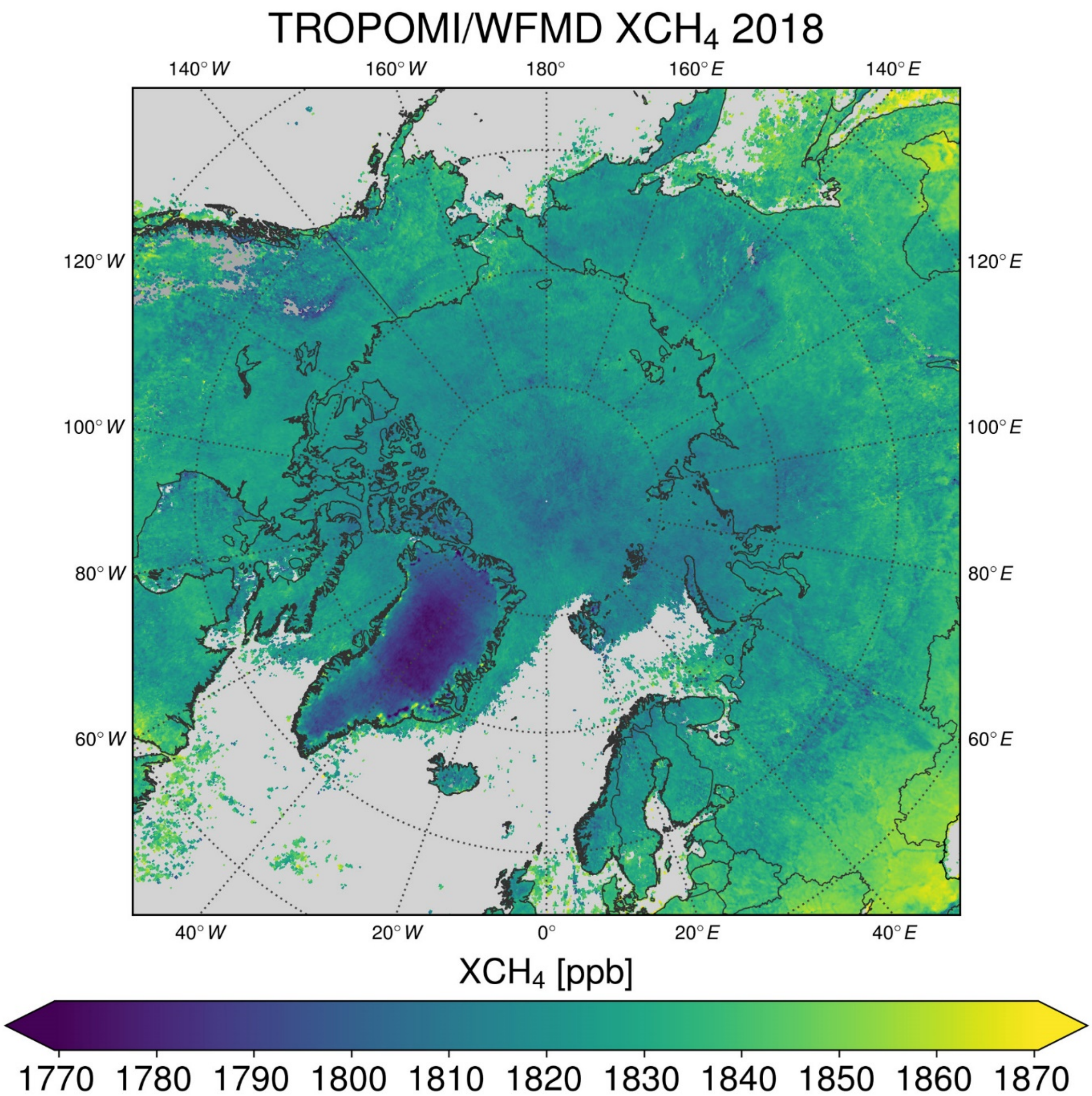

Figure 11: Polar view for the annual mean of XCH_4 at northern high latitudes.

Intense methane sources are readily detected in a single satellite overpass, e.g., methane leakage from natural gas production at one of the world's largest natural gas fields, Galkynysh in Turkmenistan (see Figure 12).

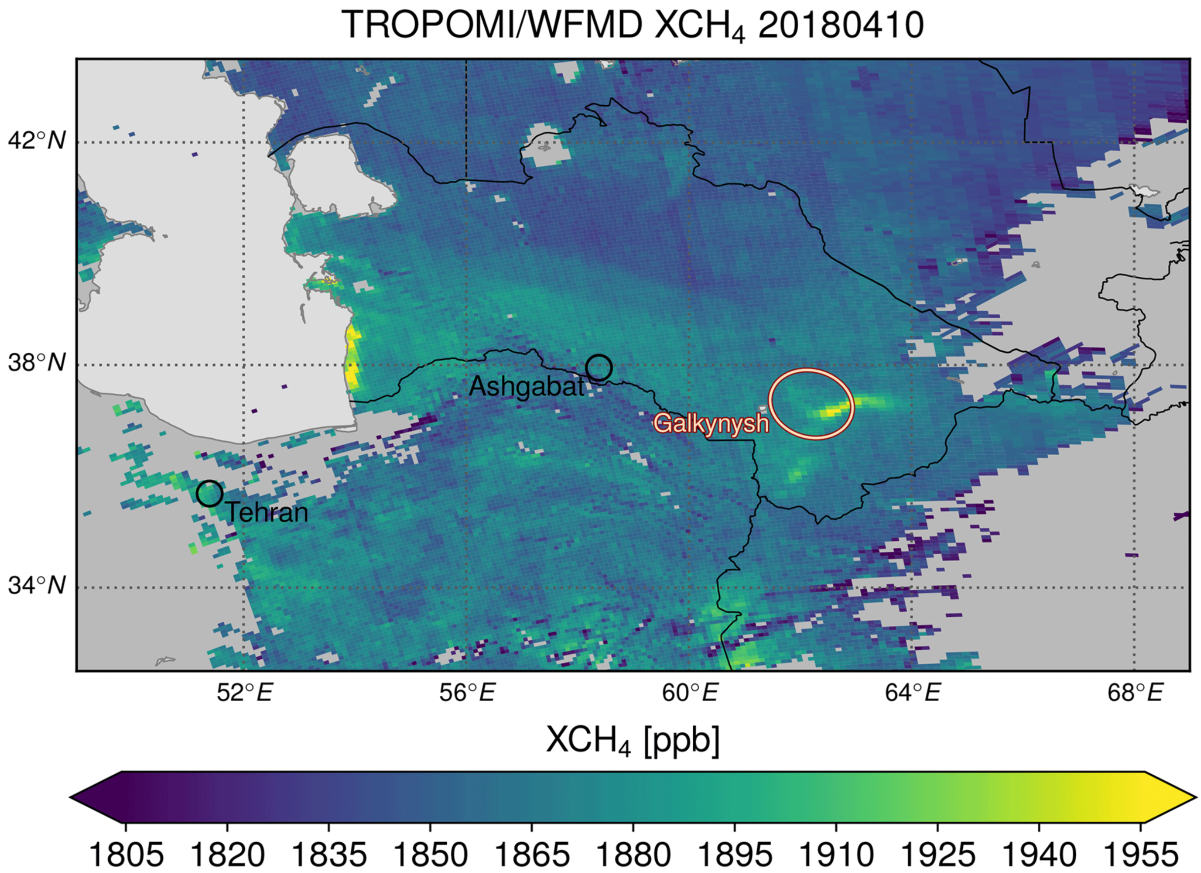

Figure 12: Methane enhancement due to emissions from one of the world's largest natural gas fields, Galkynysh in Turkmenistan.

The validation results are shown in the following sub-section.

3.1. Comparison with TCCON XCH_4

The validation data set is the GGG2014 collection of the Total Carbon Column Observing Network (TCCON) (Wunch et al., 2011). To ensure comparability, all TCCON sites use similar instrumentation (Bruker IFS 125HR) and a common retrieval algorithm. The TCCON data are tied to the WMO trace gas scale using airborne in situ measurements applying individual scaling factors for each species. The estimated TCCON accuracy (1σ) is about 3.5 ppb for XCH_4. From the validation with TCCON data at 24 TCCON sites, realistic error estimates of the satellite data are provided.

To compare the satellite data with TCCON quantitatively, it has to be taken into account that the sensitivities of the instruments differ from each other and that individual apriori profiles are used to determine the best estimate of the true atmospheric state, respectively. The first step is to correct for the apriori contribution to the smoothing equation by adjusting the measurements for a common apriori. Here we use the TCCON prior as the common apriori profile for all measurements:

$$\hat{c}_{adj} = \hat{c} + \frac{1}{m_0} \sum_l m_l \, (1 - A_l)(x^l_{a,T} - x^l_a)$$

In this equation, $\hat{c}$ represents the originally retrieved TROPOMI column-averaged dry air mole fraction, l is the index of the vertical layer, A_l the corresponding column averaging kernel of the TROPOMI algorithm, $\boldsymbol{x}_a$ and $\boldsymbol{x}_{a,T}$ the TROPOMI and TCCON apriori dry air mole fraction profiles. m_l is the mass of dry air determined from the dry air pressure difference between the upper and lower boundary of layer l and $m_0 = \sum_l m_l$ is the total mass of dry air. To minimise the smoothing error introduced by the averaging kernels we do not compare $\hat{c}_{adj}$ directly with the retrieved TCCON mole fractions $\hat{c}_T$ but rather with the adjusted expression

$$\hat{c}_{T,adj} = c_{a,T} + \left(\frac{\hat{c}_T}{c_{a,T}} - 1 \right) \frac{1}{m_0} \sum_l m_l A_l x^l_{a,T}$$

Thereby, $c_{a,T}$ represents the TCCON apriori column-averaged dry air mole fraction associated with the apriori profile $\boldsymbol{x}_{a,T}$.

For the comparison a set of collocation criteria has been specified. The representativity is maximised by as strict as possible criteria while concurrently ensuring sufficient data for a sound and stable comparison. This trade-off is resolved by the following selection. The spatial collocation criterion requires the satellite measurements to lie within a radius of 100 km around the TCCON site and that the altitude difference is smaller than 250 m. The temporal collocation criterion is set to ±2 hours. For each satellite measurement within the collocation radius, all TCCON data meeting the temporal collocation criterion are averaged to obtain a unique satellite-TCCON data pair.

The validation results are shown in Figure 13 including the mean bias μ and the scatter σ relative to TCCON for each site. The parameter σ is estimated from Huber's Proposal-2 M-estimator, which is a well-established estimator of location and scale being robust against outliers of a normal distribution. This is an appropriate choice and preferred over the standard deviation, because one is interested in the actual single measurement precision without distortion of the results by a few outliers, which are rather attributed to systematic errors, e.g. due to residual clouds. As a consequence, outliers are fully included in the computation of the systematic error but get lower weight in the robust determination of the random error, which is interpreted as a measure of the repeatability of measurements.

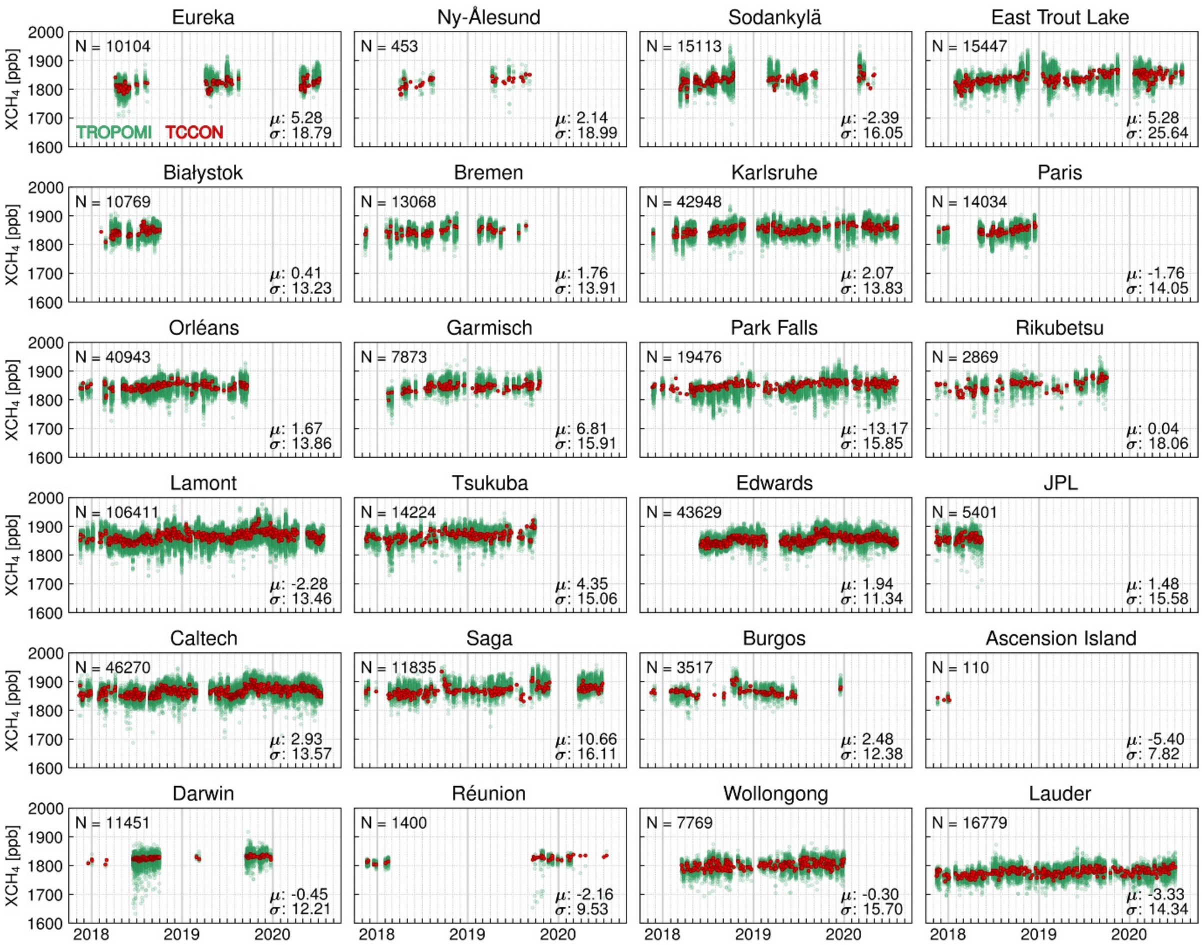

Figure 13: Comparison of the TROPOMI/WFMD v1.2 XCH_4 time series (green) with ground-based measurements from the TCCON (red). For each site, N is the number of collocations, μ corresponds to the mean bias and σ to the scatter of the satellite data relative to TCCON in ppb.

It is also checked whether the respective site biases are sensitive to the selection of the spatial collocation radius, which is an indication of sources within the satellite collocation area with only marginal influence on the TCCON measurements itself. A considerable sensitivity was found for XCH_4 at Edwards. The collocation region intersects oil production areas in California's Central Valley (in contrast to Caltech and JPL), as well as the South Coast Air Basin (SoCAB), which has a well-known methane enhancement. As such nearby sources limit the representativity of affected satellite measurements, the collocation radius is reduced to 50 km for Edwards.

The results for the individual sites are condensed to the following parameters for the overall quality assessment of the satellite data: the global offset is defined as the mean of the local biases at the individual sites, the random error is the global scatter of the differences to TCCON after subtraction of the respective regional biases, and the spatial systematic error is the standard deviation of the local offsets relative to TCCON at the individual sites as a measure of the station-to-station biases. For XCH_4 the global offset amounts to 0.75 ppb, the random error is 14.13 ppb, and the spatial systematic error is given by 4.52 ppb. The seasonal systematic error is defined as the standard deviation of the four overall seasonal offsets (using all sites combined after subtraction of the respective local offsets) relative to TCCON and amounts to 0.85 ppb. The spatio-temporal systematic error (defined as the the root-sum-square of the spatial and seasonal systematic errors) amounts to 4.60 ppb, which is on the order of the estimated (station-to-station) accuracy of the TCCON of about 3.5 ppb.

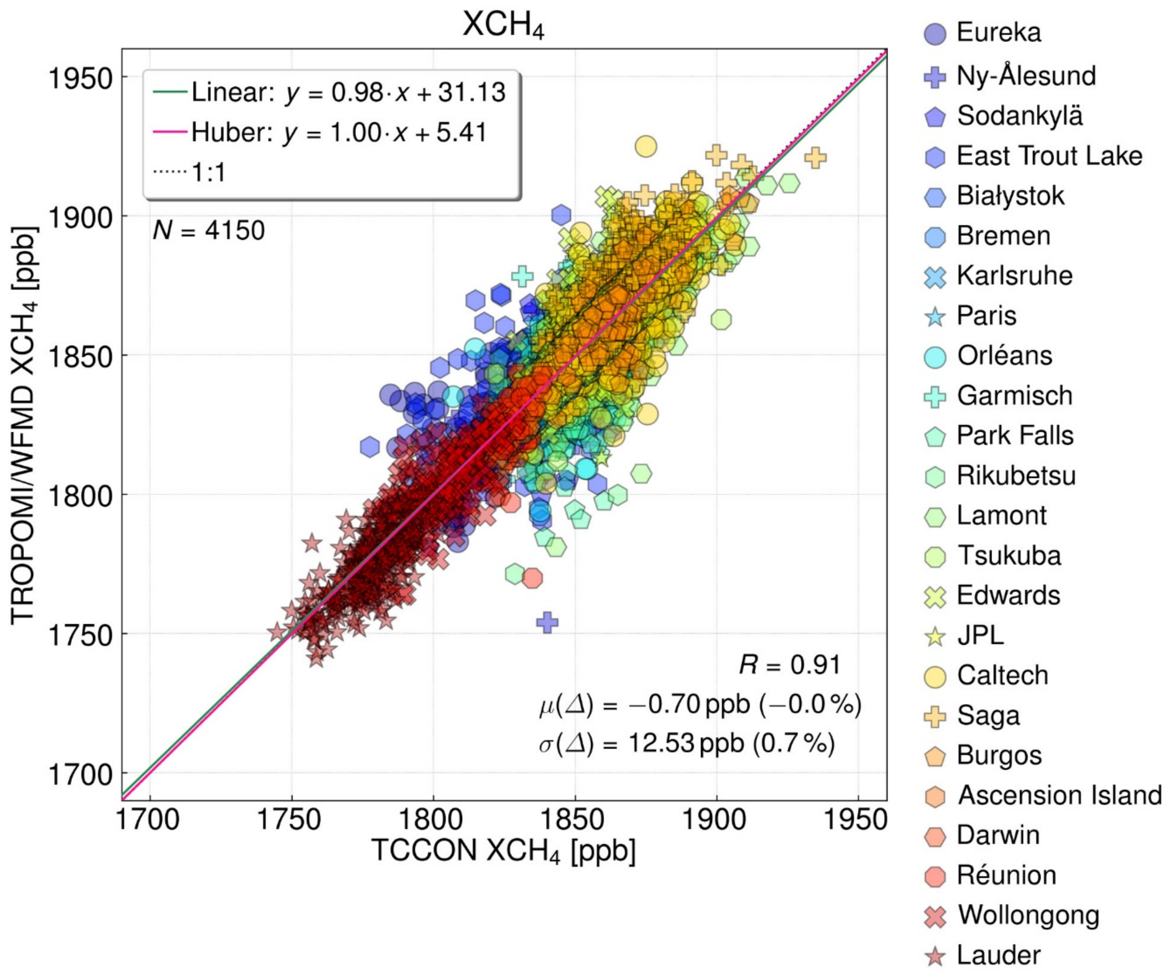

Figure 14: Comparison of the TROPOMI/WFMD data to the TCCON based on daily means. Specified are the linear regression results and the correlation of the data sets, as well as the mean and standard deviation of the difference. To analyse the impact of outliers, the regression is also performed for the Huber linear regression model, which is robust to outliers.

To further analyse how well the real temporal and spatial variations are captured by the TROPOMI data, Figure 14 shows a comparison to TCCON based on daily means for days with more than three collocations. The obvious linear relationship with a high correlation of $R = 0.91$ underlines the typical good agreement of the satellite and validation data.

There are a few outliers where the satellite values are considerably lower than the TCCON values. These occasional instances are not site specific and can probably be ascribed to days with residual or partial cloud cover interfering with the satellite retrievals. Outliers with higher values compared to TCCON are dominated by collocations at high latitude sites during the first months of 2019 and may be attributable to Arctic polar vortex air potentially causing the following related issues: associated fronts of different air masses may complicate the identification of collocations near the vortex edge and/or the stratospheric part of the methane profiles may be largely affected by the polar vortex leading to a considerable deviation from the assumed apriori profile shapes. It is verified that the impact of outliers on the regression is marginal by repeating the fit with the Huber linear regression model, which is robust to outliers and provides similar results to the standard linear regression here.

To analyse the stability, we use comparisons with the TCCON since the start of the routine operations phase of Sentinel-5P. To assess the long-term drift stability, a robust Huber regression of the monthly mean differences relative to the reference (using all data combined after subtraction of the respective regional offsets) with time is used. The resulting stability estimate is -0.01 ppb/year.

The validation results can be summarized as follows:

The natural XCH_4 variations are well captured by the satellite data. We find a random error of the TROPOMI data of 14.13 ppb (0.8%), while the spatio-temporal systematic error of the satellite data of 4.60 ppb (0.2%) is comparable to the station-to-station accuracy of the TCCON. There is no significant long-term drift in the TROPOMI/WFMD v1.2 methane data set.

4. Comparison of SWIR XCH4 TROPOMI products

In this section the XCH_4 data products are inter-compared over regions world-wide that are challenging for the CH_4 retrieval (SRON, Sect. 4.1) and over target regions (IUP-UB, Sect. 4.2 and Sect. 4.3). Over challenging regions, the products from IUP-UB (WFMD) and the scientific SRON S5P-RemoTeC TROPOMI data product are inter-compared (Section 4.1). Over target regions, the XCH_4 data products from IUP-UB (WFMD) and the operational S5P TROPOMI product are intercompared (Sect. 4.2) as well as the IUP-UB (WFMD) product and the scientific SRON S5P-RemoTeC TROPOMI product version 14_14 (referred to as “OPERbeta”).

If not stated otherwise the XCH_4 data after correction is used (variable ‘xch4’ for the WFMD product and ‘xch4_corrected’ for the SRON product). Both WFMD and SRON product apply a correction to the retrieved XCH_4. In the scientific SRON S5P-RemoTeC TROPOMI product this correction is based on the retrieved surface albedo and it is based only on TROPOMI data, so it is independent of any reference data (Lorente et al., 2021). In the WFMD product the correction uses a machine learning approach based on random forest that makes use of several variables (retrieved albedo and cloud parameter, strong H2O absorption radiance, SZA, and a XCH_4 climatology, among others (see Schneising et al. (2019)). In the SRON product, a strict filtering is applied in order to achieve maximum accuracy and precision, and to avoid errors due to unaccounted light path modifications by small scatterers. Another difference between the two products is that SRON provides XCH_4 data only over clear-sky scenes in version 14_14, which was the product version available when the intercomparison was done. A specific intercomparison for measurements over ocean is presented using version 18_17 of the SRON scientific product in Sect. 4.1.4.

4.1. Comparison of SRON and IUP-UB products for challenging regions for the retrieval performed by SRON

Regions world-wide where identified that are challenging from the point of view of CH_4 retrieval. These regions are listed in Table 3 covering scenes with occasional snow cover, as well as high and low surface albedos. The regions are discussed individually in the following subsections. For the inter-comparison of the data products, we calculated global monthly averaged maps on spatial resolution of 0.1° x 0.1° not accounting for the individual coverage of the two XCH_4 retrievals from SRON and IUP-UB. However, for line plots and correlations plots we only considered data where both products show valid XCH_4 values.

Table 3: Target regions as used for the comparisons conducted by SRON for challenging regions for the retrieval.

Region	Location	Relevance	Version
Canada/ Russia High latitudes	Lat.: 90N, 50N Lon: 180W, 180 E	Albedo contrast for low albedo	SRON v14_14 WFMD v1.2

		Snow covered scenes	
Australia	Lat.: 11 S, 39 S Lon: 113 E, 155 E	Albedo contrast for low albedo and albedo-aerosol interaction	SRON v14_14 WFMD v1.2
Sahara/North Africa	Lat.: 0, 35N Lon.: 20W, 40E	High albedo scenes not covered by ground-based stations	SRON v14_14 WFMD v1.2
Ocean		Sun-glint measurements over ocean are challenging due to low signal	SRON v18_17 WFMD v1.2

4.1.1. Comparison results for Canada/Russia

We selected a region in the higher Northern Hemisphere covering a broad range of longitudes including Canada and Russia that is characterized by a low surface albedo retrieved in the short-wave infrared spectral range. Due to the low signal over these scenes, any scattering effect on the light path can lead to errors in the retrieved XCH_4 which allows to test how both XCH_4 retrievals perform under this difficult sensing situation.

Lorente et al. (2021) found by validation with TCCON measurements that the SRON-RemoTeC retrieval for low surface albedo scenes tends to underestimate the real atmospheric XCH_4 column. To account for this error a dedicated posteriori correction of the XCH4 level 2 product was developed that corrects for the signal dependent bias of the retrieval and is independent of any reference data. By validation of the SRON RemoTeC S5P XCH_4 with TCCON retrievals and by inter-comparison with GOSAT satellite measurements it was shown that this posteriori correction of the XCH4 level 2 data product can correct the bias for low albedo scenes (see. Fig 6 in Lorente et al. (2021)).

Figure 15 shows XCH_4 measured by TROPOMI as retrieved by SRON and WFMD, as well as their ratio, the retrieved surface albedo (by SRON), and the correlation plot for the month of July 2018. For scenes where the surface albedo is low (e.g., over Russia, Figure 15d) SRON XCH_4 is higher than WFMD XCH_4. Before the correction applied in the SRON XCH_4 product, the bias between SRON and WFMD XCH_4 is -24.6 ± 21.5 ppb, and after correction this bias is reduced to 0.6 ± 21.4 ppb (Figure 15e). The posterior correction increases SRON XCH_4 over low albedo scenes to correct for the underestimation of the retrieved XCH_4. The correlation of the bias between SRON and WFMD with surface albedo is reduced after the posterior correction (Pearson’s correlation number reduces from 0.3 to 0.1).

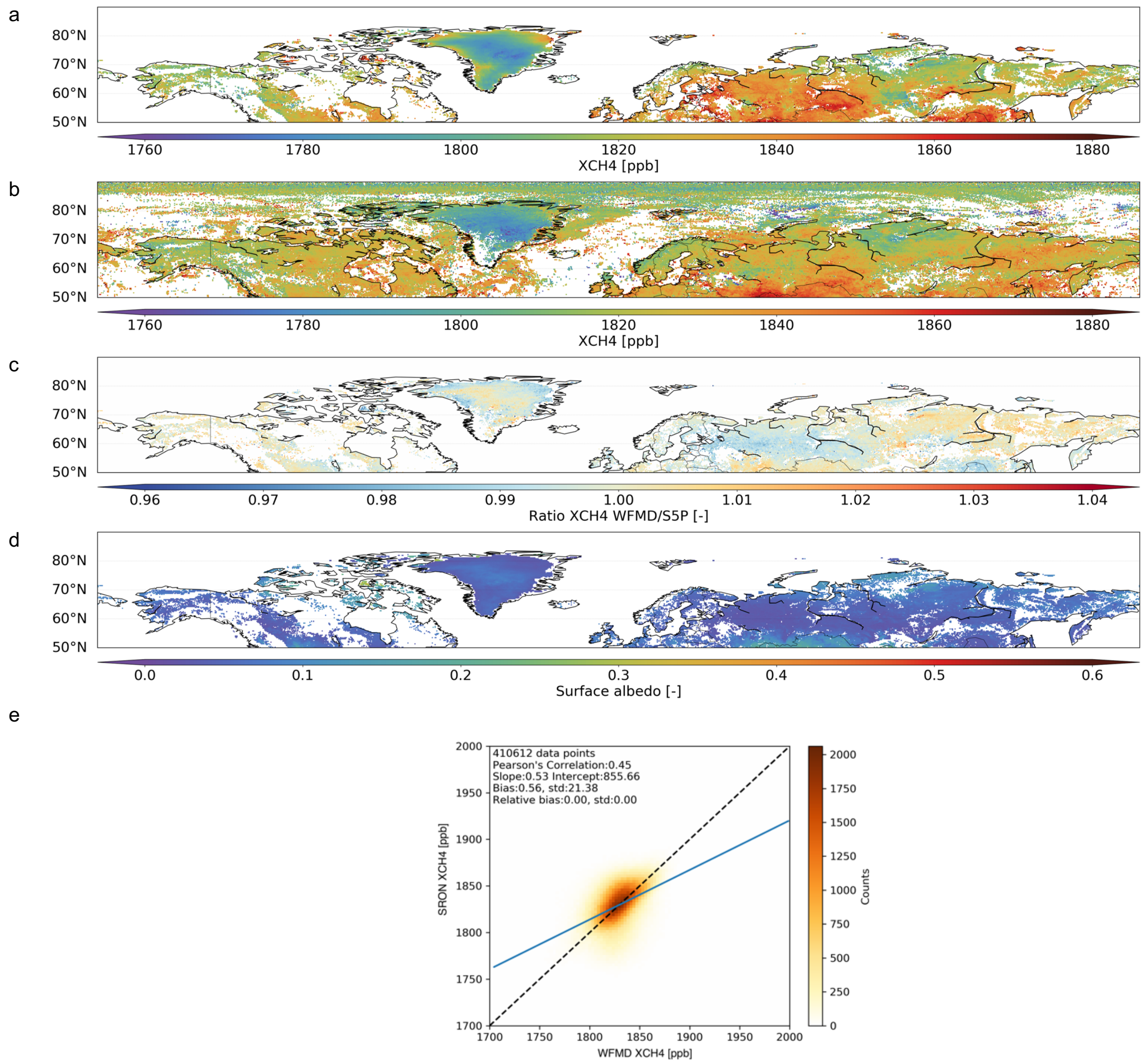

Figure 15: TROPOMI XCH_4 retrieved by (a) SRON, (b) WFMD and (c) the ratio between WFMD and SRON. (d) Surface albedo as retrieved by the SRON-RemoTeC S5P retrieval, (e) correlation plot between WFMD and SRON XCH_4 for the month of July 2018.

4.1.2. Comparison results for Australia

Australia was selected as a further example for a challenging retrieval region because it covers a wide range of surface albedos. Here, interference error between retrieval parameters describing the scattering (e.g., aerosols) and the surface albedo can lead to biases in retrieved XCH_4 values.

Figure 16 shows the SRON and IUP-UB (WFMD) XCH_4 products for the month of January 2019 over Australia. For this specific month, the bias between the two products is -7.9 ± 9.5 ppb, with XCH_4 retrieved by WFMD higher than the SRON product. The differences have a weak correlation with surface albedo (r = 0.14), with WFMD product being lower than the SRON product (blue areas on Figure 16c) over areas with relatively high albedo. Before the correction, each of the XCH_4 products has a positive correlation with the retrieved surface albedo (r = 0.6 for WFMD and r = 0.4 for SRON), which becomes lower after correction (r = -0.3 for WFMD and r = 0.2 for SRON).

Figure 17 shows the monthly mean of XCH_4 for each product and the bias between SRON – WFMD with its standard deviation. Both products follow a similar seasonality in the distribution of XCH4 over Australia (Figure 17a), so both capture correctly the geophysical variation of XCH_4. The bias is negative (WFMD XCH_4 higher than SRON) for the complete time period, and increases with time (Figure 17b).

One of the difficulties in the retrieval related to scattering errors is found over the north-western part of Australia, where there is a correlation of XCH_4 enhancements with the retrieved scattering properties in the SRON product. A zoom-in over this area (Figure 18) in the comparison with WFMD shows quite a significant variability of both products, as well as an enhancement in the aerosol optical thickness (SRON) and cloud parameter (WFMD) over this area. Please note that these two parameters are not equivalent but they can be considered as a proxy for atmospheric scattering processes.

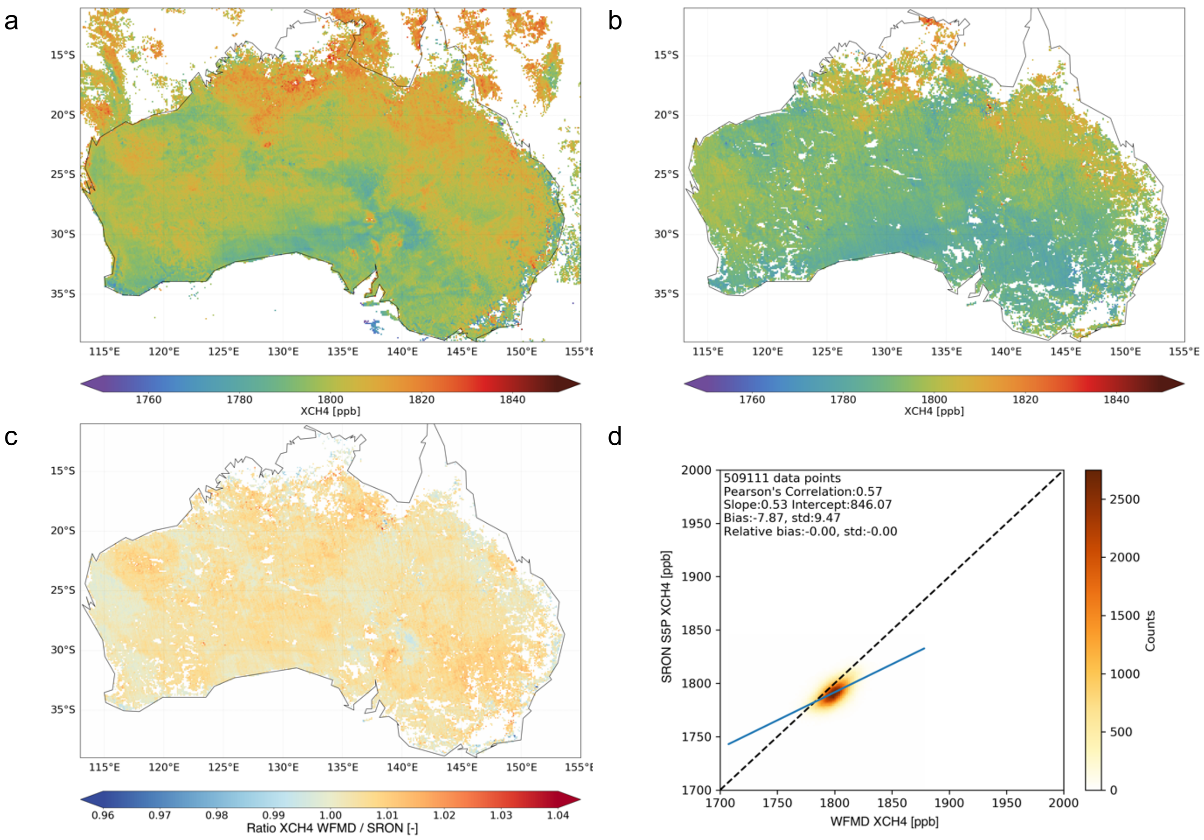

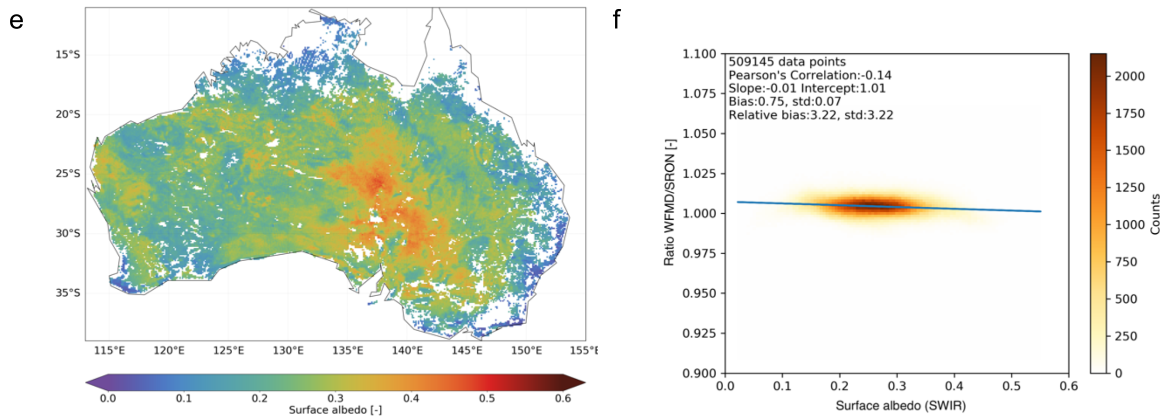

Figure 16: TROPOMI XCH4 retrieved by (a) IUP-UB with WFMD (b) SRON with the scientific S5P RemoTeC algorithm, WFMD/SRON XCH4 (a) ratio, (d) correlation, (e) retrieved SWIR surface albedo and (f) WFMD/SRON XCH4 ratio as a function of surface albedo over Australia for the period 1 Jan 2019 - 31 Jan 2019.

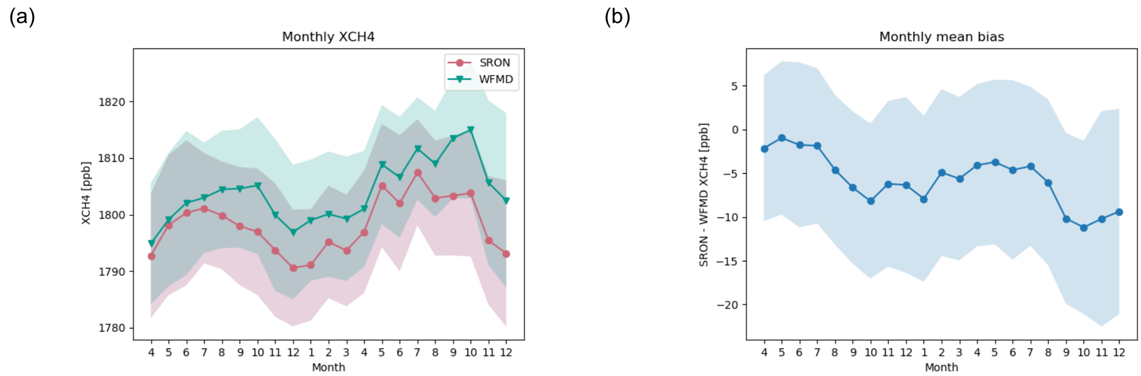

Figure 17 (a) Monthly mean XCH4 retrieved by SRON (red) and WFMD (green) with the 1-sigma standard deviation represented by the shadowed areas and (b) monthly mean bias SRON – WFMD XCH4 and its standard deviation represented by shadowed area over Australia starting on April 2018.

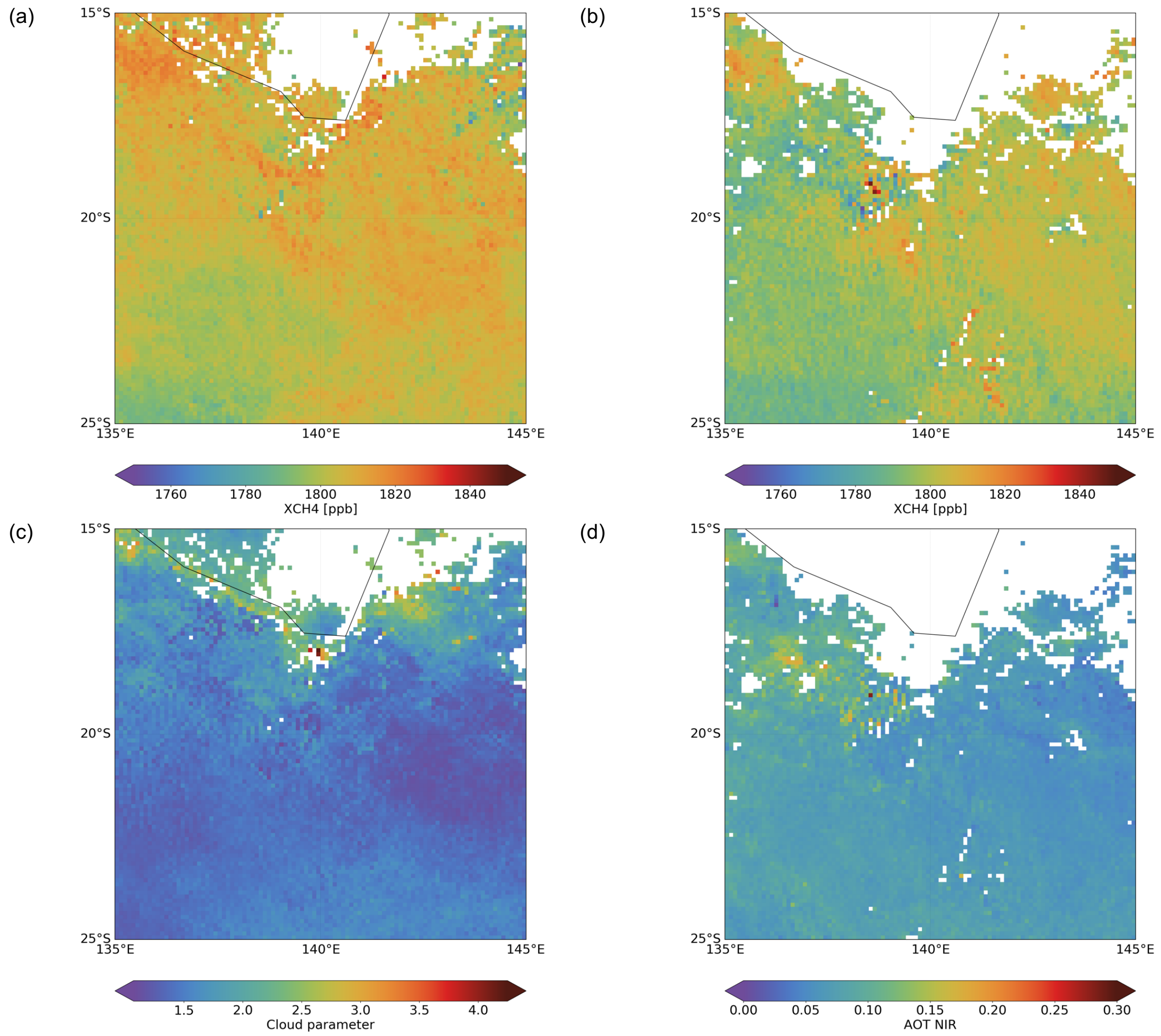

Figure 18: Monthly mean XCH_4 retrieved by (a) WFMD and (b) SRON, (c) cloud parameter in the WFMD product and (d) aerosol optical thickness in the near-infrared retrieved by SRON.

4.1.3. Comparison results for North Africa

A region with very high surface albedos in the SWIR is the Sahara Desert in Africa. However, the validation of the XCH_4 retrieval is limited here since the TCCON network is not covering this region with ground-based measurements. Hence, to assess the data quality of the TROPOMI XCH_4 retrievals over scenes with high surface albedo, satellite inter-comparison is needed, e.g., using XCH4 retrievals from measurements of the GOSAT satellite as shown in Section 2.2.

Figure 19 shows the comparison between SRON and WFMD XCH_4 over North Africa for January 2019. Both products capture enhancements around the 5N-10N latitudinal band and lower XCH_4 values over the desert areas. For this specific month, the mean bias is -9.95 ± 18.76 ppb, overall WFMD XCH_4 being higher than the SRON XCH_4 (red areas in the ratio plot in Figure 19c). Both products capture the seasonal variation of the XCH_4 distribution as shown by Figure 20. January and February 2019 are the months when the bias between the two products is higher for this specific region, where SRON retrieves a stronger decrease in XCH_4 than WFMD.

Over this area both WFMD and SRON XCH_4 show a correlation with surface albedo before the correction is applied to each of the products, with higher XCH_4 retrieved for high surface albedo scenes. This effect is corrected for by the posterior correction that is applied in both products. Thus, the bias between SRON and WFDM does not depend on surface albedo (Figure 19f).

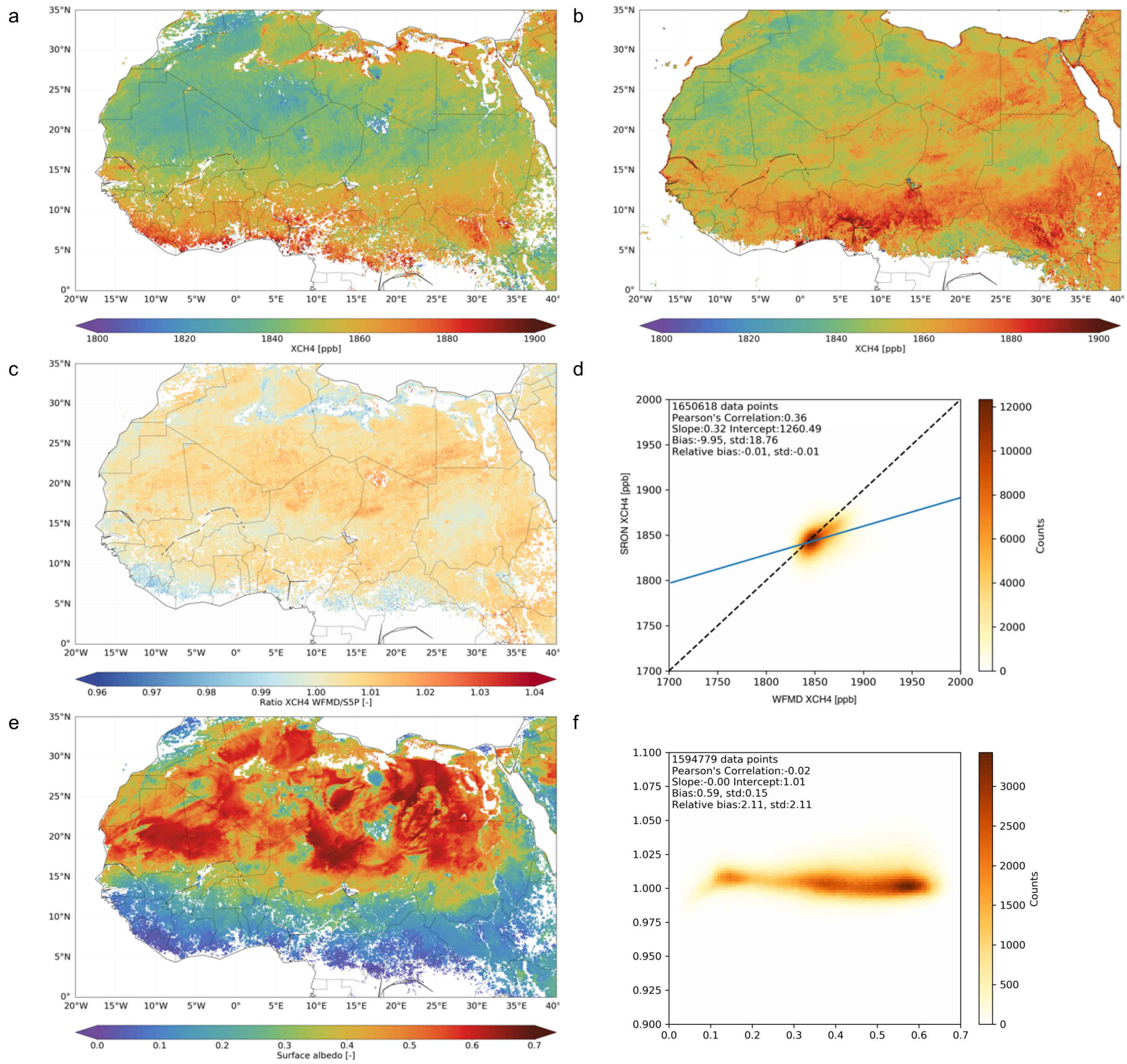

Figure 19: TROPOMI XCH_4 retrieved by (a) IUP-UB with WFMD (b) SRON with the scientific S5P RemoTeC algorithm, WFMD/SRON XCH_4 (a) ratio, (d) correlation, e) SWIR surface albedo retrieved by SRON and (f) WFMD/SRON XCH4 ratio as a function of surface albedo over Australia for the period 1 Jan 2019 - 31 Jan 2019.

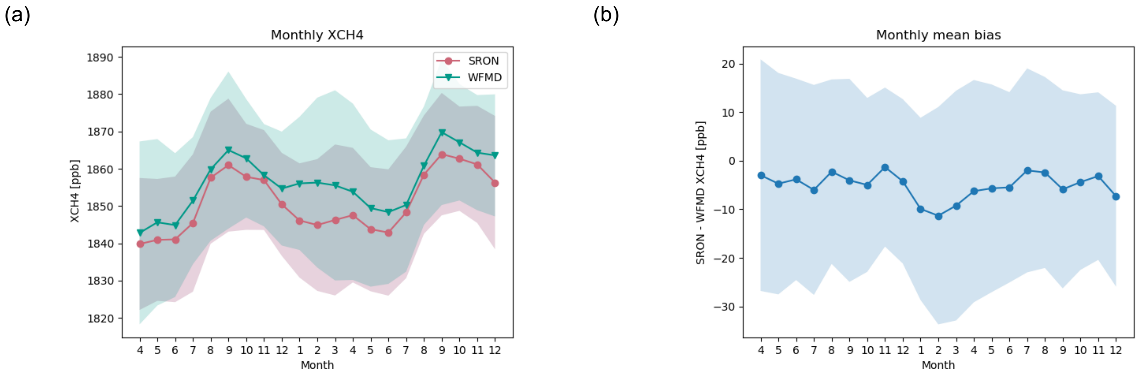

Figure 20: (a) Monthly mean XCH_4 retrieved by SRON (red) and WFMD (green) with the 1-sigma standard deviation represented by the shadowed areas and (b) monthly mean bias SRON – WFMD XCH_4 and its standard deviation represented by shadowed area over North Africa starting on April 2018.

4.1.4. Comparison results for ocean measurements

The SRON scientific XCH_4 product version 18_17 includes retrievals for measurements over ocean performed under sun-glint geometries. In this section we perform a comparison of this product with WFMD XCH_4 product v1.2 f or measurements over ocean.

Figure 21 shows XCH_4 over oceans retrieved with SRON S5P-RemoTec scientific algorithm version 18_17 (Figure 21a) and with WFMD algorithm v1.2 (Figure 21b). The bias is -2.4 ± 27.8 ppb, and the correlation plot is shown in Figure 21d. One of the main differences of the two products is that WFMD retrieves XCH_4 also out of the sun-glint area over the ocean, i.e., at latitudes greater than 60 degrees. Around the Equator and at mid-latitudes a difference in coverage is also visible. This is because of the strict cloud filtering applied in the SRON product to minimize errors due to scattering.

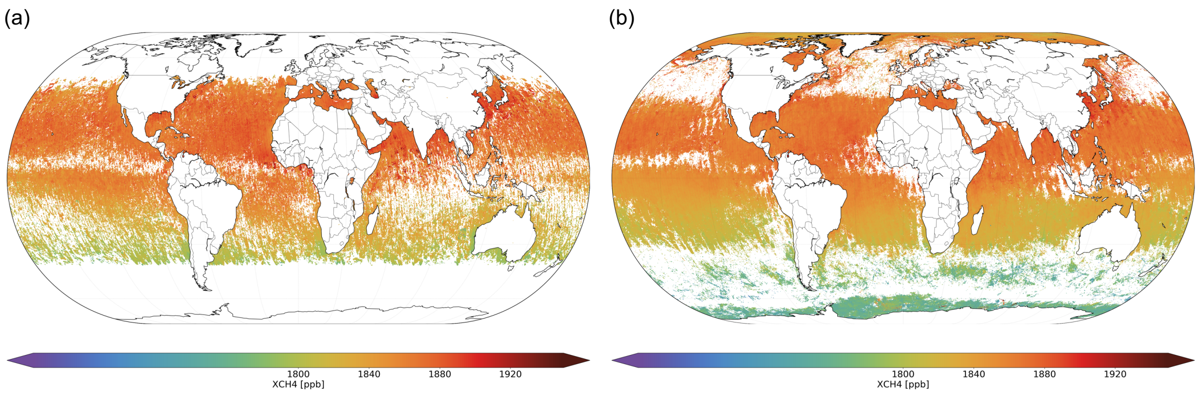

(c)

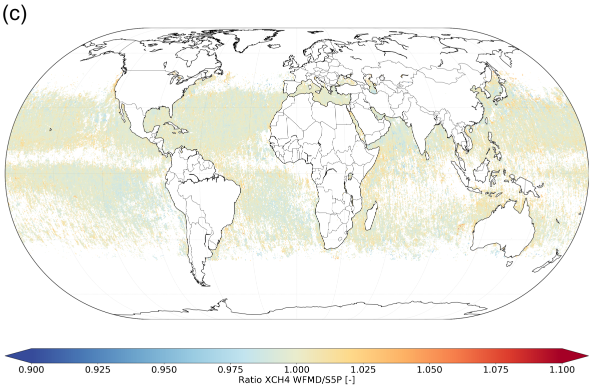

(d)

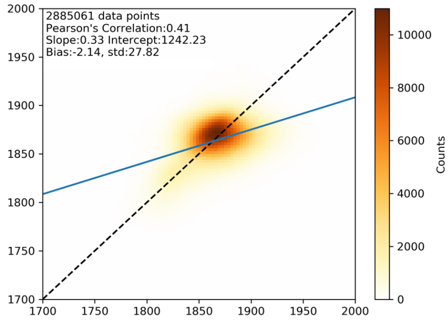

Figure 21: Average XCH_4 for 2020 retrieved by (a) SRON S5P-RemoTeC scientific algorithm version 18_17 and by (b) WFMD algorithm, (c) the ratio of both and (d) correlation plot.

4.2. Comparison of SRON and IUP-UB products performed by IUP on target regions

IUP-UB focussed on detailed comparisons for three target regions, which are listed in Table 4.

Table 4: Target regions as used for the comparisons conducted by IUP-UB.

Region ID	Region	Comments
TGD	Galkynysh and Dauletabad gas and oil fields, Turkmenistan	Mainly anthropogenic methane sources (natural gas, oil, …). See also Buchwitz et al., 2017; Schneising et al., 2020.
CAL	California, Central Valley and surrounding area, USA	Mainly anthropogenic methane sources (natural gas, oil, cattle, …). See also Buchwitz et al., 2017.
SSU	South Sudan	Mainly methane sources (wetlands), e.g., Lunt et al., 2019.

In the following sub-sections, the comparison results for these target regions are presented and discussed.

4.2.1. Result for target region TGD (Turkmenistan gas and oil fields)

Figure 22 shows a comparison for target region TGD for 10-April- 2018. Figure 22 (a) shows comparisons of TROPOMI XCH_4 product WFMD version 1.2 (Schneising et al., 2019) with the operational product ("OPER") version 01.02.02 (Hu et al., 2016) using the recommended quality filter (qa_value (here simply referred to as qa)) qa > 0.5. The top left figure shows the WFMD product and the top right map shows the OPER product. The width of the colour scales is the same for both figures (± 40 ppb) but the centre value differs and corresponds to the mean XCH_4 value for the shown scene. As can be seen, this mean value is 1860 ppb for WFMD and 1853 for OPER, i.e., OPER is lower by 7 ppb on average. The difference is however not constant but shows a spatial structure, as shown in the bottom left map. The bottom right scatter plot shows the correlation between the two (Level 2) data products along with some numerical values which quantify the comparison: Ncoloc (= 3718) is the number of collocated ground pixels, Nwfmd (= 7050) is the number of WFMD pixels and Noper (= 3718) is the number of OPER pixels. The correlation coefficient R is 0.86 indicating that the spatial pattern are well correlated. The mean difference (DIFF) OPER-WFMD is -7.96 ppb and the standard deviation (STD) of the difference is 6.96 ppb. Below the two top figures numerical values for "$DXCH_4$" are listed (in blue). $DXCH_4$ is the maximum XCH_4 value (corresponding to a single ground pixel) minus the median of the scene.

Figure 22 (b) shows the same comparison but for relaxed quality filtering (qa > 0.1) of the OPER product. Here Noper is higher (= 4851), DIFF (= -7.82 ppb) is slight less negative and STD (= 7.32) is slightly larger.

Figure 23 shows the corresponding results but for 8-May-2018 and Figure 24 for 4-June-2018.

The conclusions for these overpasses/days over target region TGD are similar as for 10-April-2018 shown in Figure 22. The coverage (or number of ground pixels) is better for WFMD compared to OPER even if the quality filtering for OPER is relaxed (qa > 0.1). The pattern of OPER-WFMD XCH4 differences is complex and on average OPER is lower compared to WFMD but the magnitude is not constant in time: the difference is -17.75 ppb for 8-May-2018 and -0.93 ppb on 4-June-2018. Despite these differences, the XCH4 spatial pattern are "similar" as also shown by the correlation coefficients R (~0.55 for 8-May-2018 and ~0.76 for 4-June-2018).

Figure 25 shows how the two data sets compare when averaging (gridding) all data for the period January – October 2018 (using a grid cell size of 0.1°x0.1°). All three XCH4 maps (top row and bottom left) show two areas of elevated methane around a longitude of 61.5°E and between 36.0°N and 37.5°N corresponding to the Galkynysh and Dauletabad gas and oil fields in Turkmenistan. The WFMD-OPER difference map (Figure 25 bottom right) shows a complex pattern but no large difference in the area corresponding to these gas fields and their surrounding area. This indicates that the difference between these two data products does not depend significantly on the (retrieved) atmospheric methane concentration, which is important in order to reliably obtain methane emission information from these data sets.

Figure 26 shows a comparison of the TROPOMI XCH_4 products WFMD and OPER (qa > 0.5, i.e., default quality filtering) for each day (overpass) during the period beginning of January 2018 to end of October 2018 for target region TGD. Shown are time series and corresponding mean values for 5 quantities:

- The XCH_4 difference OPER-WFMD (ΔXCH_4):
    - The low bias of OPER relative to WFMD is only present until beginning of May 2018, i.e., during the S5P commissioning phase. Afterwards, i.e., during the operational phase starting early May 2018, both data sets agree well (on average) within a few ppb
- The standard deviation of ΔXCH_4: 9.36 ppb on average with only little day-to-day variations
- The linear correlation coefficient: R is typically 0.67 indicating reasonable correlation of the daily spatial pattern
- The ratio of the number of observations: On average WFMD has a factor of 2.35 more observations than the OPER product (for qa > 0.5, i.e., when the recommended quality filter is used for OPER)
- $DXCH_4$, i.e., maximum XCH_4 value (corresponding to a single ground pixel) minus median of the scene: $DXCH_4$ is similar especially after early May 2018,

i.e., after the commissioning phase. The correlation is 0.54 indicating that day-to-day variations are to some extent captured similarly.

Figure 27 shows the corresponding results but using relaxed quality filtering for OPER (qa > 0.1). All results are similar but here the number of WFMD observations is only marginally higher compared to OPER (x1.37 compared to x2.35).

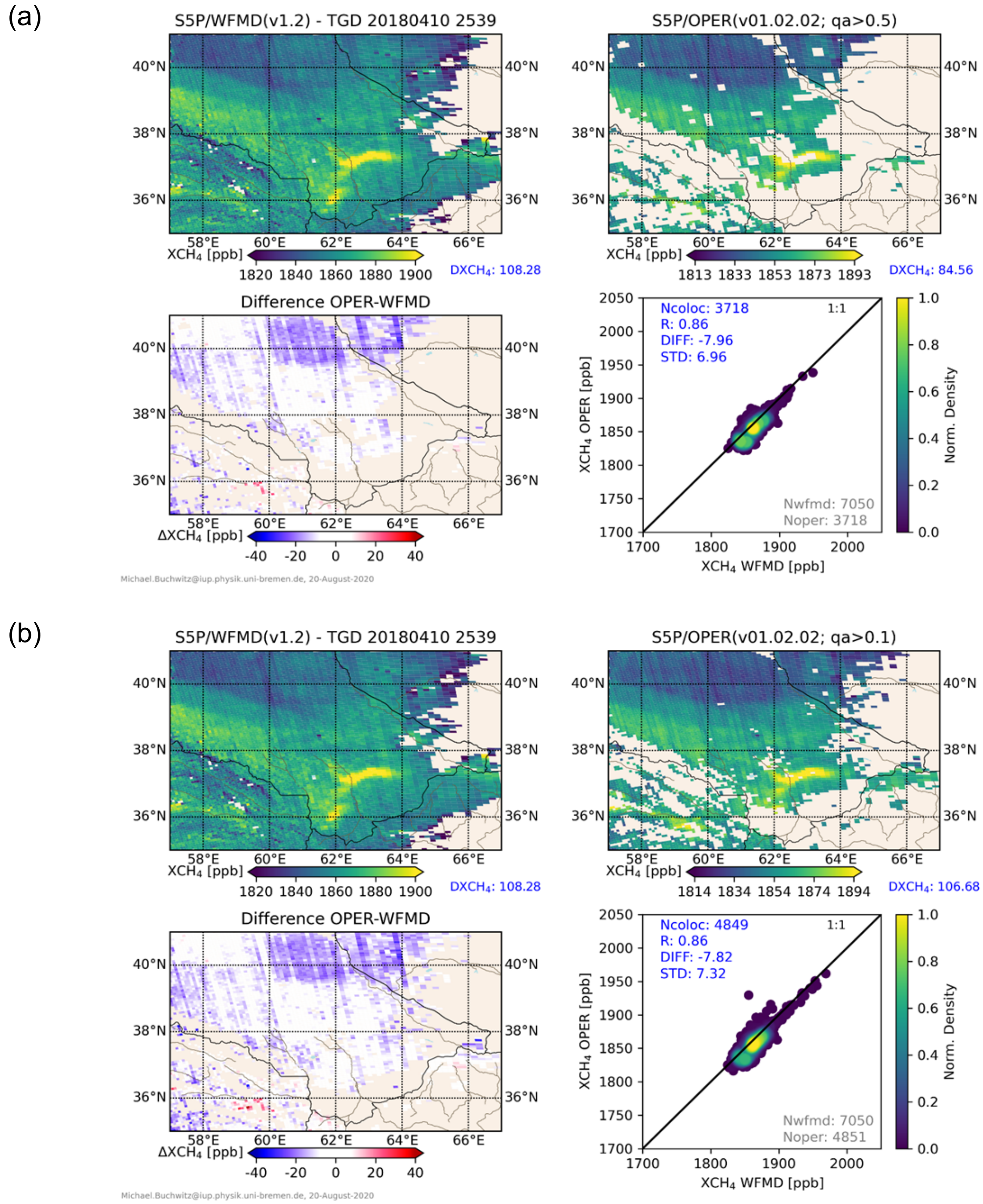

Figure 22: (a) Comparison of TROPOMI XCH_4 data products WFMD (v1.2) and OPER (v01.02.02, qa > 0.5) for target region TGD on 10-April-2018 (see main text for details). (b) Similar as (a) but for OPER with relaxed quality filtering (qa > 0.1).

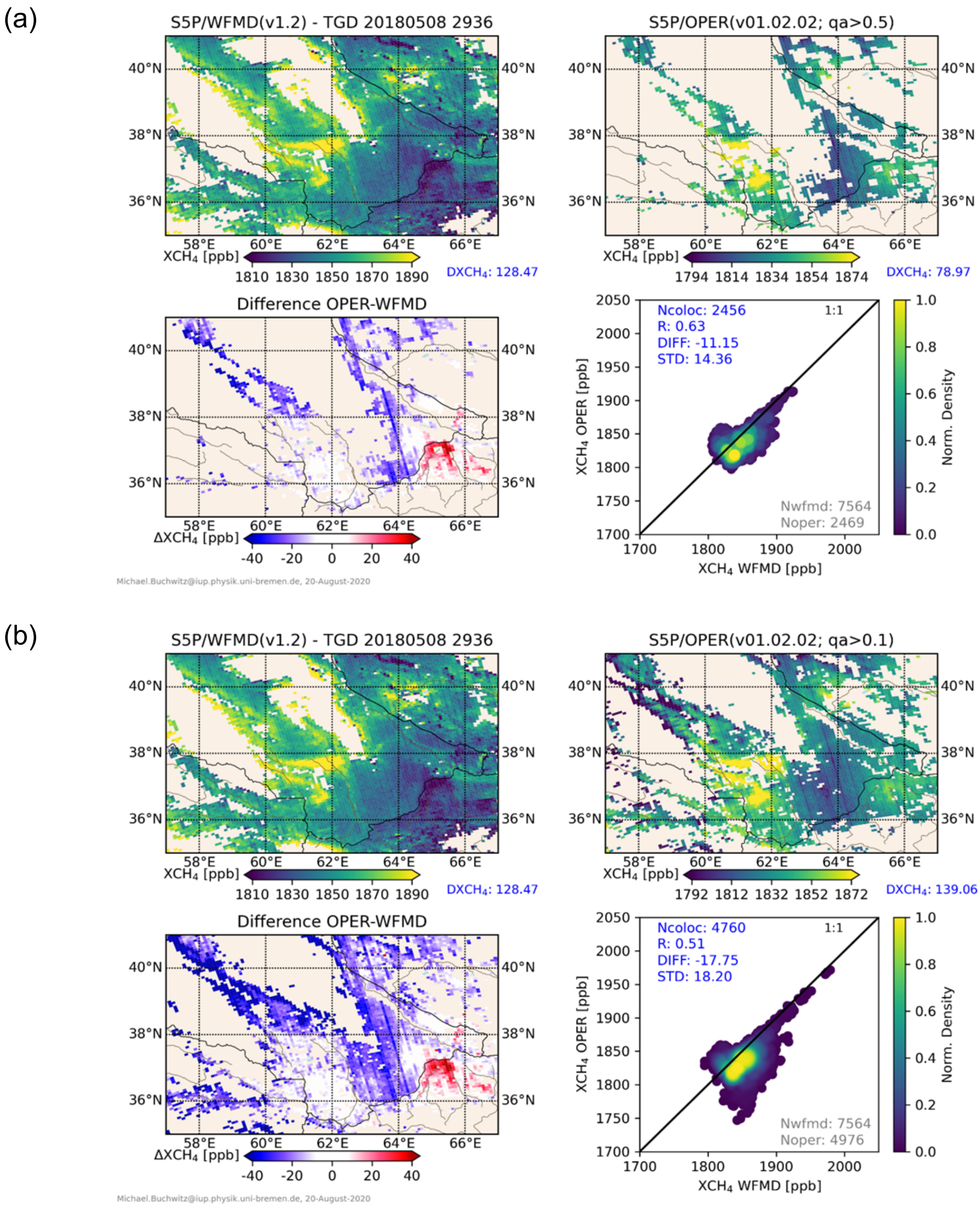

Figure 23: Similar as Figure 22 but for 8-May-2018 (target region TGD).

(a)

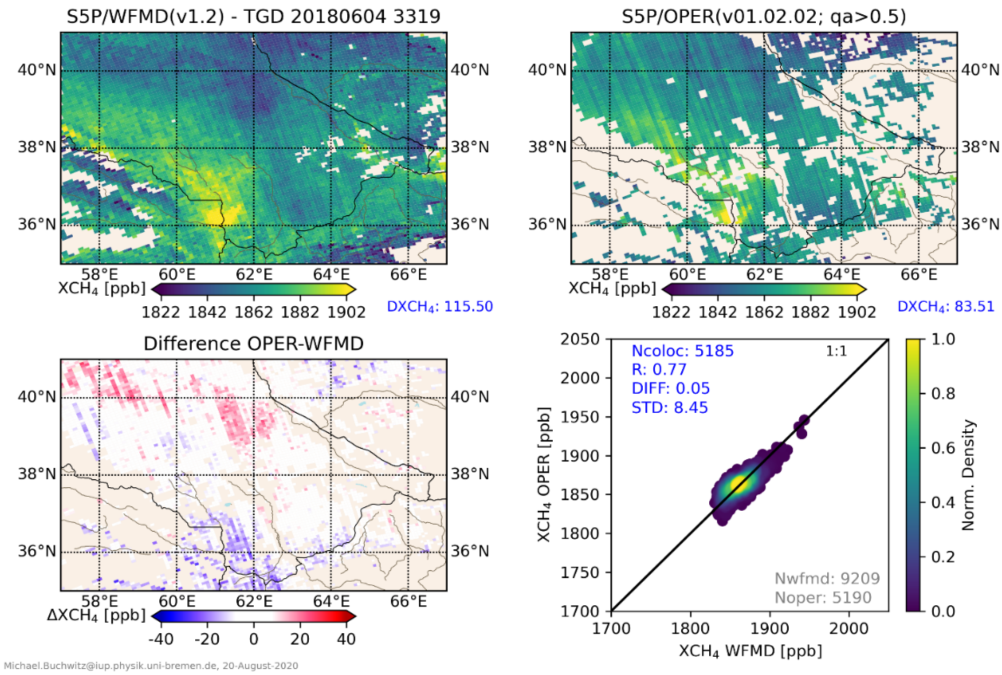

(b)

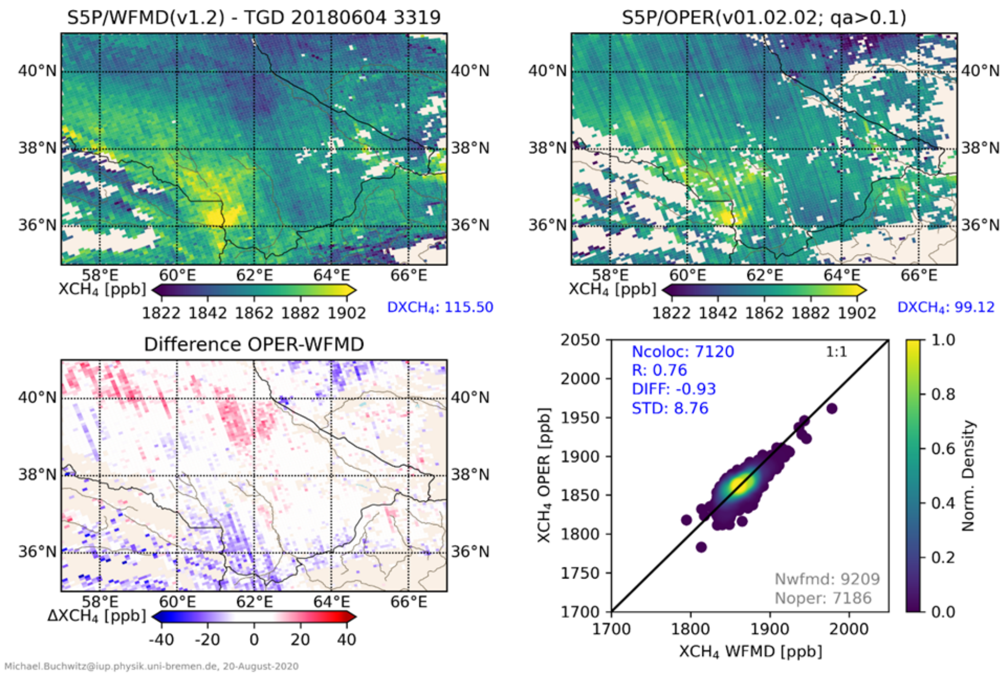

Figure 24: Similar as Figure 22 but for 4-June-2018 (target region TGD).

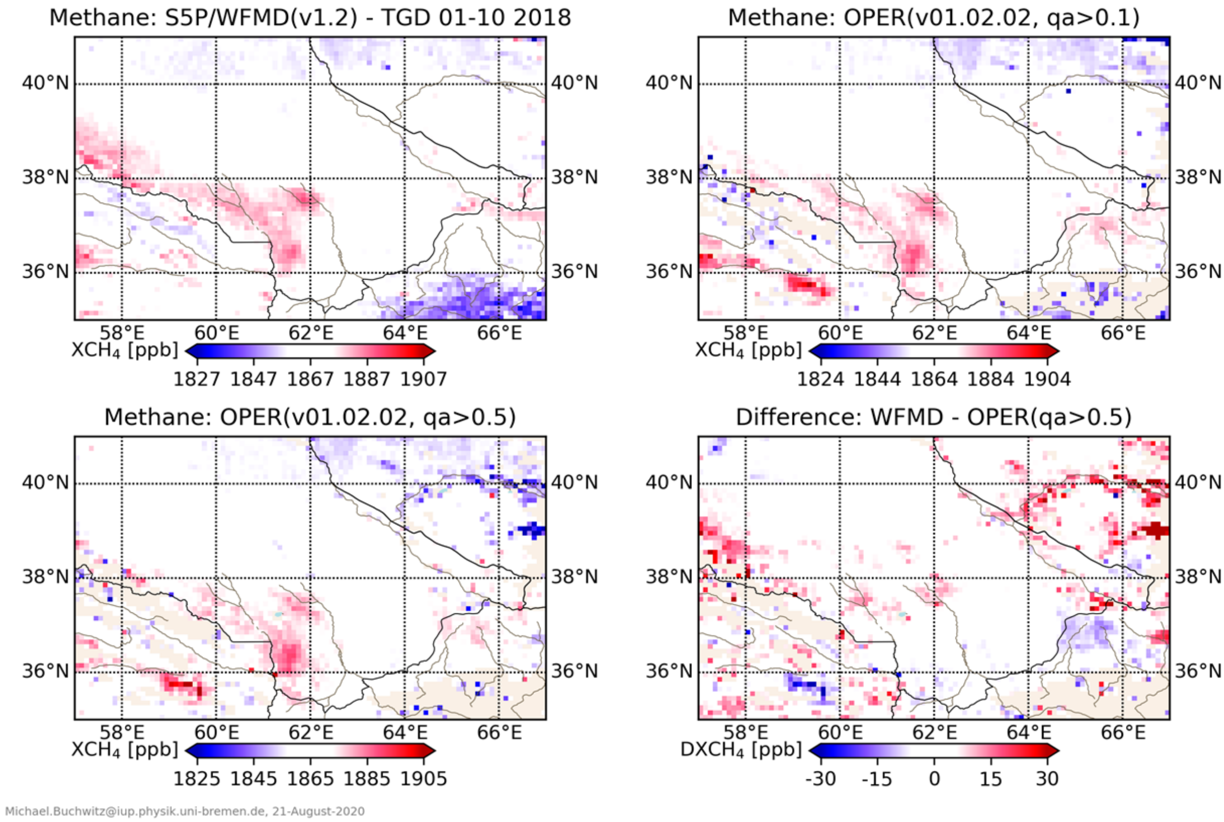

Figure 25: Comparison for target region TGD for temporally averaged data covering the period January to October 2018. Top left: WFMD XCH_4 product. Top right: OPER product with relaxed quality filtering (qa > 0.1). Bottom left: OPER product with recommended (default) quality filtering (qa > 0.5). Bottom right WFMD – OPER (qa > 0.5) XCH_4 difference.

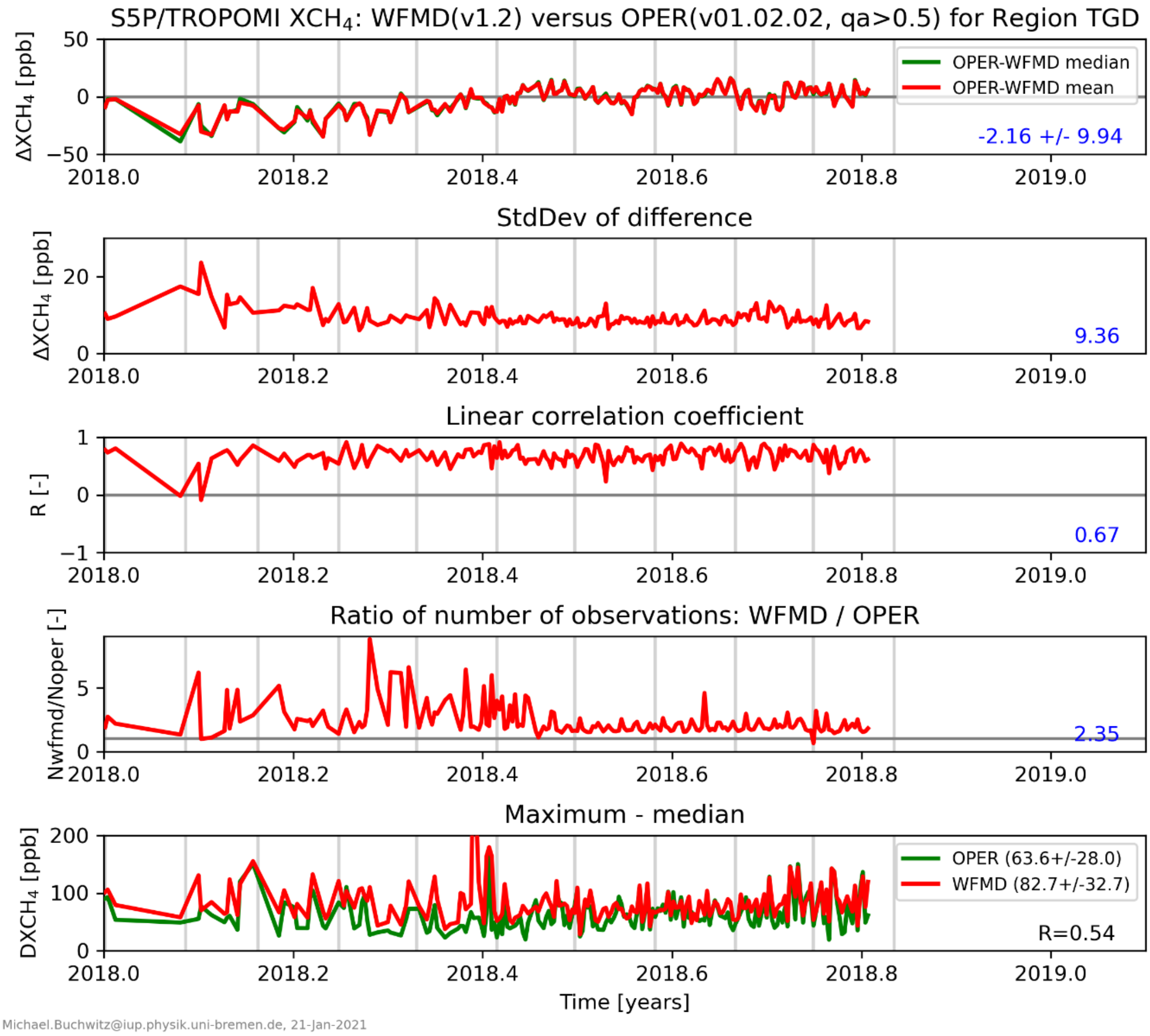

Figure 26: Comparison of TROPOMI XCH_4 products WFMD and OPER (qa > 0.5, i.e., default quality filtering) for each day (overpass) during the period beginning of January 2018 to end of October 2018 for target region TGD. Shown are 5 quantities computed for every TGD overpass. These quantities are (from top to bottom): the XCH_4 difference WFMD-OPER (red: difference of mean values, green: difference of medians), the standard deviation of the difference, the linear correlation coefficient, the ratio of the number of observations, $DXCH_4$, i.e., maximum XCH_4 value (corresponding to a single ground pixel) minus median of the scene (see main text for details). Listed in blue are the corresponding mean values as computed from the presented time series.

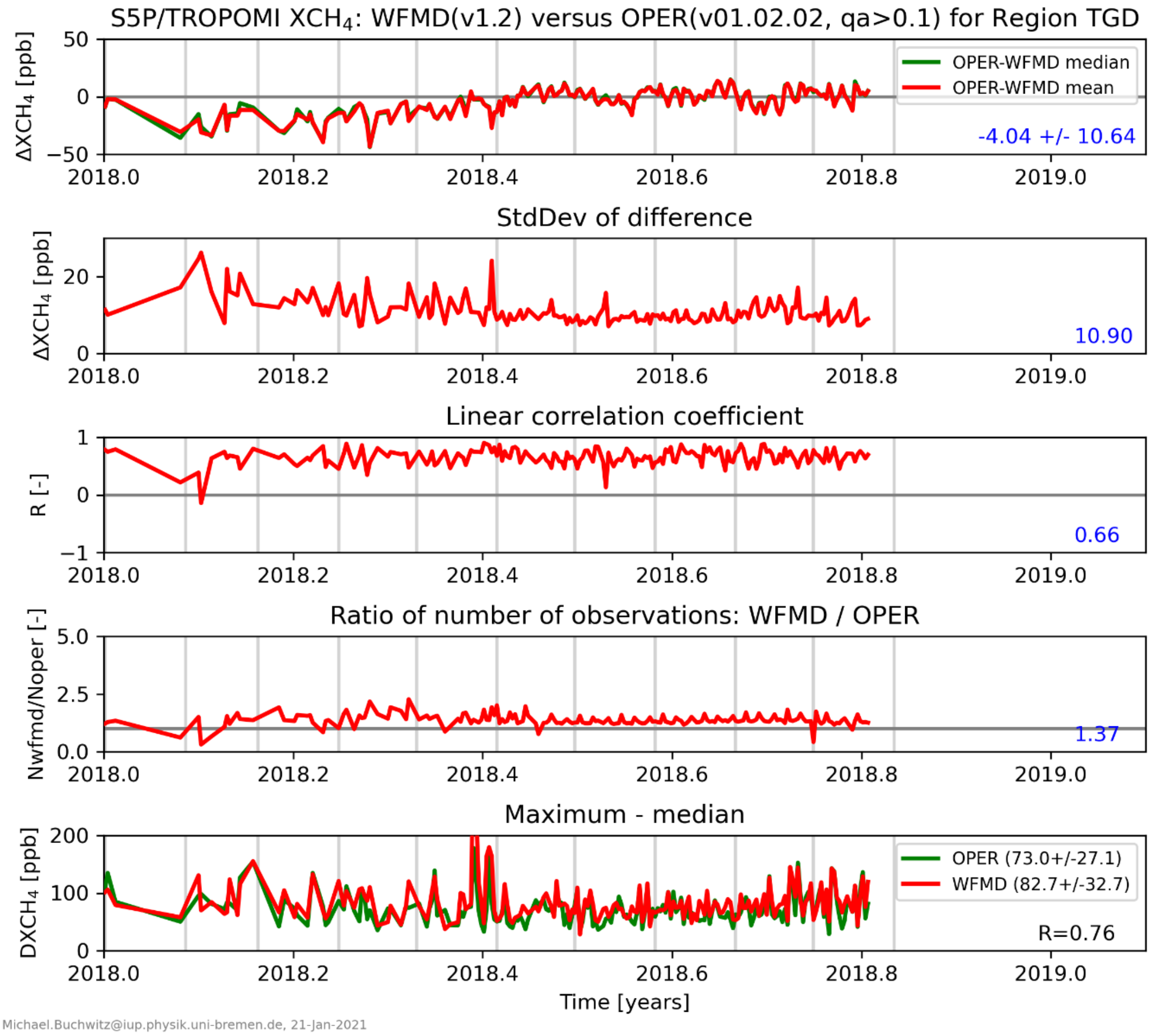

Figure 27: As Figure 26 but for relaxed quality filtering (qa > 0.1) of the OPER product.

4.2.2. Result for target region CAL (California Central Valley)

Figure 28 shows a comparison of spatial maps for target region CAL on 15-October-2018 (the structure of this figure is the same as for Figure 22). As can be seen, the spatial coverage of the OPER product is very sparse compared to WFMD, which is a typical finding for this target area.

Figure 29 shows the corresponding time series. From this figure the following can be concluded:

- XCH_4 difference OPER-WFMD (ΔXCH_4):
  - There is typically a low bias of OPER relative to WFMD until beginning of May 2018, i.e., during the S5P commissioning phase. Afterwards, i.e., during the operational phase starting early May 2018, both data sets agree well (on average) within a few ppb
- Standard deviation of ΔXCH_4: 12.39 ppb on average with only little day-to-day variations
- Linear correlation coefficient: R is typically 0.44 indicating low correlation of the daily spatial pattern
- Ratio of the number of observations: On average WFMD has a factor of 7.81 more observations than the OPER product (for qa > 0.5, i.e., when the recommended quality filter is used for OPER)
- $DXCH_4$, i.e., maximum XCH_4 value (corresponding to a single ground pixel) minus median of the scene: $DXCH_4$ is significantly higher for WFMD. The correlation is only 0.27. This is consistent with the low correlation of the spatial pattern.

Figure 30 shows the corresponding results but using relaxed quality filtering for OPER (qa > 0.1). All results are similar but here the number of WFMD observations is only a factor of 2.44 higher compared to OPER (instead of 7.81 for the default filter).

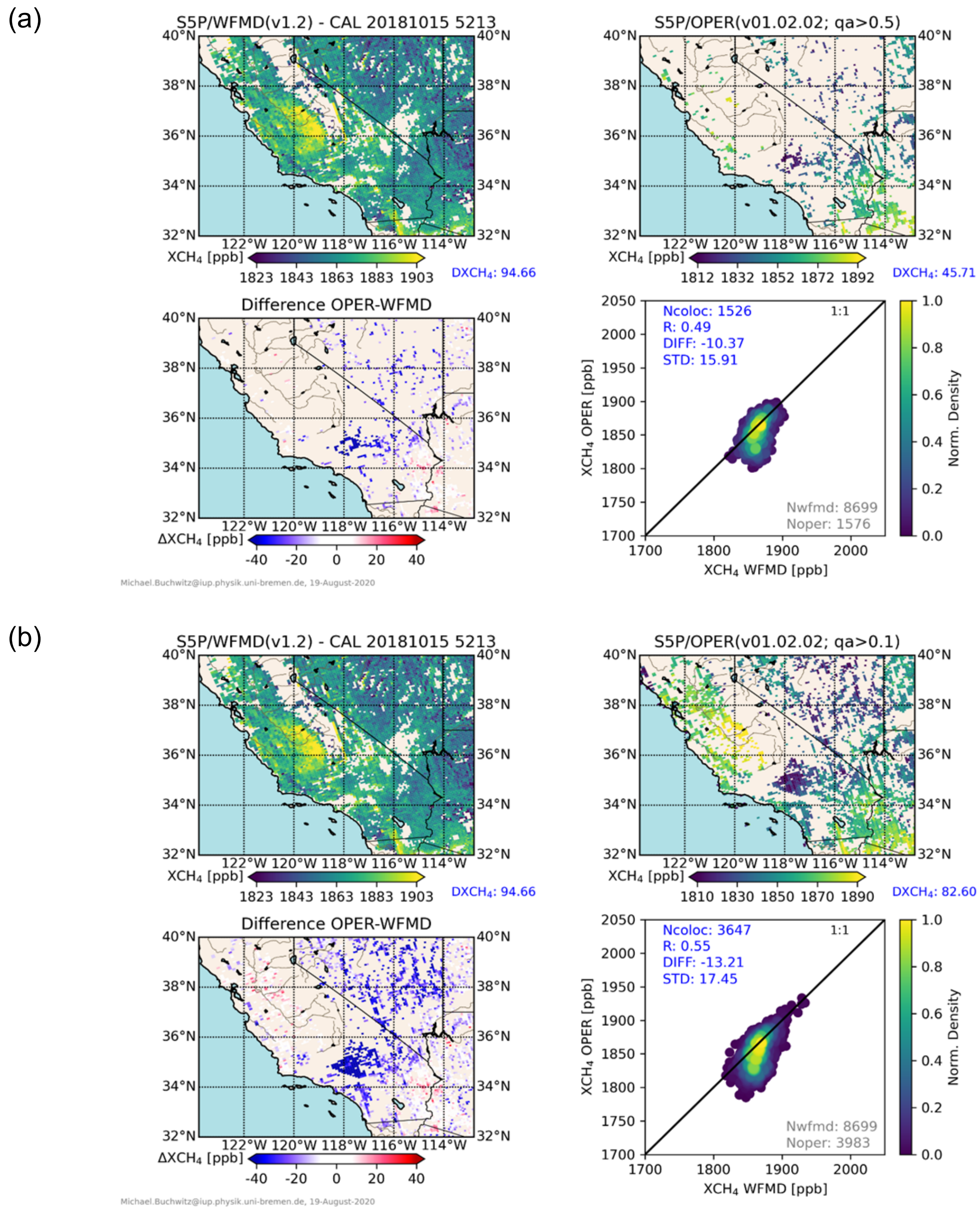

Figure 28: Similar as Figure 22 but for target region CAL and for 15-October-2018.

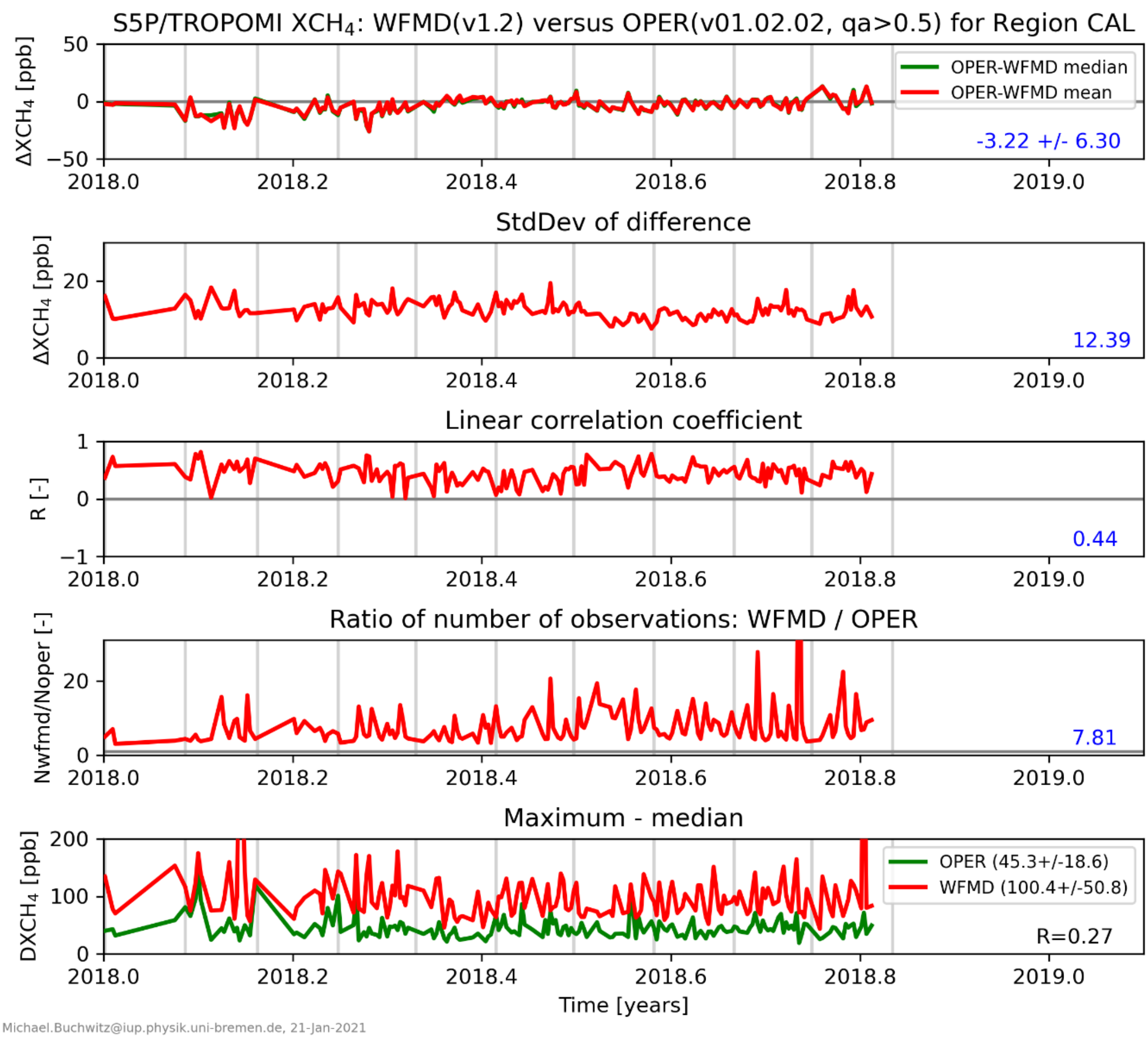

Figure 29: Comparison of TROPOMI XCH_4 products WFMD and OPER (qa > 0.5, i.e., default quality filtering) for each day (overpass) during the period beginning of January 2018 to end of October 2018 for target region CAL. Shown are 5 quantities computed for every overpass. These quantities are (from top to bottom): the XCH_4 difference WFMD-OPER (red: difference of mean values, green: difference of medians), the standard deviation of the difference, the linear correlation coefficient, the ratio of the number of observations, $DXCH_4$, i.e., maximum XCH_4 value (corresponding to a single ground pixel) minus median of the scene (see main text for details). Listed in blue are the corresponding mean values as computed from the presented time series.

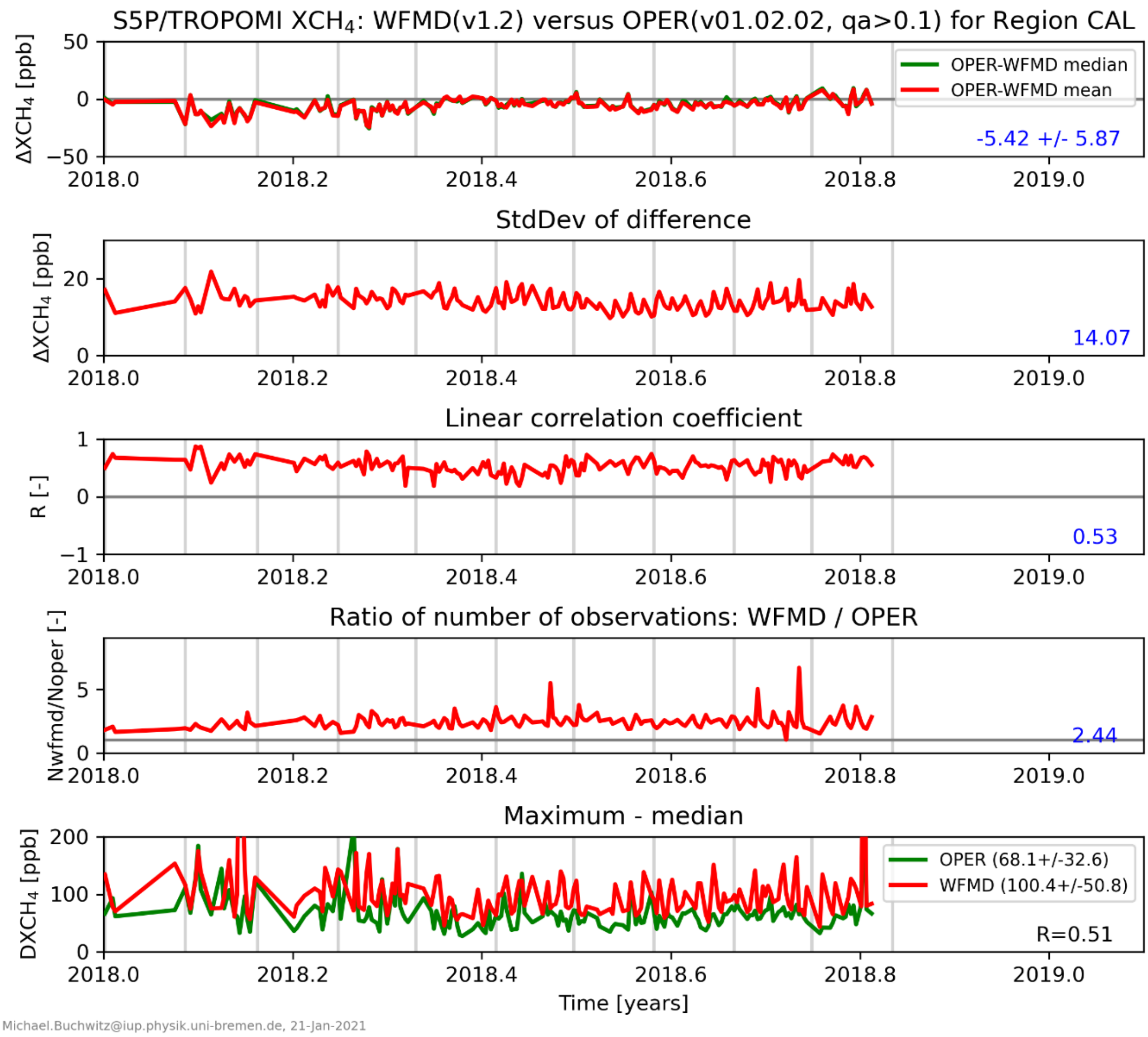

Figure 30: As Figure 29 but for relaxed quality filtering (qa > 0.1) of the OPER product.

4.2.3. Result for target region SSU (South Sudan)

Comparisons of spatial maps for three different days/overpasses are shown in Figure 31 - Figure 33. As can be seen, the spatial coverage of both products is sparse, which is a typical finding for this target region.

Figure 34 shows the corresponding time series. From this figure the following can be concluded:

- XCH_4 difference OPER-WFMD (ΔXCH_4):
    - There is typically a slight low bias of OPER relative to WFMD especially until beginning of May 2018, i.e., during the S5P commissioning phase. Afterwards, i.e., during the operational phase starting early May 2018, both data sets agree well (on average) within a few ppb.
- Standard deviation of ΔXCH_4: 11.90 ppb on average with only marginal day-to-day variations
- Linear correlation coefficient: R is typically 0.67 indicating significant correlation of the daily spatial pattern
- Ratio of the number of observations: On average WFMD has a factor of 4.56 more observations than the OPER product (for qa > 0.5, i.e., when the recommended quality filter is used for OPER)
- $DXCH_4$, i.e., maximum XCH_4 value (corresponding to a single ground pixel) minus median of the scene: $DXCH_4$ is typically higher for WFMD. The correlation is only 0.09.

Figure 35 shows the corresponding results but using relaxed quality filtering for OPER (qa > 0.1). All results are similar but here the number of OPER and WFMD observations is similar (there are 7% less observations of WFMD on average).

Figure 36 shows how the two data sets compare when averaging (gridding) all data for the period January – October 2018 (using a grid cell size of 0.1^ox0.1^o). The three XCH_4 maps (top row and bottom left) show similar large-scale pattern with typically higher values at higher latitudes and lower values at lower latitudes. At smaller scales there are however significant differences. The bottom left map for the OPER product with default filtering (qa > 0.5) shows a region of elevated methane at 30^oE and 5^oN-10^oN corresponding to a South Sudan wetland region (see, e.g., Lunt et al., 2019). This feature is also visible in the top right figure showing the OPER product with relaxed filtering (qa > 0.1) but here large parts of the surrounding area also show elevated methane. In the WFMD product this feature is much less pronounced. The OPER product with relaxed filtering shows a strong low bias covering the entire region of the Lake Victoria (33_oE, 2^oS) which is likely due to a retrieval artefact. That this feature does not appear in the filtered product shows that the filter works very well in this case.

To better isolate spatial XCH_4 anomalies, Figure 37 shows the same maps as also shown in Figure 36 but here daily anomalies have been averaged rather than absolute

XCH_4 values. The method used to compute these maps is essentially the method described in Hakkarainen et al., 2019, which has also been used in Buchwitz et al., 2020, and is referred to as DAM (Daily Anomalies via (latitude band) Medians). This method removes large-scale variations of the XCH_4 "background". As can be seen, the South Sudan wetland region appears to be better visible in the anomaly maps and the elevated methane is higher for the OPER products compared to the WFMD products. That indicates that very likely (depending on inversion method) the OPER product would yield higher wetland emissions compared to the WFMD product.

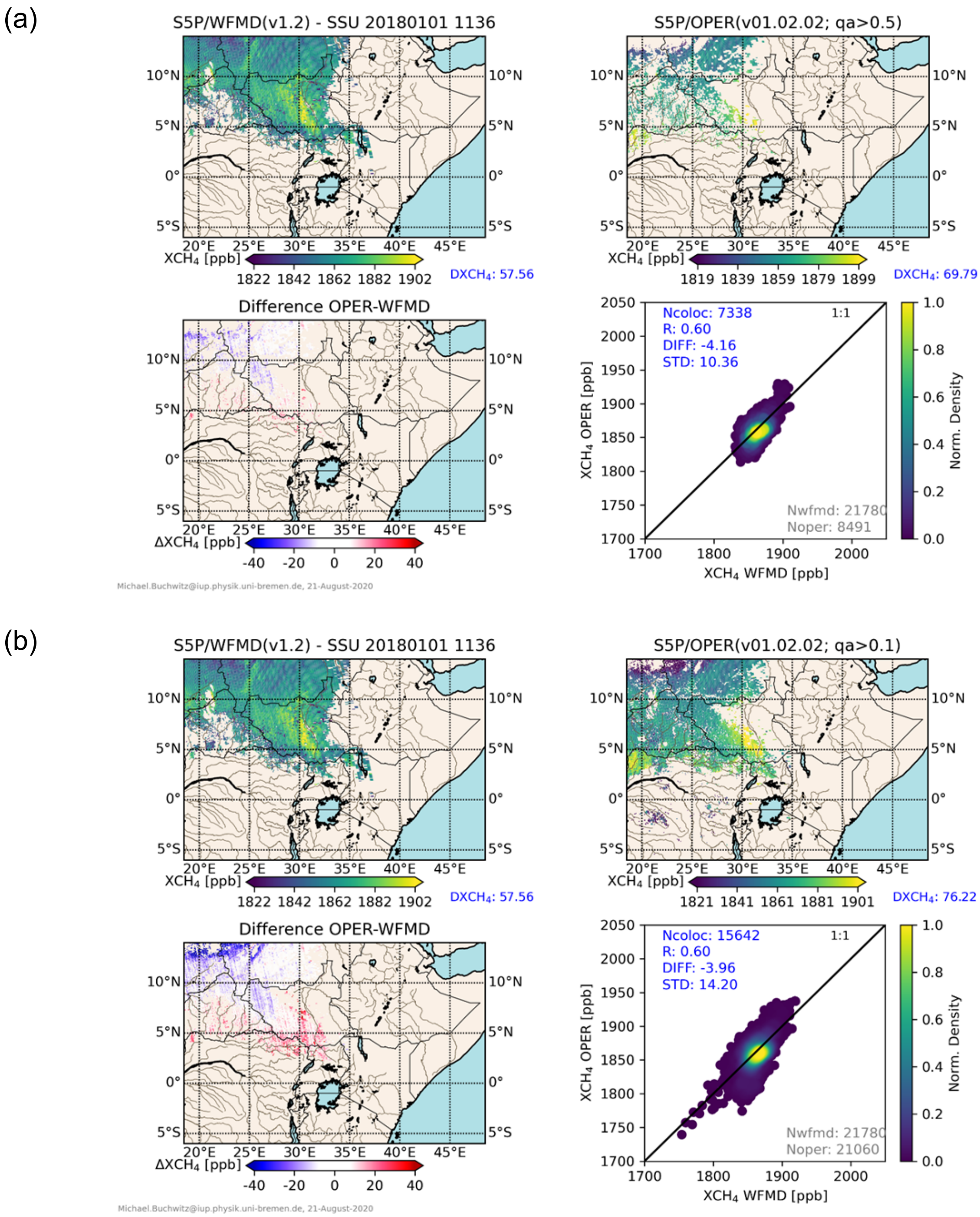

Figure 31: Similar as Figure 22 but for target region SSU on 1-January-2018.

(a)

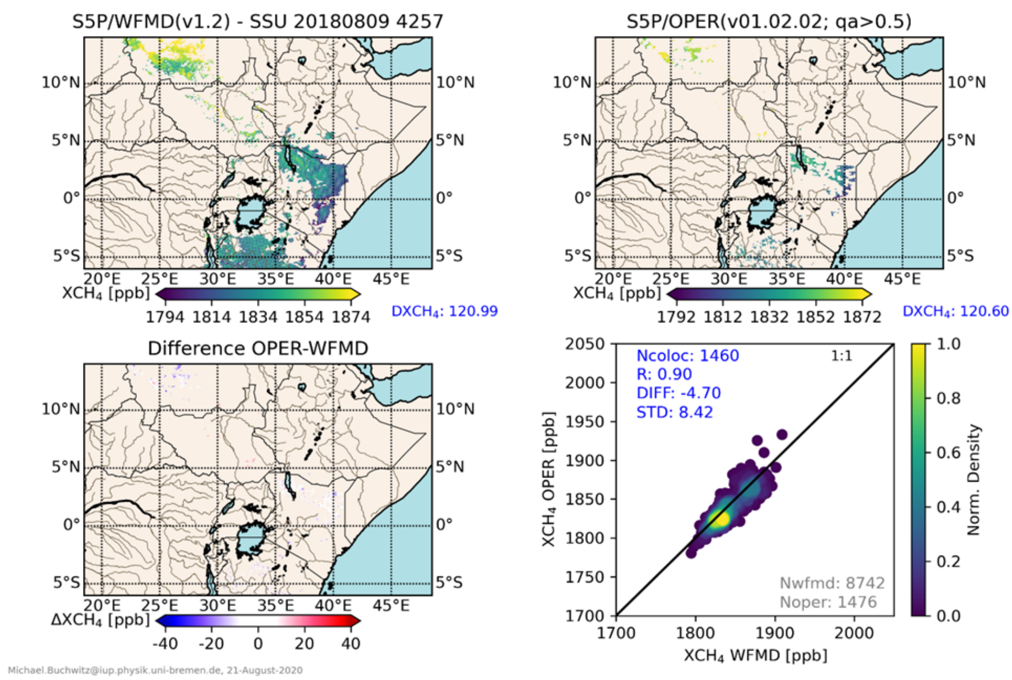

(b)

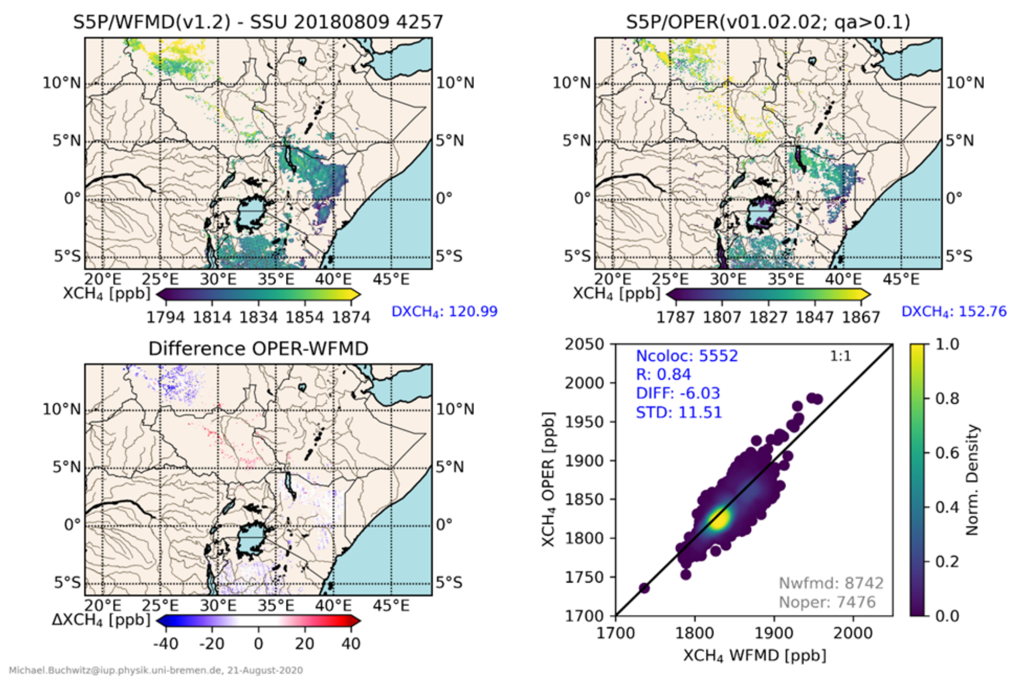

Figure 32: Similar as Figure 31 but for 9-August-2018.

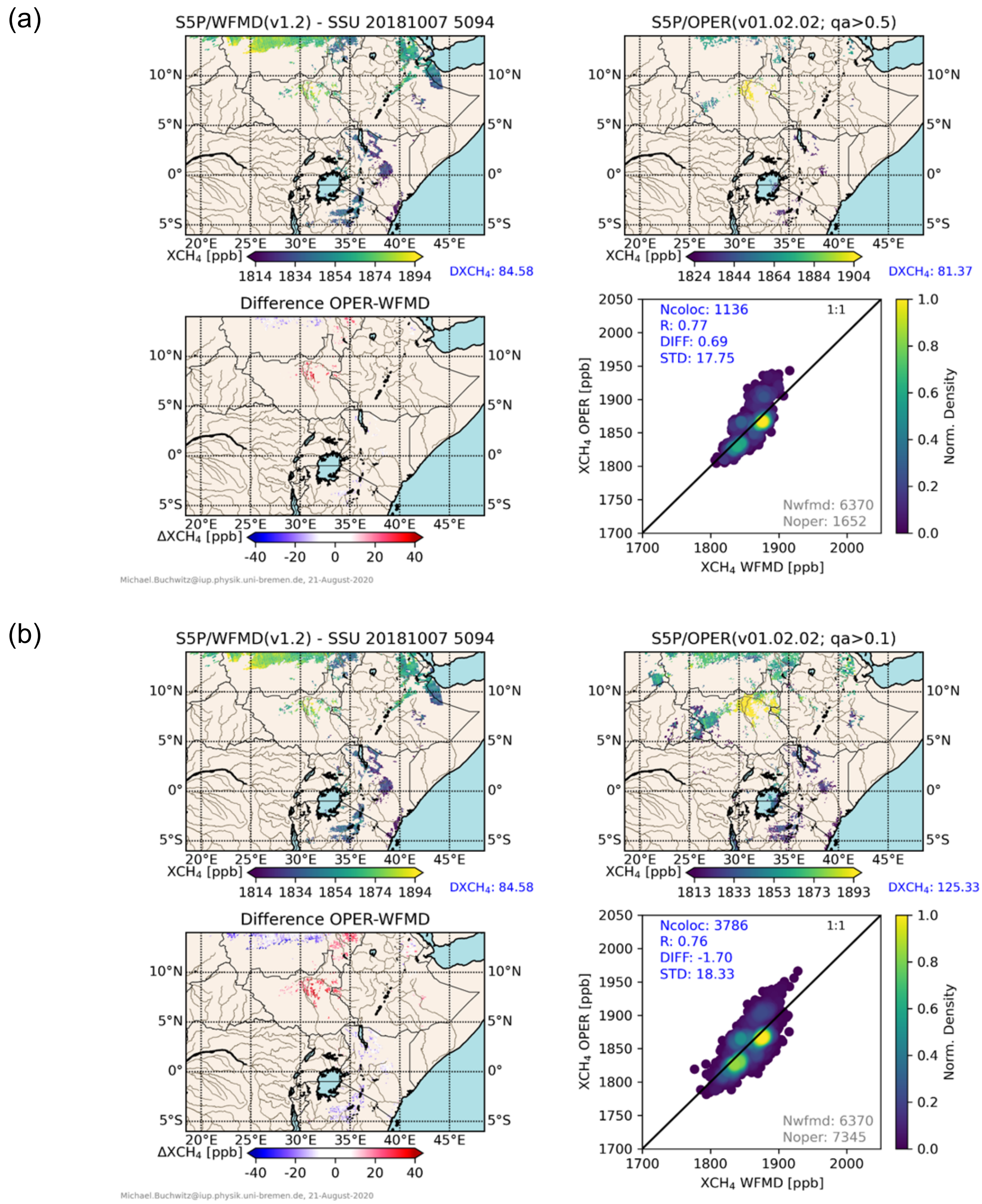

Figure 33: Similar as Figure 31 but for 7-October-2018.

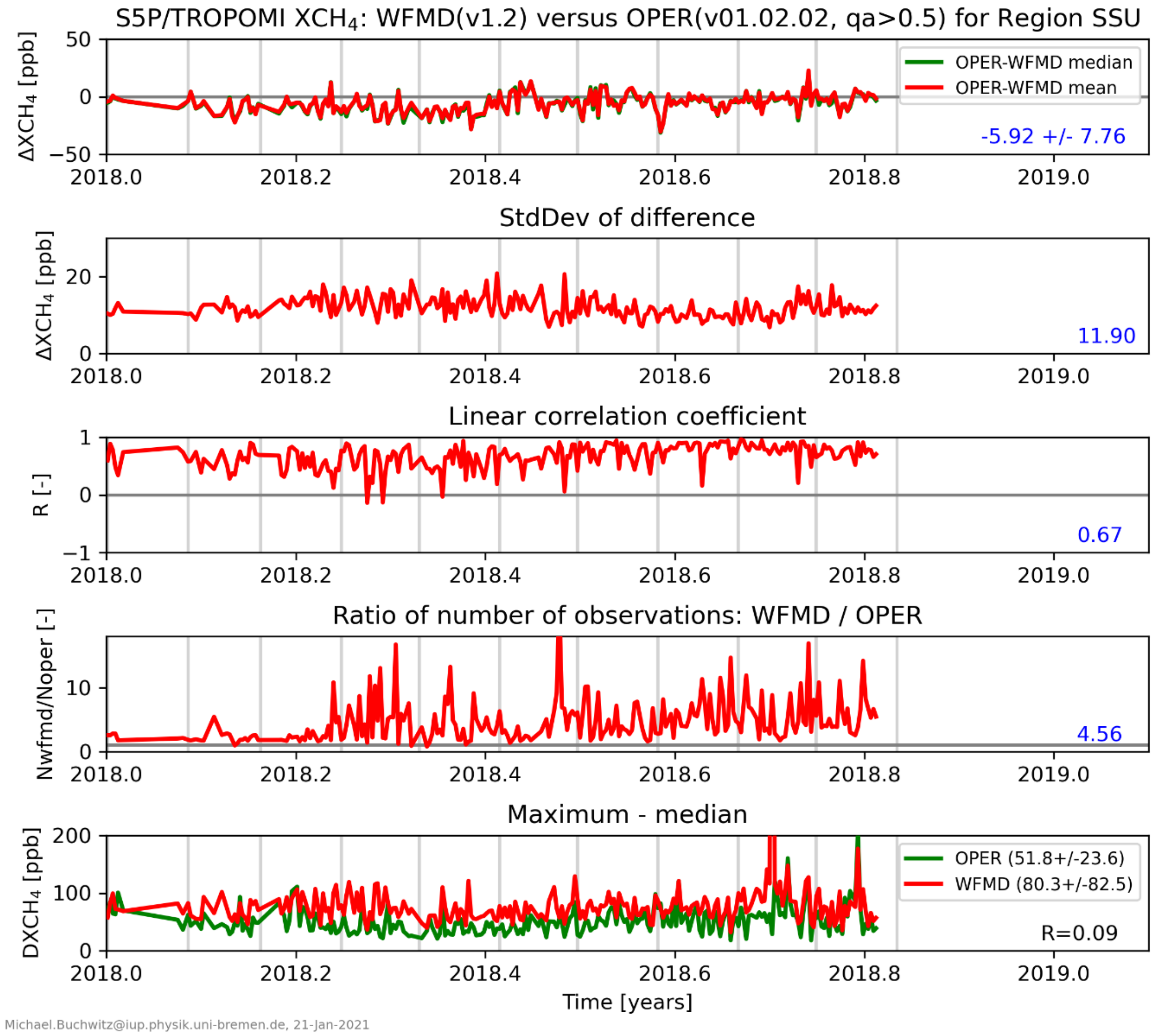

Figure 34: Comparison of TROPOMI XCH_4 products WFMD and OPER (qa > 0.5, i.e., default quality filtering) for each day (overpass) during the period beginning of January 2018 to end of October 2018 for target region SSU. Shown are 5 quantities computed for every overpass. These quantities are (from top to bottom): the XCH_4 difference WFMD-OPER (red: difference of mean values, green: difference of medians), the standard deviation of the difference, the linear correlation coefficient, the ratio of the number of observations, $DXCH_4$, i.e., maximum XCH_4 value (corresponding to a single ground pixel) minus median of the scene (see main text for details). Listed in blue are the corresponding mean values as computed from the presented time series.

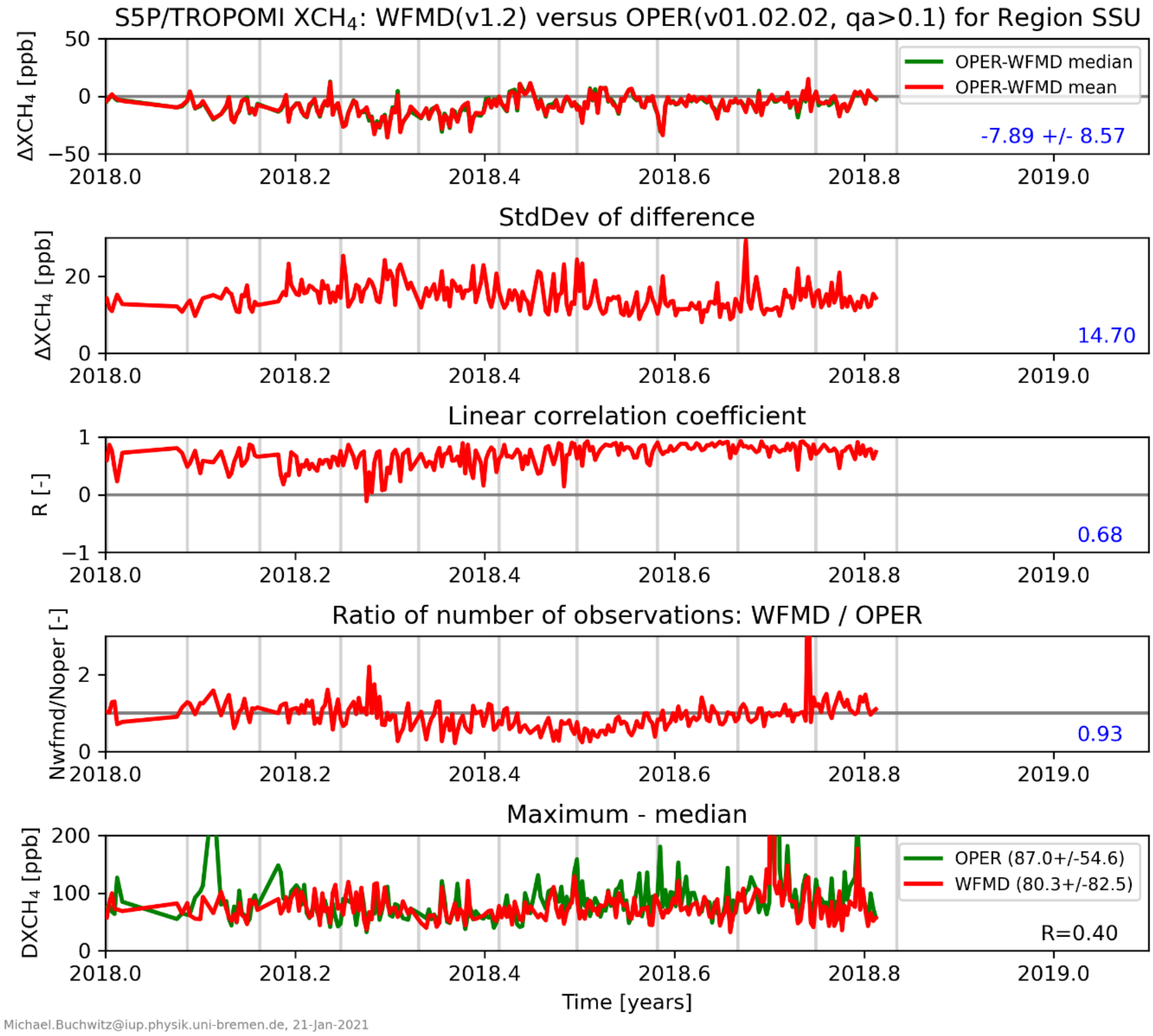

Figure 35: As Figure 34 but for relaxed quality filtering (qa > 0.1) of the OPER product.

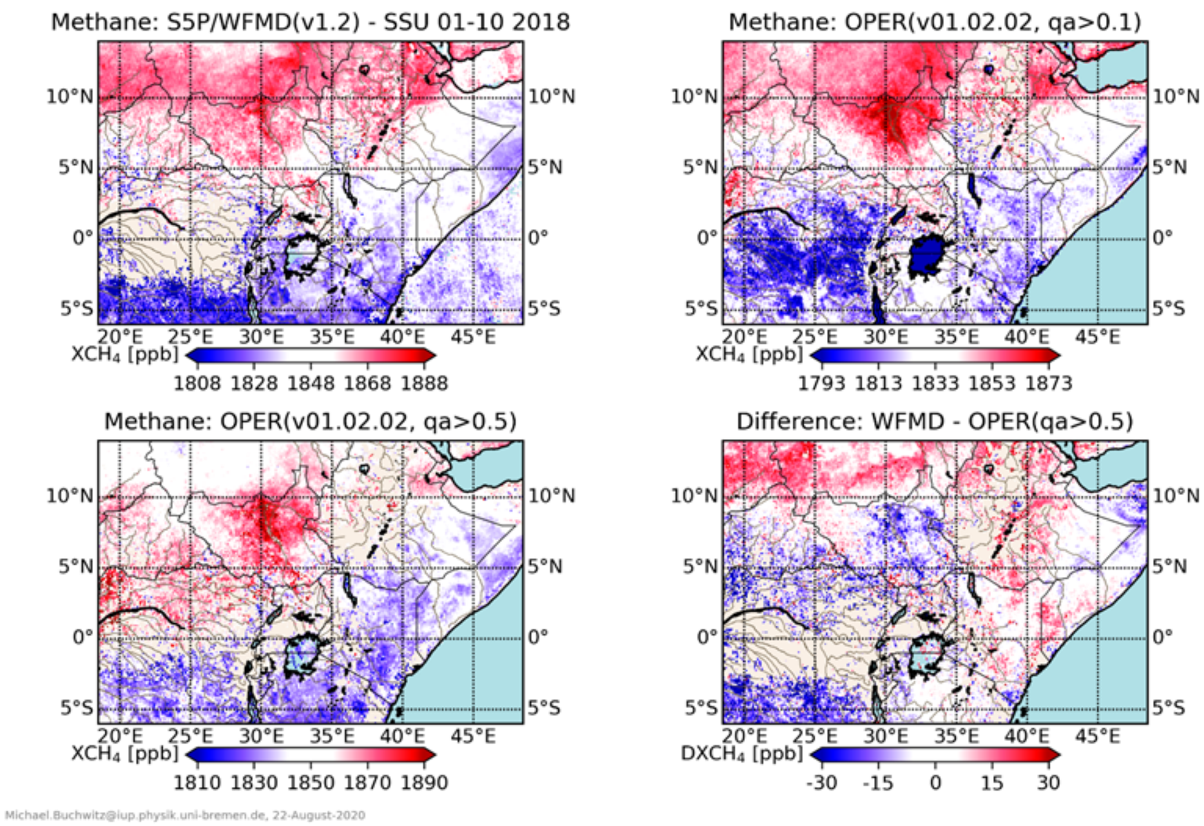

Figure 36: Comparison for target region SSU for temporally averaged data covering the period January to October 2018. Top left: WFMD XCH_4 product. Top right: OPER product with relaxed quality filtering (qa > 0.1). Bottom left: OPER product with recommended (default) quality filtering (qa > 0.5). Bottom right WFMD – OPER (qa > 0.5) XCH_4 difference.

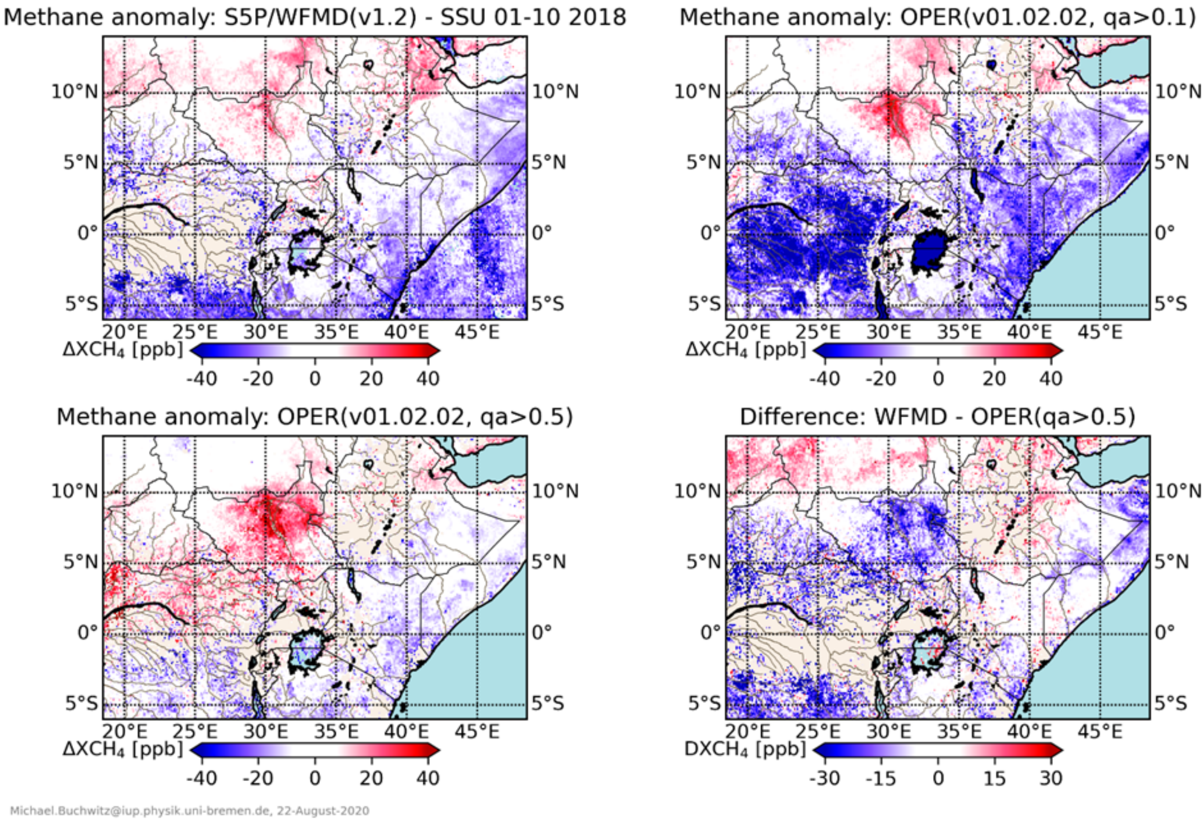

Figure 37: Similar as Figure 36 but for averages of daily anomalies instead of averaging absolute XCH_4 values.

4.3. Comparisons with prototype operational product ("OPERbeta") from Lorente et al. (2021)

SRON generated an improved version (v14_14) of the S5P XCH_4 algorithm (RemoTeC) to generate an improved operational product, which was activated in the operational processing in June 2021 (see Table 2). The status of this activity is described in Lorente et al. (2021). We downloaded the corresponding data set and refer to it a "OPERbeta" in this section.

To find out to what extent this new product improves the comparison with the WFMD version 1.2 product we performed additional comparisons similar as the ones for product OPER as shown in the previous section.

We focus on those target regions and scenes as also presented in the previous section to enable direct comparison of OPERbeta with OPER and WFMD.

The results in terms of comparisons of XCH_4 maps are shown in Figure 38 - Figure 42. The comparison is limited to the OPER and OPERbeta products with recommended quality filtering (qa > 0.5). As can be seen, there is some difference between the OPER and OPERbeta products but overall they are quite limited.

A summary of the comparison is shown in Table 5. As can be seen, the number of observations (Nobs) is higher for OPERbeta compared to OPER but still significantly lower than for WFMD. The linear correlation of the spatial pattern and the standard deviation of the difference to WFMD has been improved, i.e., the spatial pattern of OPERbeta is in better agreement now with WFMD. The mean bias however has typically increased somewhat, i.e., the comparison suggests a low bias of OPERbeta compared to WFMD.

It is therefore of interest to show comparisons of these two data sets with TCCON. Figure 43 shows a comparison of WFMD (version 1.2) with TCCON (source: Schneising et al., 2021) and OPERbeta (source: Lorente et al., 2021). The mean difference to TCCON and the standard deviation of the difference are shown as a function of the latitudes of the different TCCON sites.

The difference WFMD – TCCON is +0.6 ± 4.4 ppb (slight but not significant high bias of WFMD relative to TCCON) for the mean differences per TCCON site and the mean value of the standard deviation of the individual ground pixel comparisons is 14.8 ppb (which can be interpreted as average single ground pixel random error or "precision").

The difference OPERbeta – TCCON is -4.0 ± 5.4 ppb (low bias but not significant taking into account the 1-sigma scatter) for the mean differences per TCCON site and the mean value of the standard deviation of the individual ground pixel comparisons is 12.9 ppb.

(a)

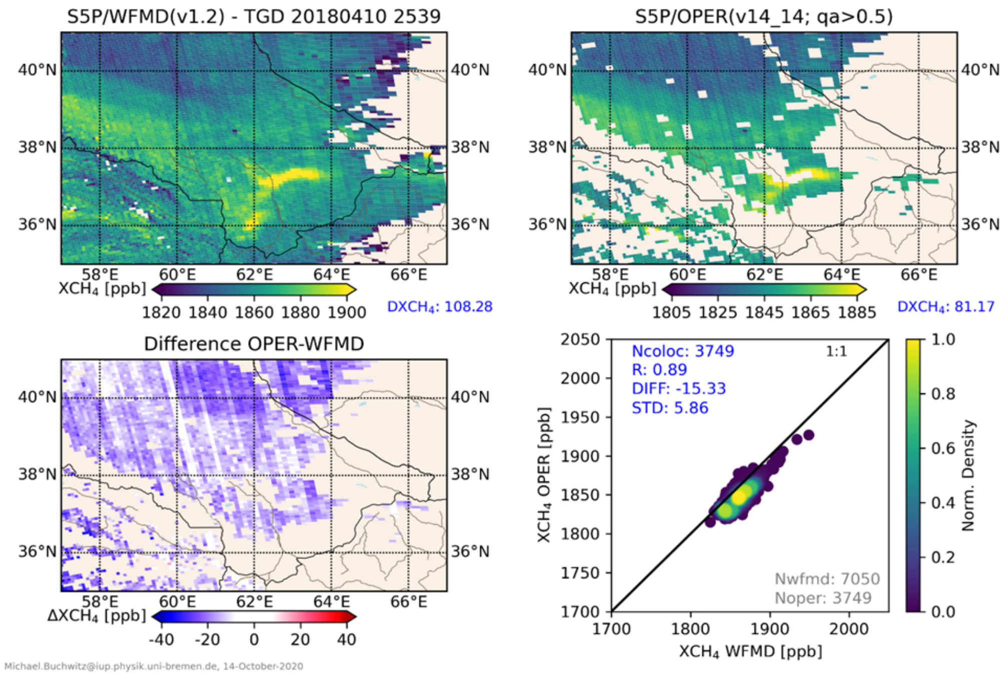

(b)

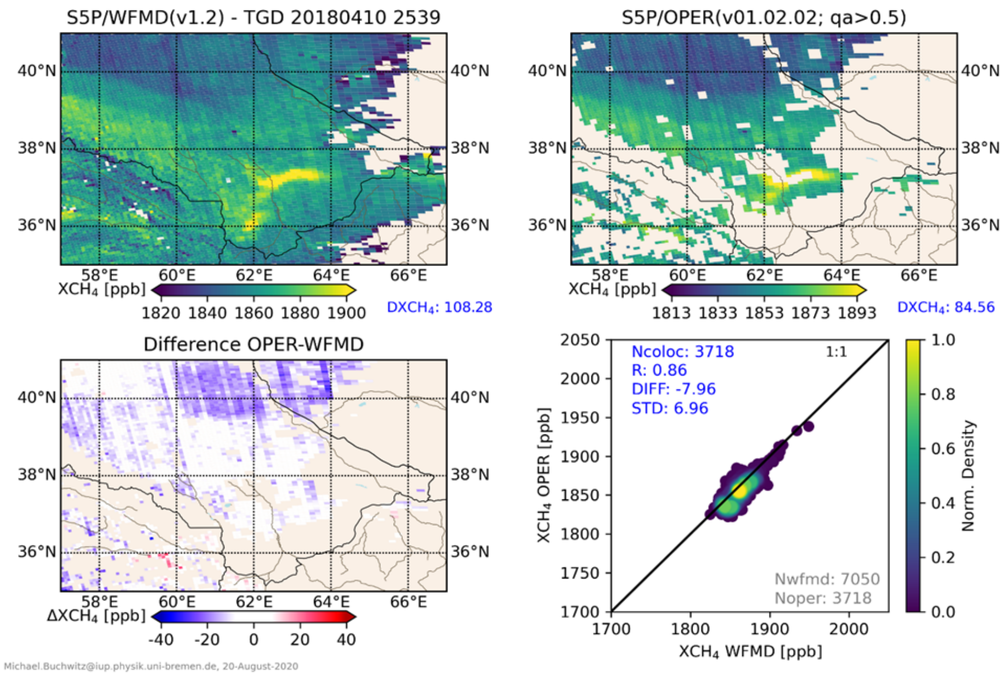

Figure 38: Comparisons of (a) WFMD XCH_4 with OPERbeta (version 14_14) from Lorente et al., 2021, for region TGD on 10-April-2020. (b) Similar as (a) but for OPER.

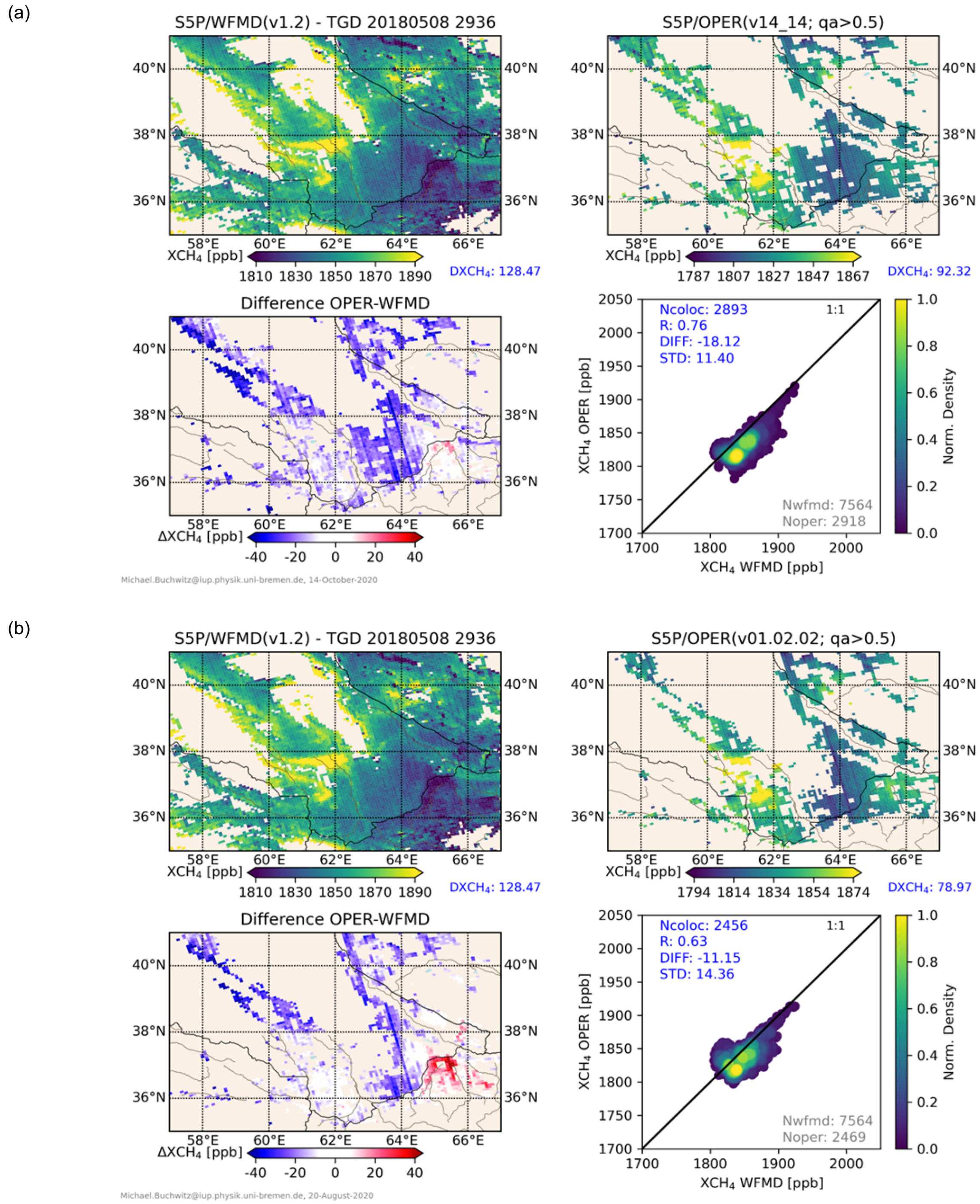

Figure 39: Similar as Figure 38 but for 8-May-2018 (target region TGD).

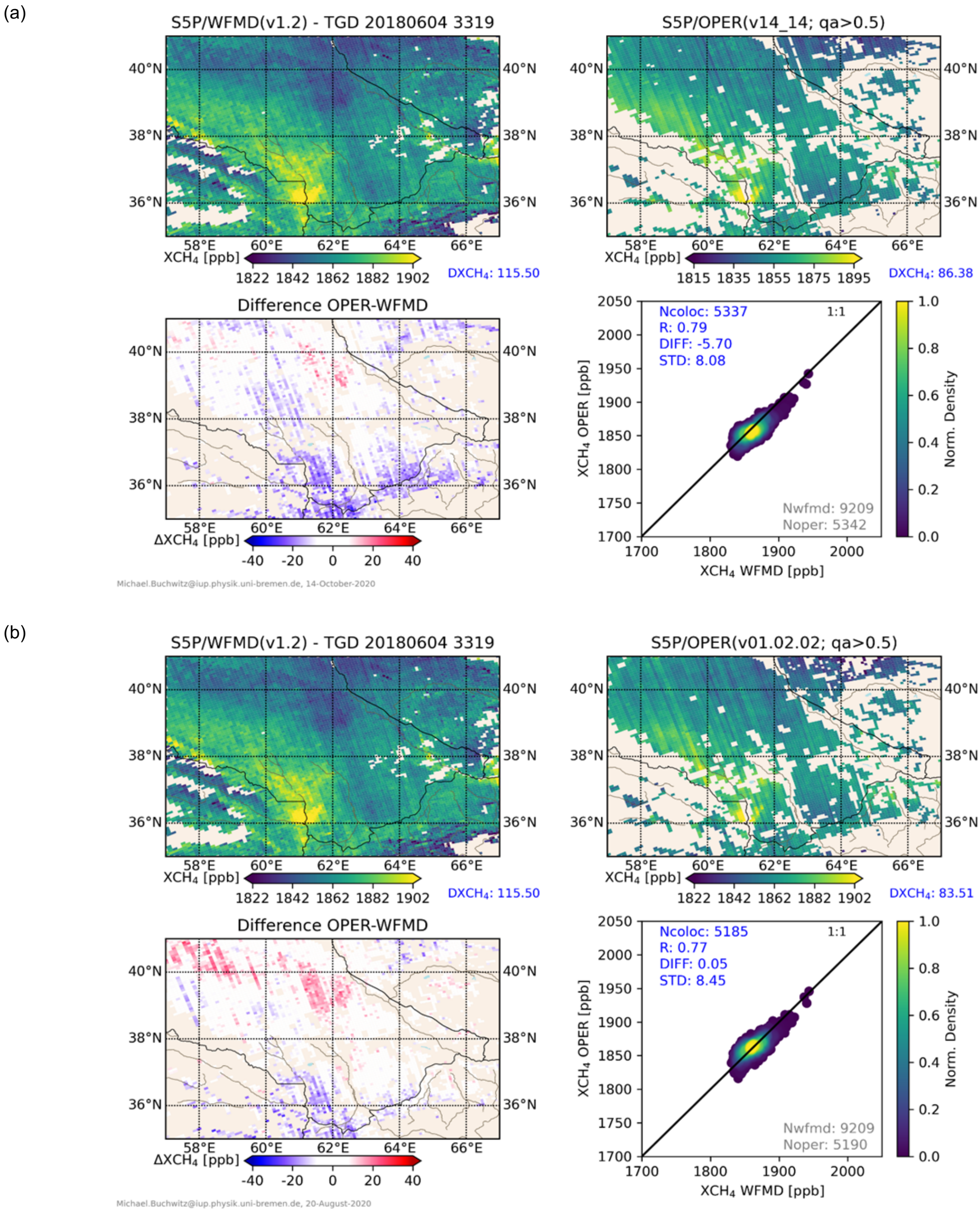

Figure 40: Similar as Figure 38 but for 4-June-2018 (target region TGD).

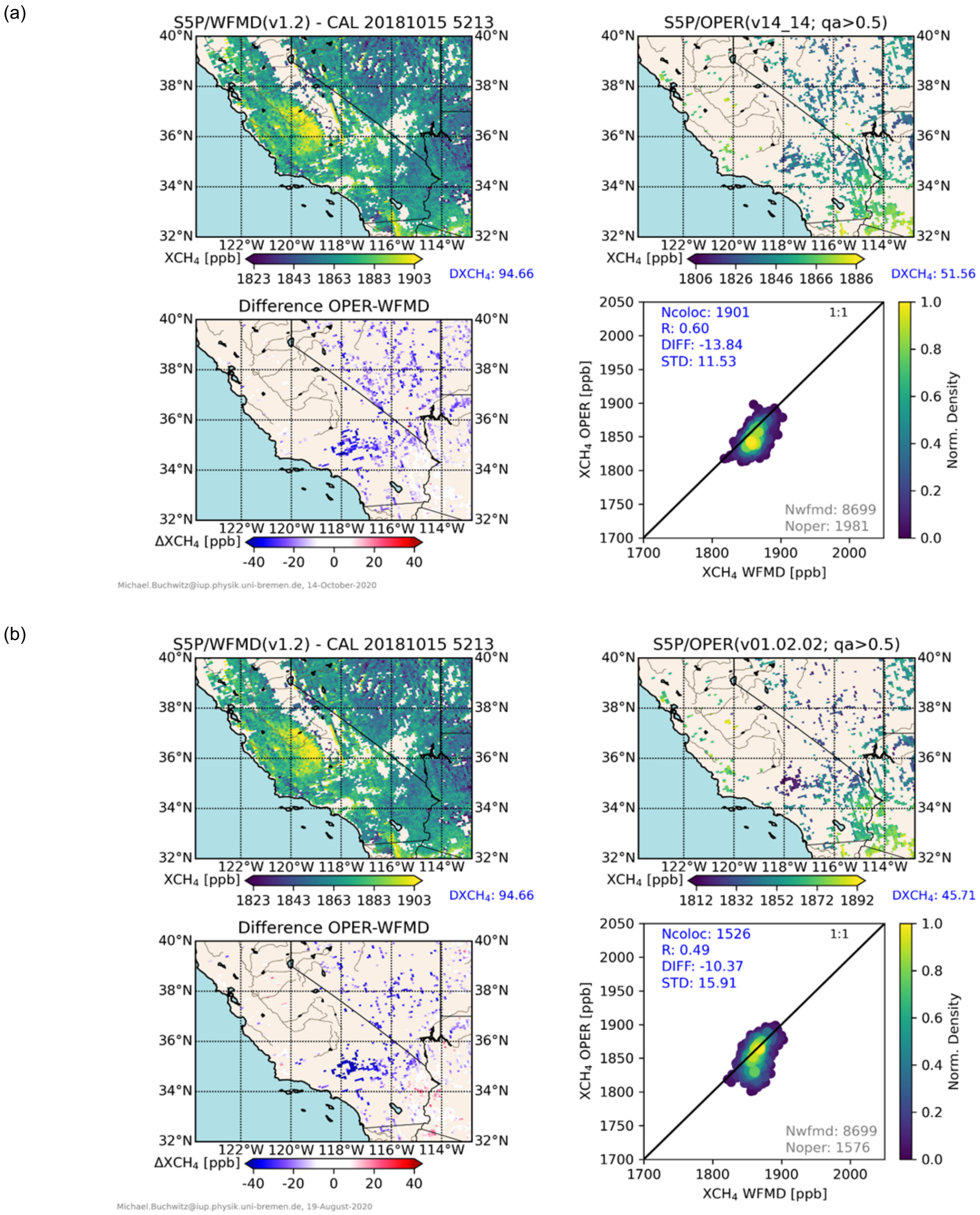

Figure 41: Similar as Figure 38 but for target region CAL and 15-October-2018.

(a)

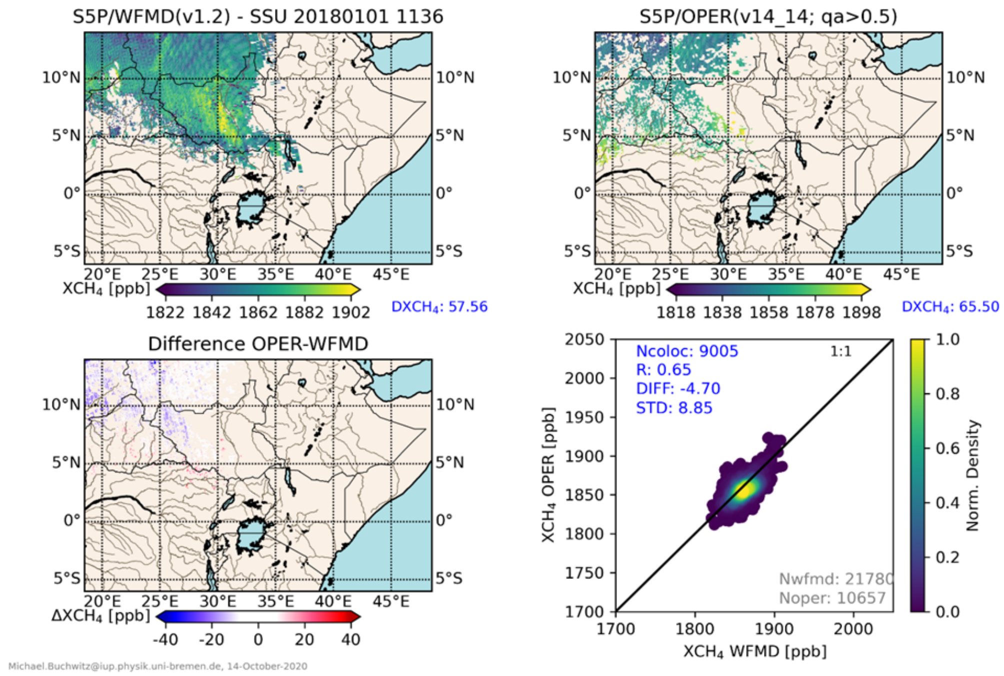

(b)

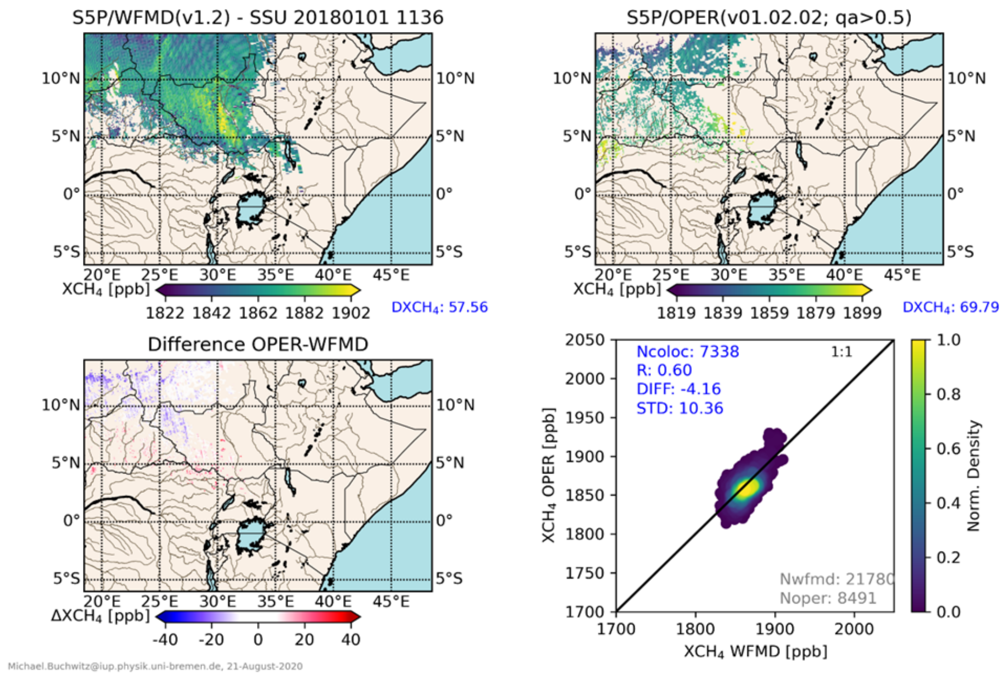

Figure 42: Similar as Figure 38 but for target region SSU and 1-January-2018.

Table 5: Overview of the WFMD, OPER and OPERbeta XCH_4 target region comparisons.

No	Target	Day in 2018	Orbit	Nobs			Correlation with WFMD		Diff (OPER-WFMD) ± StdDev	
				WFMD	OPER	OPERbeta	OPER	OPERbeta	OPER	OPERbeta
1	TGD	10-Apr	2539	7050	3718	3749	0.86	0.89	-8.0 ± 7.0	-15.3 ± 5.9
2	-"-	8-May	2936	7564	2469	2918	0.63	0.76	-11.2 ± 14.4	-18.1 ± 11.4
3	-"-	4-Jun	3319	9209	5190	5342	0.77	0.79	+0.1 ± 8.5	-5.7 ± 8.1
4	CAL	15-Oct	5213	8699	1576	1981	0.49	0.60	-10.4 ± 15.9	-13.8 ± 11.5
5	SSU	1-Jan	1136	21780	8491	10657	0.60	0.65	-4.2 ± 10.4	-4.7 ± 8.9
6	-"-	9-Aug	4257	8742	1476	1592	0.90	0.93	-4.7 ± 8.4	-4.7 ± 7.9
7	-"-	7-Oct	5094	6370	1652	1998	0.77	0.78	+0.7 ± 17.8	-0.9 ± 19.1

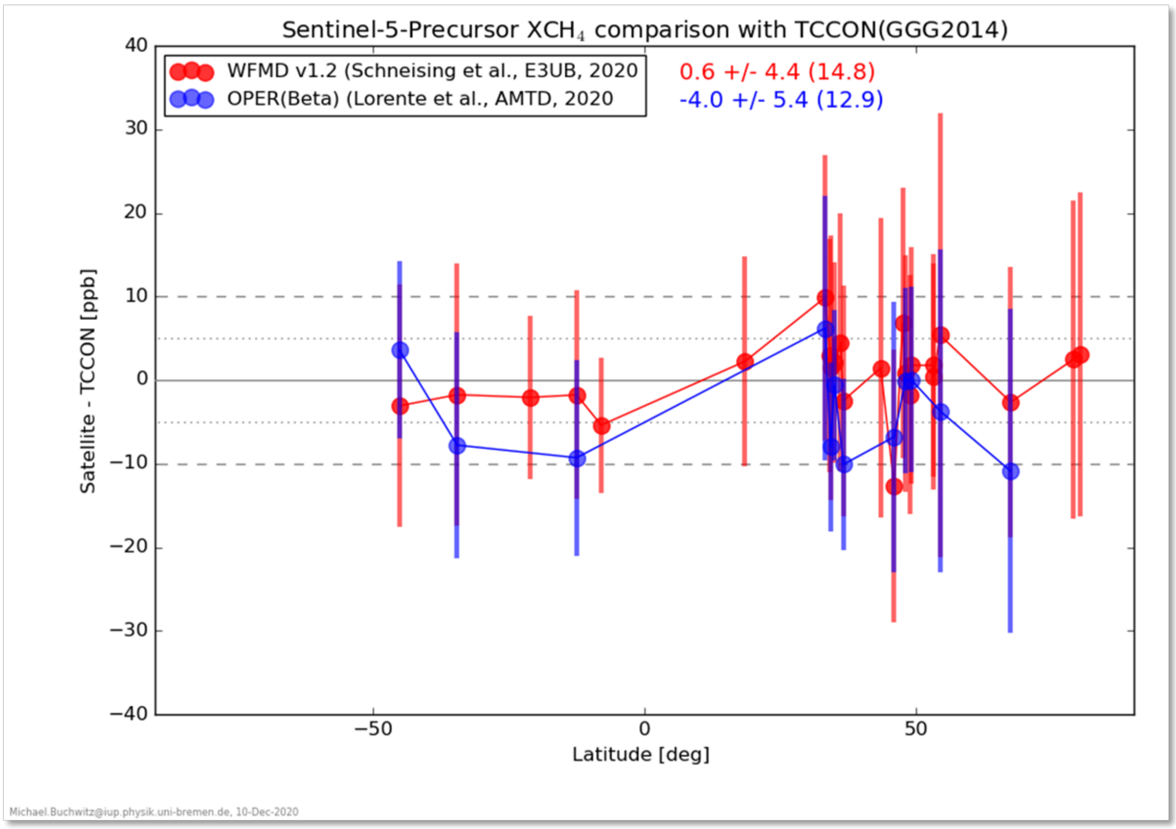

Figure 43: Comparison of the validation of products WFMD and OPERbeta with TCCON.

4.4. Comparisons at high latitudes

High latitudes are challenging for S5P XCH_4 retrieval for many reasons mostly related to low spectral radiances (poor reflectivity of snow, ice and water in the 2.3 µm spectral region used for retrieval) and low sun elevation, i.e., large solar zenith angles.

Initial comparisons have also been conducted for high northern latitudes as shown in Figure 44. As can be seen, product WFMD has better coverage (also over land, at least to some extent) and shows less “strange features” compared to OPER, which are likely related to surface reflectivity related retrieval issues.

S5P XCH_4 scientific product (Schneising et al., 2019, WFMD, v1.2)

S5P XCH_4 operational product (Hu et al., 2016, RemoTeC, v01.02.01, qa>0.5 (= recommended filter))

April 2018

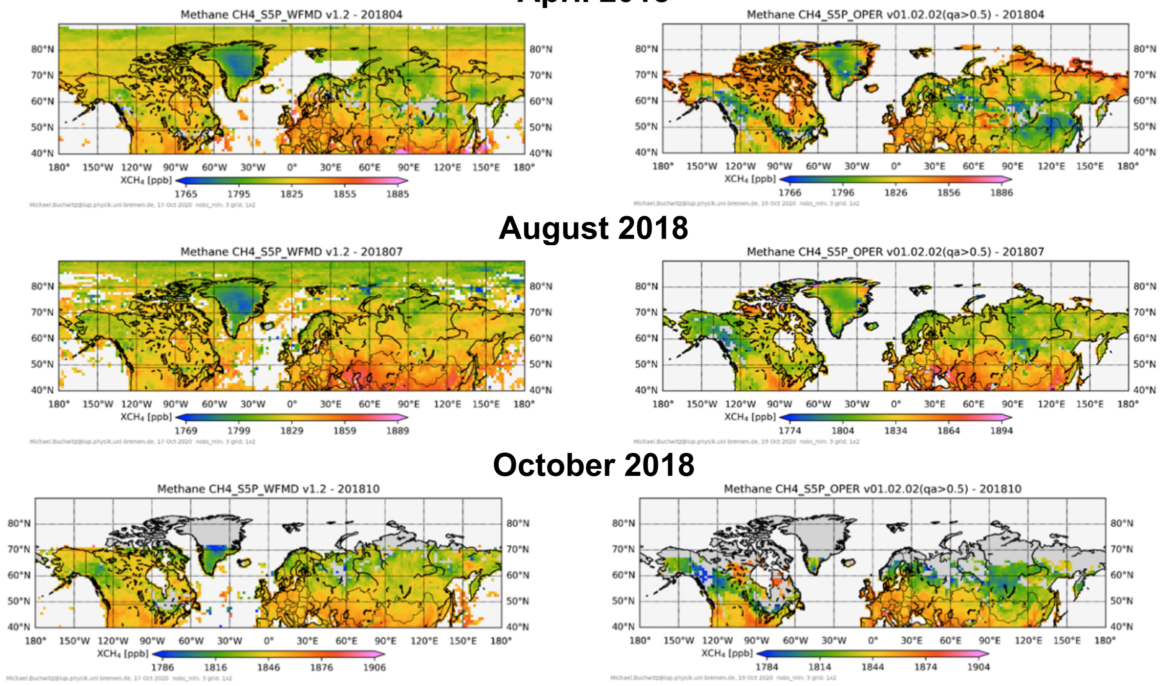

Figure 44: Comparison of monthly XCH_4 values for high northern latitudes of product WFMD (left) with OPER (right) for three months. From top to bottom: April, August and October 2018.

4.5. Algorithm improvements parallel to Methane+

In this section we present algorithm improvements from both the WFMD-UB product and the SRON S5P-RemoTeC XCH_4 scientific product that were developed in parallel to the Methane+ project.

The WFMD product v1.5 (Schneising et al., 2021c) has been generated with an improved retrieval algorithm (Schneising et al., 2021b) compared to product version 1.2 (Schneising et al., 2019). As explained in more detail in Schneising et al., 2021b, the following algorithm modifications have been implemented for v1.5 compared to v1.2 (for details including all references see Schneising et al., 2021b): Use of improved input data bases (surface information (elevation, roughness), meteorological information (ERA5)) and improved post-processing (e.g., modified training data sets with additional features) for bias correction and quality filtering.

The SRON S5P-RemoTeC XCH4 scientific algorithm accounts for the spectral dependence of the surface reflectance by fitting a polynomial in the inversion. In version 14_14 and 18_17, the fit includes a 2nd order polynomial. Recent analysis has shown that increasing the order to 3 improves the representation of surface features in the retrieval. In Sect. 4.5.2 we present example cases where this modification of the spectral fit removes artifacts related to the underlying surface features and significantly improves the XCH4 data product.

4.5.1. Additional comparisons including TROPOMI WFMD v1.5 XCH_4

In this sub-section we present additional comparisons for several regions for the following three TROPOMI S5P XCH_4 data products:

- OPER V01: The first version of the OPERational data product, i.e., the same product also used for the comparisons shown in the previous sub-sections; here we use only data with the recommended quality filtering (qa=1)

- WFMD v1.2 as also used in previous sub-sections

- WFMD v1.5: The latest version of the IUP-UB S5P XCH_4 data product; this product covers the time period October 2017 to December 2020 and has been generated in the framework of the ESA Climate Change Initiative (CCI) GHG-CCI+ project (https://climate.esa.int/en/projects/ghgs/). The product will be made available via the CCI Open Data Portal Website but is currently already available from the Univ. Bremen S5P/Tropomi WFMD website.

In the following sub-sections we present comparisons for the following regions:
- Northern Siberia, Russia
- Etosha Pan, Namibia

4.5.1.1. Comparisons for Northern Siberia, Russia

Froitzheim et al., 2021, present OPERational TROPOMI XCH_4 retrievals over Northern Siberia and argue that features of locally elevated methane in this Siberian permafrost region are due to methane release from carbonate rock formations. Barré et al., 2021, discuss the same features but argue that the locally elevated retrieved XCH_4 visible in the OPERational product are high bias outliers due to surface reflectivity related issues not properly dealt with by the retrieval algorithm.

Comparisons of XCH_4 over this region are shown in Figure 45. The first column shows the OPERational product V01 and the “features” discussed in Froitzheim et al., 2021, are clearly visible, especially in the middle and top panels (August 2019 and 2020). In contrast, these pattern of elevated XCH_4 are hardly visible in the WFMDv1.2 product (middle column) and they are essentially not present in the WFMDv1.5 product (right column), which has improved post-processing steps (quality flagging and bias correction) compared to WFMDv1.2 and is therefore more accurate compared to v1.2. Our analysis corroborates Barré et al., 2021, arguing that the mentioned features are high bias outlier of the OPERational data product.

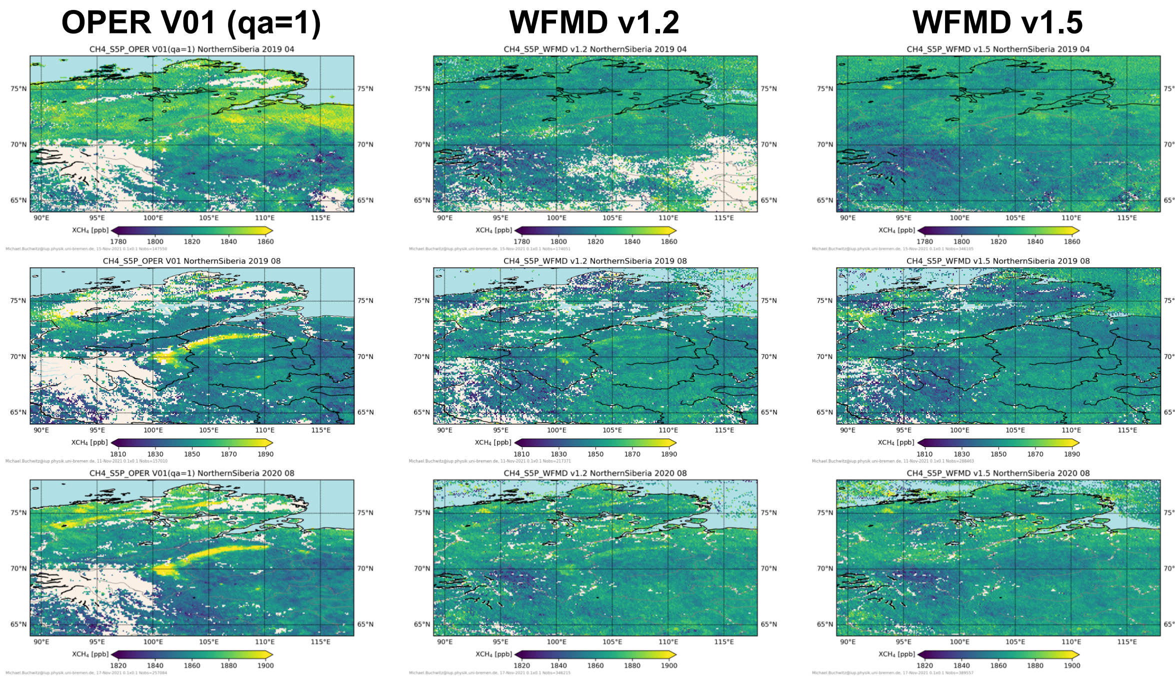

Figure 45: Comparison of the three TROPOMI XCH_4 data products over Northern Siberia. Top row: April 2019, middle row: August 2019, bottom row: August 2020.

4.5.1.2. Comparisons for Etosha Pan, Namibia

The Etosha Pan in Namibia is typically a dry salt-encrusted area (https://en.wikipedia.org/wiki/Etosha_pan). However, after a heavy rain it acquires a thin layer of water, which is heavily salted by the mineral deposits on the surface. The Etosha pan is also listed in the Ramsar convention on wetlands of international importance (https://www.ramsar.org/). Wetlands are known methane sources but to what extent the Etosha Pan emits methane is not well known.

The WFMD XCH_4 data products shows elevated XCH_4 over the Etosha Pan in Namibia as can be seen in Figure 46 (middle and right columns). These pattern of locally elevated XCH_4 are not visible in the OPERational product when this product is filtered using the recommended filtering method (i.e., using qa=1). The resulting data gaps of the OPERational data product are visible in Figure 46 (left columns, esp. bottom panel).

At present it cannot be ruled out that the high values of XCH_4 in the WFMD products are high bias outliers due to surface reflectivity related issues. Preliminary analysis of the WFMD algorithm indicates that this potential problem can be solved by a modification of the WFMD algorithm but future analysis will confirm if this is possible or not and to what extent the WFMD algorithm can be further improved.

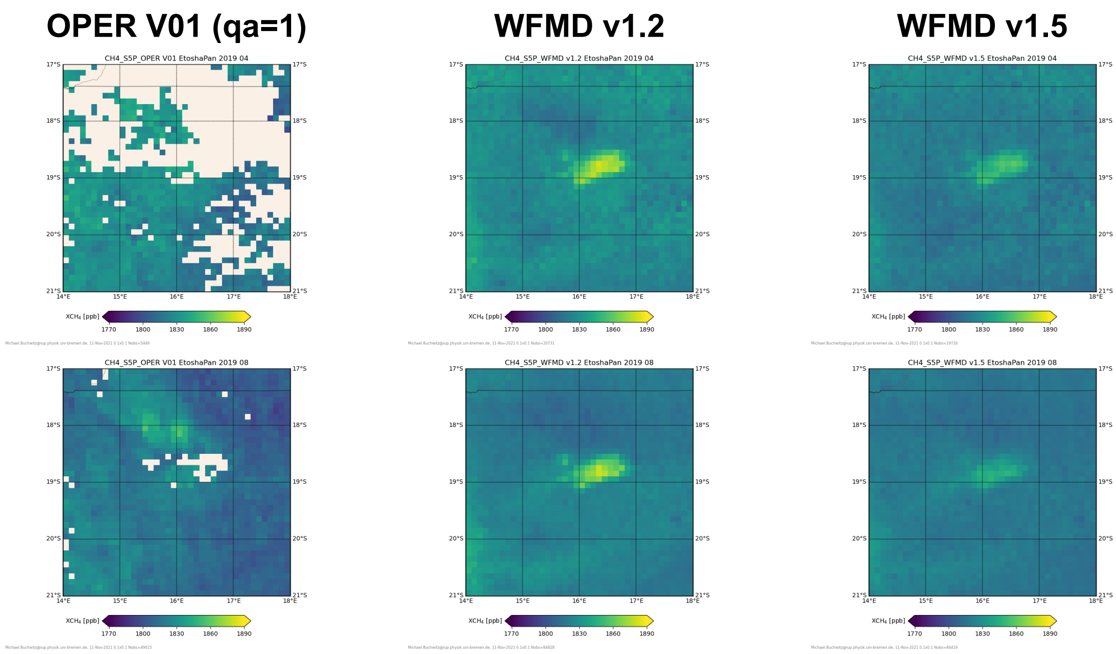

Figure 46: Comparison of the three TROPOMI XCH_4 data products over the Etosha Pan, Namibia, and surrounding area. Top row: April 2019, bottom row: August 2019.

4.5.2. Improvements of SRON S5P-RemoTeC scientific XCH4 product

We present in this section two example cases where we show the improved treatment of surface reflectance spectral dependence. We compare in a qualitative way these improvements with respect to version 18_17 of the SRON S5P-RemoTeC scientific product.

4.5.2.1. Northern Siberia, Russia

The first example has already been discussed with the WFMD v1.5 product in section □. Figure 47a shows XCH4 retrieved with SRON S5P-RemoTeC version 18_17, which fits a 2nd order polynomial for surface reflectance where a significant enhancement in XCH4 is visible. Figure 47b shows XCH4 retrieved with a 3rd order polynomial, and Figure 47c the difference between the both (a) and (b). Increasing the order of the polynomial largely reduces the XCH4 enhancement. Figure 47d shows the difference in the fit quality (by means of χ^2), with blue meaning a decrease in χ^2 with higher order polynomial, thus an improved fit quality. Increasing the order of the polynomial has its strongest effect over the area where the enhanced XCH4 is found, and results in an improved XCH4 product. In other areas increasing the order of the polynomial results in higher XCH4 (although smaller effect), which is also an improvement as these are typically areas with low albedo where the SRON S5P-RemoTeC XCH4 product underestimates XCH4.

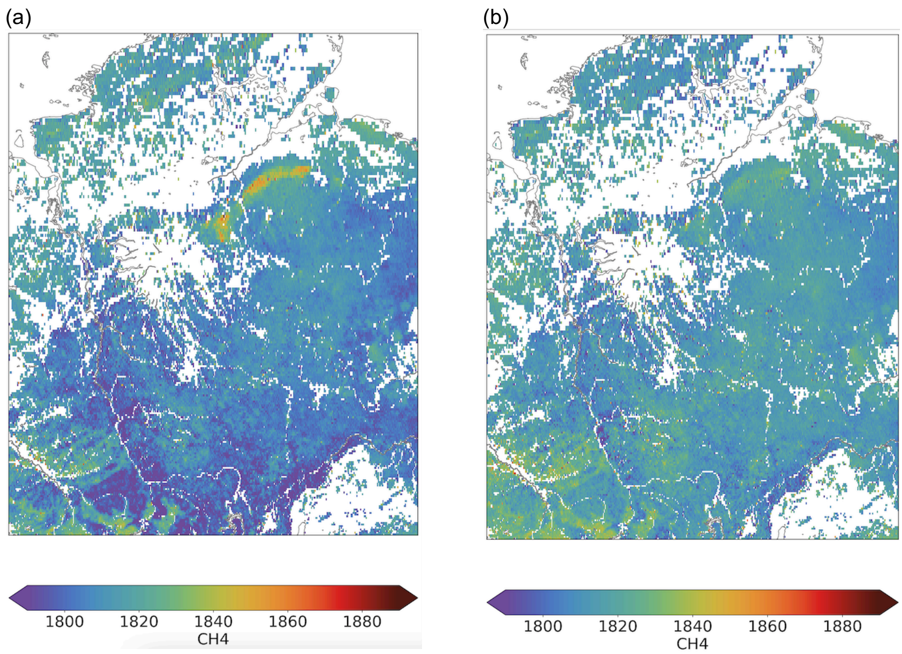

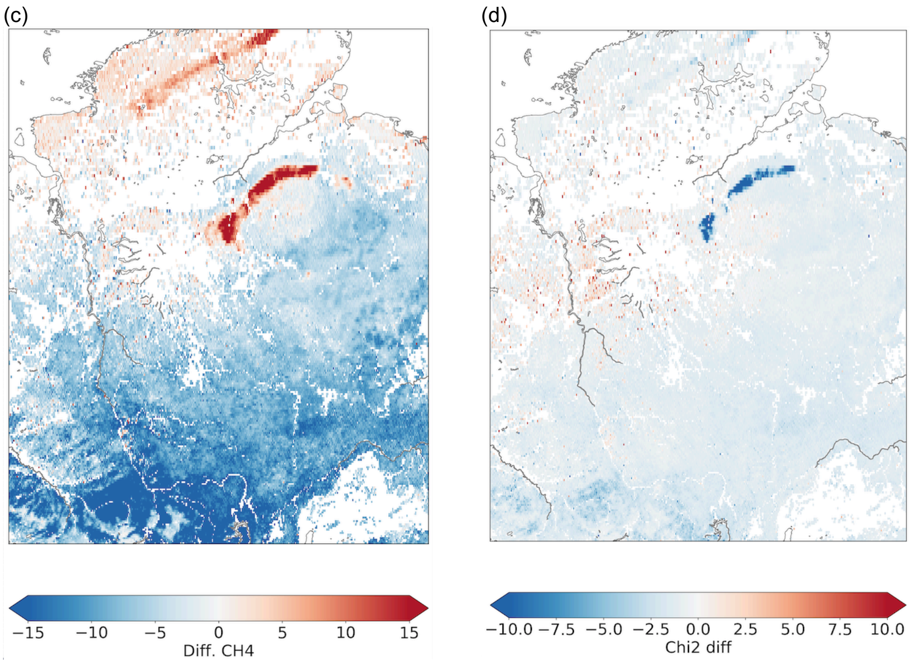

Figure 47: XCH4 averaged in a 0.1 x 0.1 degree grid retrieved with (a) second order polynomial and (b) third order polynomial for the fit of the surface reflectance spectral dependence. (c) Difference between (a) and (b) and, (d) the difference in χ^2 for each of the retrievals.

4.5.2.2. Australia

This example has already been discussed in Figure 18 on section 4.1.2, where SRON S5P-RemoTeC XCH4 product version 14_14 shows elevated XCH4 correlated with the retrieved aerosol optical thickness. Increasing the order of the polynomial to fit the surface spectral dependence removes this artifact. Figure 48 shows XCH4 retrieved with SRON S5P-RemoTeC version 18_17, which fits a 2nd order polynomial for surface reflectance where a localized enhancement in XCH4 is visible. Figure 48b shows XCH4 retrieved with a 3rd order polynomial, and Figure 48c the difference between the both (a) and (b). In a similar way as for the feature over Siberia, increasing the order of the polynomial removes the XCH4 enhancement. Figure 48d shows the difference in the fit quality (by means of χ^2), with blue meaning a decrease in χ^2 with higher order polynomial, thus an improved fit quality. Increasing the order of the polynomial has its strongest effect over the area where the enhanced XCH4 is found, and results in an improved XCH4 product. Outside of the localized artifact, increasing the order of the polynomial results in slightly higher XCH4, which is an improvement as these are typically areas with low albedo where the SRON S5P-RemoTeC XCH4 product underestimates XCH4.

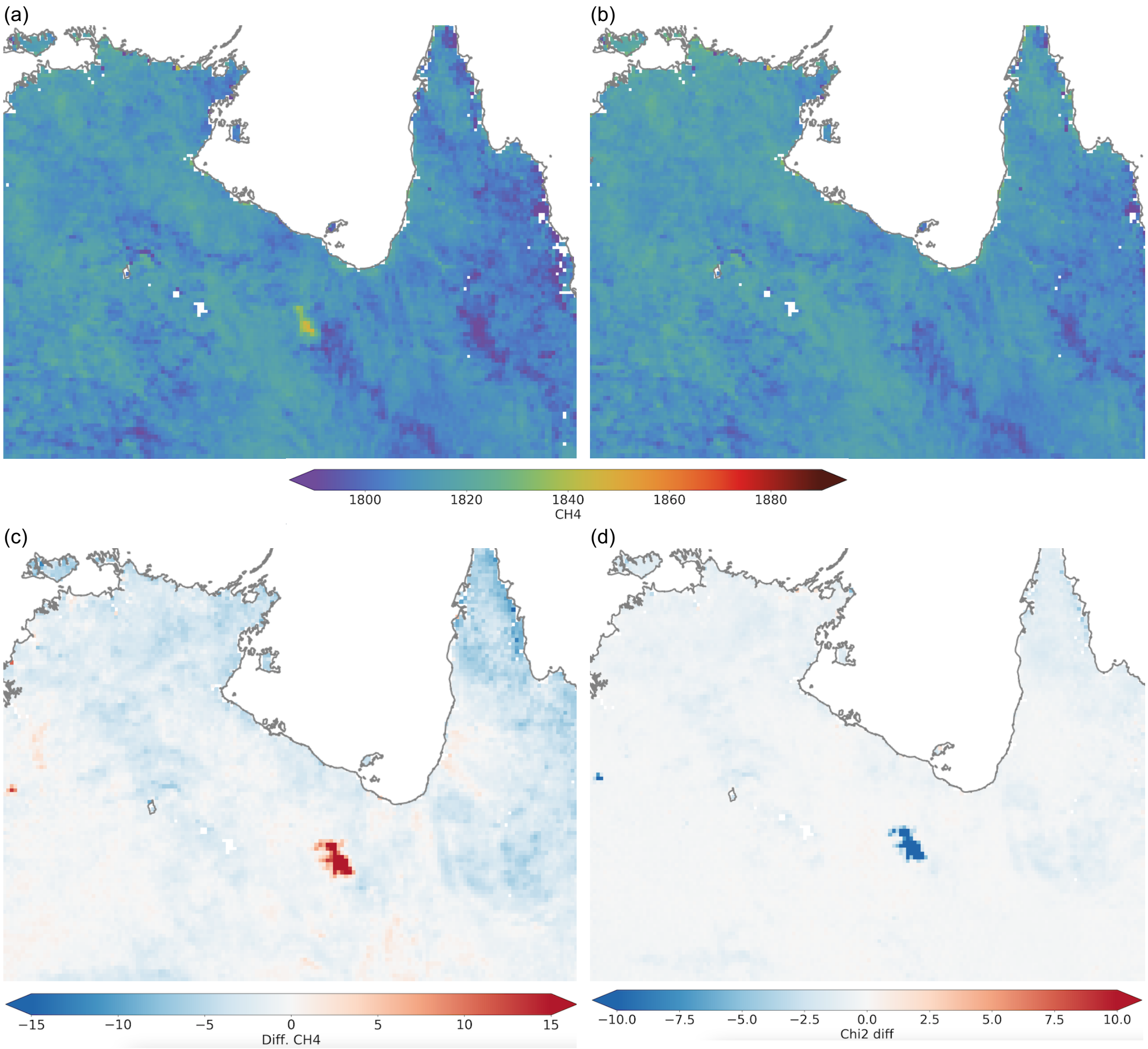

Figure 48: XCH4 averaged in a 0.1 x 0.1 degree grid retrieved with (a) second order polynomial and (b) third order polynomial for the fit of the surface reflectance spectral dependence. (c) Difference between (a) and (b) and, (d) the difference in χ^2 for each of the retrievals.

5. SUMMARY

In this Validation Report (VR) we have assessed the data quality of the SWIR XCH4 products by validation with external independent reference measurements (ground-based measurements from TCCON network and satellite measurements from GOSAT). Furthermore, a detailed inter-comparison between the data products has been performed over challenging regions and over target regions, with the aim of identifying and work out differences between the data products. This document serves as a reference in the next phase of the project where the data products will be assimilated.

SRON the Netherlands for Space Research focused in this project in providing the SRON S5P-RemoTeC scientific TROPOMI XCH_4 product with the latest updates that will be implemented in the operational processing in the processor update foreseen for June 2021. The objective is to validate this scientific (beta) product to assess the quality of data after the improvements have been implemented. Furthermore, SRON focusses on the analysis over regions that are challenging for the retrieval to asses that the developments implemented in the SRON S5P-RemoTeC scientific product work in the right direction.

Related to the SRON activities within the project, in the document we have presented the following: on one hand, the validation with independent ground-based measurements and an inter-comparison with the GOSAT satellite, and on the other hand the comparison between the IUP-UB WFMD XCH_4 product. The validation of the scientific SRON S5P-RemoTeC XCH_4 product with ground-based measurements of the TCCON network shows a very good agreement, with a bias of -3.4 ppb (-0.2%) and station-to-station variability of 5.6 ppb (0.3%), well below the mission requirements for accuracy and precision of 1%. The intercomparison with GOSAT shows an agreement of -10.3 ± 16.8 ppb. Both these results highlight the high quality of the SRON S5P-RemoTeC XCH_4 product.

In Sect. 4.1, SRON focussed on a detailed comparison addressing the retrieval performance over regions world-wide that are challenging for the CH_4 retrieval. Over high latitude regions over Canada and Russia the main challenge for the retrievals are the scenes with low surface albedo that lead to an underestimation of XCH4 due to scattering errors. The comparison between WFMD and SRON products confirms that the bias correction corrects for this effect, as also confirmed by the validation with TCCON and comparison with GOSAT. Over Australia both products overcome the dependence of the retrieved XCH_4 on surface albedo with the posterior correction. Over North Africa scenes with high surface albedos are predominant, and both SRON and WFMD product correct for high XCH4 retrieved over these scenes. Both products capture the seasonal and geographical variation with good agreement over these regions, with overall WFMD XCH_4 being higher than SRON XCH4 by 8 ppb.

The Institute of Environmental Physics of the University of Bremen (IUP-UB) focussed in this project on the following aspects: (i) Provision of a S5P/TROPOMI XCH_4 data set retrieved with the scientific algorithm "Weighting Function Modified Differential Optical Absorption Spectroscopy" (WFM-DOAS or WFMD). This data set is referred to as WFMD data set in this document. (ii) Validation of this WFMD data set by comparisons with TCCON ground-based XCH_4 retrievals. (iii) Comparisons of the WFMD data set with the operational Copernicus S5P/TROPOMI XCH_4 product (referred to as OPER product in this document) focussing on selected regions showing locally elevated methane. In addition, other comparisons have been conducted such as comparisons with a new S5P/TROPOMI XCH_4 data set generated at SRON with a prototype version of the operational (RemoTeC) algorithm. The corresponding data product is referred to as OPERbeta in this document.

Concerning these IUP-UB activities the following is reported in this document: (i) The S5P/TROPOMI XCH_4 WFMD data set (version 1.2) provided for this project covers the time period November 2017 to July 2020. (ii) Validation results are reported in this document. The validation of the S5P/TROPOMI WFMD v1.2 XCH_4 product can be summarized as follows: It has a random error of 14.13 ppb (0.8%), a spatio-temporal systematic error of 4.60 ppb (0.2%), and no significant long-term drift. (iii) Detailed comparisons are shown for three regions showing locally elevated methane: A region in Turkmenistan, the Galkynysh and Dauletabad gas and oil fields (region ID: TGD). The Central Valley in California, a major methane source region due to emissions from oil, natural gas, cattle and other sources (region ID: CAL). A region in South Sudan (region ID: SSU) known for wetland methane emissions. The comparisons of the WFMD and OPER XCH_4 products show quite consistent results for all three areas: The daily spatially resolved XCH_4 maps show a reasonable to good correlation (the linear correlation coefficient R is typically in the range 0.4 – 0.9, depending on area and time period) but the differences of the maps show a complex pattern with large-scale and small-scale features, which are currently not well understood. The standard deviation of the differences are on the order 10-15 ppb (~0.5 -1 %) and the mean difference is typically around 5 ppb (0.25%). The WFMD product typically has much better coverage (depending on day and area the WFMD product has typically 2-7 times more data compared to OPER). Comparisons of WFMD with the OPERbeta product indicates that OPERbeta is improved compared to OPER with respect to number of observations (if the standard quality filter qa>0.5 is used). Also, the linear correlation of the spatial pattern with the WFMD product is slightly better for OPERbeta compared to OPER and also the standard deviation of the differences are somewhat reduced.

Furthermore, also additional comparisons with the latest version of the WFMD product (v1.5) are shown for several regions. Based on these comparisons it is concluded that the WFMD v1.5 product is improved compared to v1.2 in terms of accuracy and coverage. Nevertheless, there are also some areas of potential biases, such as over the Etosha Pan in Namibia. Based on these comparisons it is also concluded that the OPERational V01 product shows high bias outliers in parts of Northern Siberia. The outliers over Northern Siberia are related to surface spectral features that are not properly accounted for in the S5-P RemoTeC algorithm. We have shown that increasing the order of the polynomial that accounts for the surface reflectance spectral dependence in the inversion removes these biases and also other known artifacts as the surface spectral features are better represented.

6. Acronyms and abbreviations

Acronym	Meaning
ID	Identifier
CAL	Target region ID for region "California, Central Valley"
IUP-UB	Institute of Environmental Physics of the University of Bremen
OPER	Operational TROPOMI XCH_4 data product
OPERbeta	Beta version of new operational TROPOMI XCH_4 data product
SSU	Target region ID for region "South Sudan"
TCCON	Total Carbon Column Observing Network
TGD	Target region ID for region "Turkmenistan, Galkynysh and Dauletabad gas and oil fields"
TROPOMI	
WFMD	Weighting Function Modified Differential Optical Absorption Spectroscopy
WFM-DOAS	See WFMD

7. References

Barré, J., Aben, I., Agustí-Panareda, A., Balsamo, G., Bousserez, N., Dueben, P., Engelen, R., Inness, A., Lorente, A., McNorton, J., Peuch, V.-H., Radnoti, G., and Ribas, R.: Systematic detection of local CH_4 anomalies by combining satellite measurements with high-resolution forecasts, Atmos. Chem. Phys., 21, 5117–5136, https://doi.org/10.5194/acp-21-5117-2021, 2021.

Buchwitz, M., Schneising, O., Reuter, M., Heymann, J., Krautwurst, S., Bovensmann, H., Burrows, J. P., Boesch, H., Parker, R. J., Somkuti, P., Detmers, R. G., Hasekamp, O. P., Aben, I., Butz, A., Frankenberg, C., Turner, A. J., Satellite-derived methane hotspot emission estimates using a fast data-driven method, Amos. Chem. Phys., 17, 5751-5774, doi:10.5194/acp-17-5751-2017, 2017.

Buchwitz, M., Reuter, M., Noel, S., Bramstedt, K., Schneising, O., Hilker, M., Fuentes Andrade, B., Bovensmann, H., Burrows, J. P., Di Noia, A., Boesch, H., Wu, L., Landgraf, J., Aben, I., Retscher, C., O'Dell, C. W., and Crisp, D.: Can a regional-scale reduction of atmospheric CO2 during the COVID-19 pandemic be detected from space? A case study for East China using satellite XCO_2 retrievals, Atmos. Meas. Tech. Discuss., https://doi.org/10.5194/amt-2020-386, in review, 2020.

Frey, M., Sha, M. K., Hase, F., Kiel, M., Blumenstock, T., Harig, R., Surawicz, G., Deutscher, N. M., Shiomi, K., Franklin, J. E., Bösch, H., Chen, J., Grutter, M., Ohyama, H., Sun, Y., Butz, A., Mengistu Tsidu, G., Ene, D., Wunch, D., Cao, Z., Garcia, O., Ramonet, M., Vogel, F., and Orphal, J.: Building the COllaborative Carbon Column Observing Network (COCCON): long-term stability and ensemble performance of the EM27/SUN Fourier transform spectrometer, Atmos. Meas. Tech., 12, 1513–1530, https://doi.org/10.5194/amt-12-1513-2019, 2019.

Froitzheim, N., J. Majka, D. Zastrozhnov, Methane release from carbonate rock formations in the Siberian permafrost area during and after the 2020 heat wave, Proceedings of the National Academy of Sciences (PNAS), Aug 2021, 118 (32) e2107632118; DOI: 10.1073/pnas.2107632118, https://www.pnas.org/content/118/32/e2107632118, 2021.

Hakkarainen, J., Ialongo, I., Maksyutov, S., and Crisp, D.: Analysis of Four Years of Global XCO2 Anomalies as Seen by Orbiting Carbon Observatory-2, Remote Sensing, 11, 850, doi:10.3390/rs11070850, pp. 20, 2019.

Hase, F., Cuesta, J. and Birk, M.: SEOM-IAS validation report, DLR, IAS-D09-PRJ-066, 2018.

Hu, H., Hasekamp, O., Butz, A., Galli, A., Landgraf, J., Aan de Brugh, J., Borsdorff, T., Scheepmaker, R., and Aben, I.: The operational methane retrieval algorithm for

TROPOMI, Atmos. Meas. Tech., 9, 5423–5440, https://doi.org/10.5194/amt-9-5423-2016 , 2016.

Lorente, A., Borsdorff, T., Butz, A., Hasekamp, O., aan de Brugh, J., Schneider, A., Wu, L., Hase, F., Kivi, R., Wunch, D., Pollard, D. F., Shiomi, K., Deutscher, N. M., Velazco, V. A., Roehl, C. M., Wennberg, P. O., Warneke, T., and Landgraf, J.: Methane retrieved from TROPOMI: improvement of the data product and validation of the first 2 years of measurements, Atmos. Meas. Tech., 14, 665–684, https://doi.org/10.5194/amt-14-665-2021, 2021.

Lunt, M. F., Palmer, P. I., Feng, L., Taylor, C. M., Boesch, H., and Parker, R. J.: An increase in methane emissions from tropical Africa between 2010 and 2016 inferred from satellite data, Atmos. Chem. Phys., 19, 14721–14740, https://doi.org/10.5194/acp-19-14721-2019, 2019.

Schneising, O., Buchwitz, M., Reuter, M., Bovensmann, H., Burrows, J. P., Borsdorff, T., Deutscher, N. M., Feist, D. G., Griffith, D. W. T., Hase, F., Hermans, C., Iraci, L. T., Kivi, R., Landgraf, J., Morino, I., Notholt, J., Petri, C., Pollard, D. F., Roche, S., Shiomi, K., Strong, K., Sussmann, R., Velazco, V. A., Warneke, T., and Wunch, D.: A scientific algorithm to simultaneously retrieve carbon monoxide and methane from TROPOMI onboard Sentinel-5 Precursor, Atmos. Meas. Tech., 12, 6771-6802, https://doi.org/10.5194/amt-12-6771-2019, https://doi.org/10.5194/amt-12-6771-2019, 2019.

Schneising, O., Buchwitz, M., Reuter, M., Vanselow, S., Bovensmann, H., and Burrows, J. P.: Remote sensing of methane leakage from natural gas and petroleum systems revisited, Atmos. Chem. Phys., 20, 9169-9182, https://doi.org/10.5194/acp-20-9169-2020, 2020.

Schneising, O., et al., End-to-End ECV Uncertainty Budget (E3UB) for TROPOMI WFM-DOAS XCH_4, technical report ESA Climate Change Initiative “Plus” (CCI+), 8-Jan-2021, version 4, pp. 23, 2021.

Schneising, O., et al., Algorithm Theoretical Basis Document (ATBD) for TROPOMI WFM-DOAS (TROPOMI/WFMD) XCH_4 (version 1.5), Technical Report ESA Climate Change Initiative “Plus” (CCI+), Product v1.5, 12.7.2021, pp. 77, https://www.iup.uni-bremen.de/carbon_ghg/products/tropomi_wfmd/atbd_wfmd.pdf, 2021b.

Schneising, O., et al., Product User Guide (PUG) for TROPOMI WFM-DOAS (TROPOMI/WFMD) XCH_4 (version 1.5), Technical Report ESA Climate Change Initiative “Plus” (CCI+), Product v1.5, 12.7.2021, pp. 17, https://www.iup.uni-bremen.de/carbon_ghg/products/tropomi_wfmd/data/v15/pug_wfmd.pdf, 2021c.

Sha, M. K., Langerock, B., Blavier, J.-F. L., Blumenstock, T., Borsdorff, T., Buschmann, M., Dehn, A., De Mazière, M., Deutscher, N. M., Feist, D. G., García, O. E., Griffith, D. W. T., Grutter, M., Hannigan, J. W., Hase, F., Heikkinen, P., Hermans, C., Iraci, L. T., Jeseck, P., Jones, N., Kivi, R., Kumps, N., Landgraf, J., Lorente, A., Mahieu, E., Makarova, M. V., Mellqvist, J., Metzger, J.-M., Morino, I., Nagahama, T., Notholt, J., Ohyama, H., Ortega, I., Palm, M., Petri, C., Pollard, D. F., Rettinger, M., Robinson, J., Roche, S., Roehl, C. M., Röhling, A. N., Rousogenous, C., Schneider, M., Shiomi, K., Smale, D., Stremme, W., Strong, K., Sussmann, R., Té, Y., Uchino, O., Velazco, V. A., Vigouroux, C., Vrekoussis, M., Wang, P., Warneke, T., Wizenberg, T., Wunch, D., Yamanouchi, S., Yang, Y., and Zhou, M.: Validation of methane and carbon monoxide from Sentinel-5 Precursor using TCCON and NDACC-IRWG stations, Atmos. Meas. Tech., 14, 6249–6304, https://doi.org/10.5194/amt-14-6249-2021, 2021.

Tu, Q., Hase, F., Blumenstock, T., Kivi, R., Heikkinen, P., Sha, M. K., Raffalski, U., Landgraf, J., Lorente, A., Borsdorff, T., Chen, H., Dietrich, F., and Chen, J.: Intercomparison of atmospheric CO2 and CH4 abundances on regional scales in boreal areas using Copernicus Atmosphere Monitoring Service (CAMS) analysis, COllaborative Carbon Column Observing Network (COCCON) spectrometers, and Sentinel-5 Precursor satellite observations, Atmos. Meas. Tech., 13, 4751–4771, https://doi.org/10.5194/amt-13-4751-2020, 2020.

Wunch, D., Toon, G. C., Blavier, J.-F. L., Washenfelder, R. A., Notholt, J., Connor, B. J., Griffith, D. W. T., Sherlock, V., and Wennberg, P. O.: The Total Carbon Column Observing Network, 369, 2087–2112, https://doi.org/10.1098/rsta.2010.0240, 2011.

Wunch, D., Toon, G. C., Sherlock, V., Deutscher, N. M., Liu, C., Feist, D. G., and Wennberg, P. O.: The Total Carbon Column Observing Network's GGG2014 Data Version, Tech. rep., Carbon Dioxide Information Analysis Center, Oak Ridge National Laboratory, Oak Ridge, Tennessee, U.S.A., https://doi.org/10.14291/tccon.ggg2014.documentation.R0/1221662, 2015.